

# **ASSESSMENT REPORT**

## **EMERALD FIELDS RESOURCE CORPORATION**

### **PEARSON PROPERTY**

### **Emerald Fields Pearson Group Claims**

### **GOLD EXPLORATION IN 2006**

NTS 092C08, 092C09, and 092C10,  
Bounded by UTM coordinates (NAD 83 Canada, Zone 10N):  
369000 and 421000 East; 5365000 and 5403900 North

Centre coordinates (NAD 83 Canada, Zone 10):  
395000 East, 5384450North

**By:**

Monika Sumara

Geophysicist

**Submitted: 21 December 2006**

Emerald Fields Resource Corporation.

1546 Pine Portage Road

Kenora, ON

P9N 2K2

## TABLE OF CONTENTS

INTRODUCTION.....	4
1.0 DESCRIPTION OF CLAIMS .....	5
2.0 GEOLOGY.....	8
3.0 GEOLOGIC EVALUATION.....	9
4.0 GEOPHYSICAL SURVEYING .....	9
4.1 Aeromagnetic Surveying Method.....	9
4.2 Units of Measurement .....	9
4.3 Survey Location .....	10
4.4 Terrain Clearance .....	10
4.5 Data Processing and Presentation.....	11
4.6 Interpretation and Evaluation of Geology .....	12
4.7 Magnetic Maps .....	12
5.0 Conclusions and Recommendations.....	14
6.0 REFERENCES.....	15
7.0 GEOTECHNICAL SOFTWARE PROGRAMS USED .....	15
8.0 COST STATEMENT .....	16
8.1.1 Geochemical Sampling.....	16
8.1.2 Geophysical Surveying.....	16
8.1.3 Geological Evaluation .....	17
8.1.4 Costs of Preparing Report .....	17
8.1.5 Administration Costs .....	18
8.1.6 Costs Allocated to Each Individual Claim Block .....	19
9.0 LIST OF PERSONNEL .....	22
9.1 Emerald Fields Resource Corporation Personnel.....	22
10.0 STATEMENT OF QUALIFICATIONS.....	23

## LIST OF FIGURES

Figure 1. Emerald Fields claim blocks index map. ....	8
Figure 2. Emerald Fields 2006 Aeromagnetic Survey Location Map (1:50,000) .....	10
Figure 3. Total Magnetic Field Map of 2006 Aeromagnetic Survey.....	12
Figure 4. Vertical Derivative Grid 2006 Aeromagnetic Survey.....	13
Figure 5. Analytic Signal Grid of 2006 Aeromagnetic Survey.....	13

## LIST OF TABLES

Table 1. Emerald Fields Summary of Work Completed.....	4
Table 2. Emerald Fields claim names and tenure numbers. ....	7
Table 3: Total Geochemistry Costs (All Claim Blocks).....	16
Table 4: Geophysical Analysis Costs (All Claim Blocks).....	16
Table 5: Geophysical Analysis Costs (All Claim Blocks).....	17
Table 6: Assessment Report Costs (All Claim Blocks). ....	17
Table 6: Administration Costs (All Claim Blocks). ....	18
Table 8. Emerald Fields claim names, tenure numbers and cost allocated per claim. ....	20
Table 9. Table of Personnel. ....	22

## APPENDICES

Appendix A. Airborne Magnetometer Survey, Technical Report – Fugro Airborne Surveys Corp.

Appendix B. Review of Aeromagnetic Data over the Pearson Property – M. Sumara

Appendix C. Preliminary Review of Ultramafic Rock Occurrences Near Port Renfrew, Southern Vancouver Island – D. Canil

Appendix D. Preliminary Report of Pearson Property Geology – Dr. Richard Ernst

## INTRODUCTION

This report describes the results of exploration activities including prospecting, geological evaluations and an airborne geophysical survey conducted in June 2006 investigating the gold potential of Emerald Fields Pearson Group Claims (tenures listed in full in Table 2.) This group, which consists of one hundred claims, is centred at approximately 124°22' west longitude, 48°33' north latitude, approximately 10 km north of Port Renfrew, BC, Canada. The total area of the Emerald Fields Pearson Group Claims measures 36,345.69 ha. Access to the claim sites is south via a forestry road off of Provincial Highway #17. Index map of the claim group is shown in Figure 1.

The following table summarizes the work performed on all the claims, which is subsequently described in detail in the following report sections:

No.	Work Description	Detail
1	Geochemical Survey	N/A
2	Geophysical Survey: Total Line Kilometres of Geophysical Surveying completed (Airborne Magnetometer Survey by FUGRO)	1972 lineal km's
3	Geophysical Survey: Review of Aeromagnetic Data over the Pearson Property – report by M. Sumara	36,345.69 ha All Tenure Claims (See Table 2)
4	Total Meters of drilling completed	N/A
5	Geological Survey: Preliminary Review of Ultramafic Rock Occurrences Near Port Renfrew, Southern Vancouver Island, by D. Canil	36,345.69 ha All Tenure Claims (See Table 2)
6	Geological Survey: Preliminary Report of Pearson Property Geology – by Dr. Richard Ernst	36,345.69 ha All Tenure Claims (See Table 2)
7	Total Area of Topographic Surveying completed	N/A
8	Total Area Prospected	N/A
9	Total Number of Soil Samples Collected	N/A
10	Total Number of Silt Samples Collected	N/A
11	Total Number of Rock Chip Samples Collected	N/A
12	Total Line Kilometres Cut in Grid Establishment	N/A

*Table 1. Emerald Fields Summary of Work Completed.*

The claims were staked by Gary M. Pearson in 1996. Emerald Fields Resource Corporation (Emerald Fields) subsequently optioned the claim block from Gary Pearson and became the operator of the property effective 2003. The 2006 work program in the above mentioned claim blocks consisted of an airborne magnetometer survey sampling as shown in Table 1, as well as two geological studies completed by Dr. D. Canil of the University of Victoria, and Dr. Richard Ernst of Ottawa.

The Emerald Fields Pearson Group Claims are comprised of one hundred claims as listed below in Table 2.

## **1.0 DESCRIPTION OF CLAIMS**

The claims described in this report are covered by NTS map sheet 092C/08, 092C/09 and 092C/10. The claims are registered to Emerald Fields Resource Corporation. Claim names, and tenure numbers are summarized in the table below. The total area covered by the Emerald Fields Pearson Group Claims measures 36345.69 ha.

No	Tenure Number	Claim Name/Property
1	358261	GALLEON 8
2	360704	GALLEON 8-3
3	361465	GALLEON 50
4	370610	GALLEON 53
5	373375	GALLEON 70
6	373376	GALLEON 71
7	373716	GALLEON 57
8	374247	GALLEON 80
9	374409	OBIN
10	374714	DAN 1
11	375070	DAN 4
12	378446	8-Jan
13	378447	JACK
14	378824	DAN 9
15	378825	DAN 10
16	378826	DAN 11
17	379141	ABBEY
18	379142	PACMIST 4
19	379144	GHOST
20	379145	PACMIST 3
21	379146	OUTHOUSE
22	379328	PRINCESS
23	379889	PRINCESS 2
24	379890	ROCCOD
25	381142	TIMBER
26	381143	JAY JAY
27	385855	WHISTLE 1
28	386342	WHISTLE 2
29	390305	COHO 2
30	390306	COHO 3
31	390462	COHO #4
32	390463	COHO #5
33	390464	COHO #6
34	394662	GALLEON 8-2
35	394977	SNUG
36	394978	HARBOUR
37	394979	FIFTY-FIVE
38	408828	NOSE
39	409241	NOSE 2
40	414631	GALLEON 54
41	508322	RENFREW 1
42	508323	RENFREW 2
43	508324	RENFREW 3
44	508325	RENFREW 4
45	508326	RENFREW 5
46	508458	
47	508534	
48	508539	
49	508552	
50	508555	

51	508576	
52	508577	
53	508578	
54	508593	
55	508594	
56	508595	
57	508601	
58	508619	
59	508631	
60	508649	
61	508661	
62	508712	
63	508714	
64	508715	
65	508723	
66	508756	
67	508770	
68	515294	
69	515295	
70	515296	
71	515297	
72	515299	
73	515300	
74	515301	
75	515302	
76	515303	
77	519016	
78	519584	
79	519585	
80	519586	
81	519587	
82	519588	
83	519590	
84	519591	
85	520492	
86	520493	
87	520494	
88	520495	
89	520496	
90	520497	
91	520498	
92	520499	
93	520500	
94	520501	
95	520502	
96	520503	
97	520616	THOR
98	534763	
99	534765	
10	534816	

*Table 2. Emerald Fields claim names and tenure numbers.*

## Emerald Fields Claims Location Map

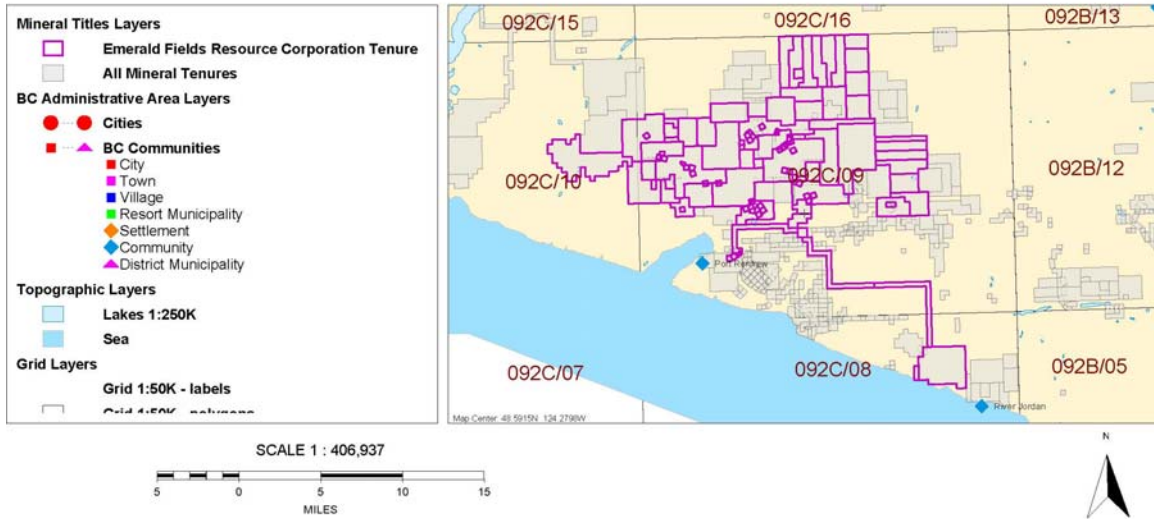


Figure 1. Emerald Fields claim blocks index map.

## 2.0 GEOLOGY

The prominent geological formations of South-Western Vancouver Island are the Island Intrusions, an Early to Middle Jurassic Island Plutonic Suite, consisting of granitic rocks and Tertiary dikes and sills. The Island Intrusions break through the following volcanic and sedimentary rocks: the Paleozoic Sicker Group, the Mississippian to Permian Buttle Lake Group, the Lower Jurassic Bonanza Group, the Upper Triassic Vancouver Group, the Upper Cretaceous Nanaimo Group, and the Jurassic to Cretaceous Leech River Complex.

The Cowichan Lake area just to the North of the Pearson and Karen, specifically the southeastern part of the Cowichan uplift, sees mainly the Sicker and Buttle Lake groups, which are the primary target of volcanogenic massive sulphide deposits. Mining exploration has profited from the base and precious metal mineral prosperity of the region. Deposits have been found in structures such as skarns, shears, quartz veins and volcanogenic massive sulphides.

Regional geology indicates that this area is possibly prospective for Iron Oxide Copper-Gold (IOCG) style deposits. IOCG deposits are characteristically large, iron rich systems that consist of variable amounts copper, silver and gold and potentially uranium.

### **3.0 GEOLOGIC EVALUATION**

Geological prospecting and field mapping was conducted in target areas identified by regional geology and geophysics (as defined in the report attached in Appendix 'B'). Based on regional indications and claim prospecting, the prospector was able to isolate outcrop of interest which he identified as quartz vein, schist and various intrusives and collected samples continuously along the feature.

Two separate geological studies were conducted and the results of these analyses are included in the appendix section of this report. Appendix C contains the Preliminary Review of Ultramafic Rock Occurrences near Port Renfrew, Southern Vancouver Island by D. Canil of the University of Victoria. His team carried out a field mapping study and the preliminary findings are included in the above review. Appendix D Preliminary contains the Report of Pearson Property Geology by Dr. Richard Ernst, an Ottawa geologist who specializes in igneous formations.

### **4.0 GEOPHYSICAL SURVEYING**

The airborne geophysical program on the Pearson claim block was carried out in June of 2006 by Fugro Airborne Services Corporation who was contracted to fly a low altitude, magnetometer survey over the key area of interest. The Fugro crew consisted of four people and was stationed in Port Renfrew for the duration of the survey. Data was collected in NAD83, UTM Zone 10N and all grids and map products are in that same projection.

#### **4.1 Aeromagnetic Surveying Method**

The helicopter based magnetometer survey was flown by Fugro and completed over a period spanning between Jun 12, 2006 and June 20, 2006. The grid measured 22km by 7km and consisted of N-S lines at 100m spacing and E-W tie lines at 500m spacing for a total distance of 1972 line kilometres.

Altitude control was accomplished via onboard helicopter altimeter. The target elevation of 60m average altitude was achieved with a mean variation of 15m. This was deemed acceptable for the rugged terrain of the southern part of Vancouver Island.

Expanded description of equipment and parameters of the aeromagnetic survey can be found in Appendix A in the technical survey report prepared by Fugro.

#### **4.2 Units of Measurement**

All survey planning and data collection including gridding and mapping was done in NAD83, UTM Zone 10N, Canada Mean coordinates.

The unit of magnetic measurement is the nanotesla (nT.)

### 4.3 Survey Location

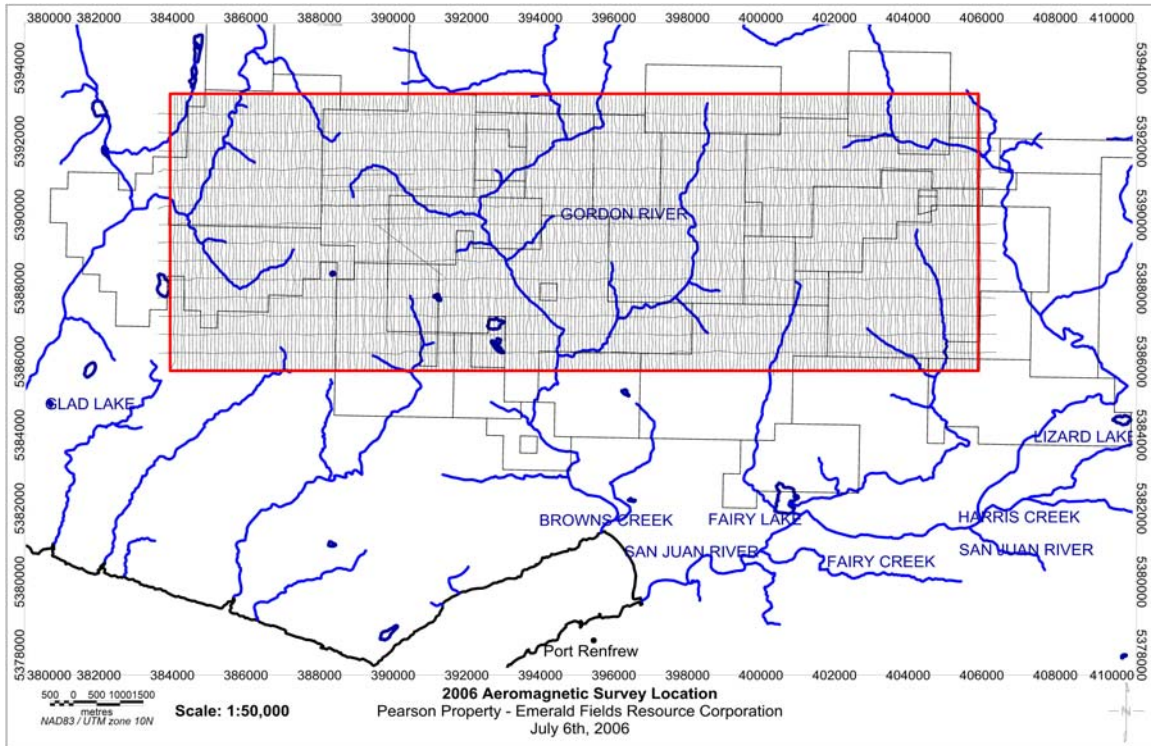


Figure 2. Emerald Fields 2006 Aeromagnetic Survey Location Map (1:50,000)

A magnetic survey was flown for Emerald Field Resource Corporation, from June 12 to June 18 2006, over a survey block located near Port Renfrew, British Columbia. The survey area is centered on NTS map sheet 92C/9, 10 (Figure 2).

Survey coverage consisted of approximately 1972 line-km, including 308 line-km of tie lines. Flight lines were flown in an azimuthal direction of 90°/270° with a line separation of 100 metres. Tie lines were flown orthogonal to the traverse lines with a line separation of 500 metres.

### 4.4 Terrain Clearance

Mean terrain sensor clearance was 60 m, except where precluded by safety considerations, e.g., restricted or populated areas, severe topography, obstructions, tree canopy, aerodynamic limitations, etc.

## **4.5 Data Processing and Presentation**

The raw range data from at least four satellites are simultaneously recorded by both the base and mobile GPS units. The geographic positions of both units, relative to the model ellipsoid, are calculated from this information. Differential corrections, which are obtained from the base station, are applied to the mobile unit data to provide a post-flight track of the aircraft, accurate to within 2 m. Speed checks of the flight path are also carried out to determine if there are any spikes or gaps in the data.

The corrected WGS84 latitude/longitude coordinates are transformed to the coordinate system used on the final maps. Images or plots are then created to provide a visual check of the flight path. All data was collected and processed in the NAD 83, Zone 10 projection. A standard sequence of geophysical processing was applied to the aeromagnetic data as described in the steps below.

The aeromagnetic data was gridded using the bi-directional method with a 25m cell size, and a Total Magnetic Field image was created. In addition, two other grids were created which included the Vertical Derivative and Analytics Signal in order to investigate the magnetic characteristics of the geology in this area.

The Vertical Derivative is commonly applied to total magnetic field data to enhance the shallowest geological sources. Isolating short wavelength magnetic features enhances the response of near surface features at the expense of deeper sources and provides a more direct correlation between magnetic anomalies and geological map units.

The Analytic Signal grid is a valuable geophysical interpretation tool in locating the edges of magnetic source bodies, particularly where remanence complicates interpretation. The analytic signal is the square root of the sum of the squares of the derivatives in the x, y, and z directions.

### **Diurnal Corrections**

Basemag readings were carried out by Fugro as was the diurnal correction of the raw data.

### **Lag Correction**

A lag shift of -5 fiducial was used in the lag correction.

### **Heading Correction**

Heading corrections were performed by the survey data acquisition system as part of the aircraft compensation system. The correction parameters were determined by a heading test flight at the start of the survey.

### **Statistical Leveling of Total Magnetic Field**

A statistical leveling of the magnetic data was done first on the tie lines, and then a full level was done on all lines. A least-squares trend line was calculated through an error channel to derive a trend error curve, which was then added to the channel to be leveled. The trend curve was then saved for later inspection.

## 4.6 Interpretation and Evaluation of Geology

The detailed 2006 aeromagnetic data reveals a great deal of structural variety as compared to the widespread high level magnetic response visible on a regional scale. The geology consists mainly of the metamorphic Westcoast Complex which includes: gneiss, amphibolite, migmatite, and quartz diorite. These Paleozoic and Mesozoic age rocks are characterized by a moderately strong magnetic response, with NW trending, linear, magnetically low structures. The prominent geological features within the survey area are the two groups of intrusive rocks which consist of the early to middle Jurassic Island Plutonic Suite and are signified by a higher magnetic domain.

The geological map, MINFILE Occurrence MAP 092C, Cape Flattery, Ministry of Energy, Mines and Petroleum Resources, BC, was used in the geophysical interpretation. A compilation of anomalies throughout the survey block is summarized the Review of Aeromagnetic Data over the Pearson Property by M. Sumara in Appendix B. The interpreted anomalies were analyzed and prioritized based on signal strength, structure, size as well as any evidence of mineral showings or drillhole results. The information provided by the magnetics suggests six significant anomalies of interest however, further geological follow-up and investigation is strongly recommended, particularly over anomalies where there is only magnetic data available.

## 4.7 Magnetic Maps

The aeromagnetic data was gridded and presented in the three primary maps: Total Magnetic Field, Vertical Derivative and Analytics Signal.

All geophysical grids and maps are provided at an appropriate scale (1:50,000) on the data CD included with this report. Contoured data is also provided at that scale.

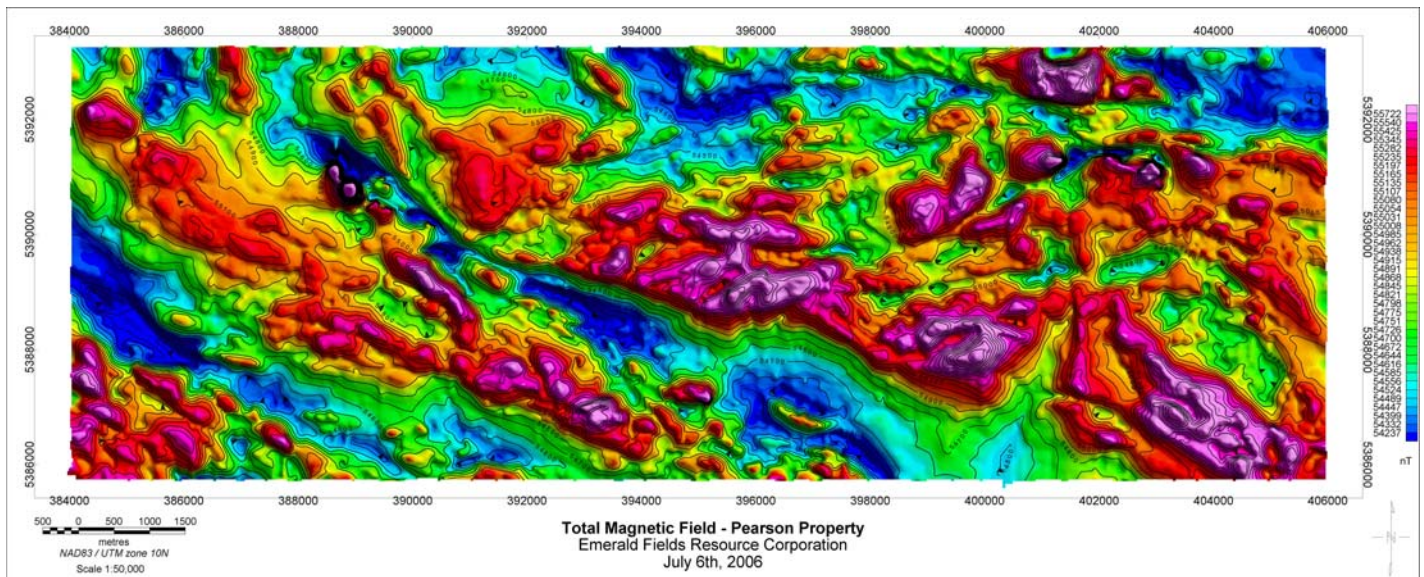


Figure 3. Total Magnetic Field Map of 2006 Aeromagnetic Survey.

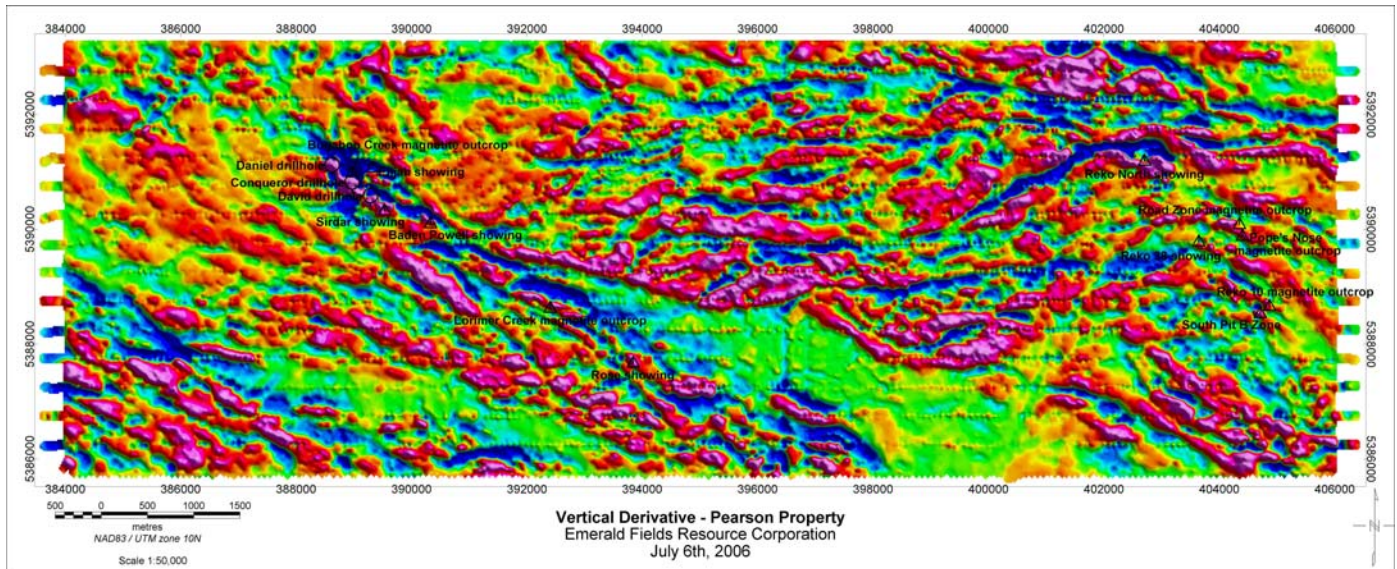


Figure 4. Vertical Derivative Grid 2006 Aeromagnetic Survey

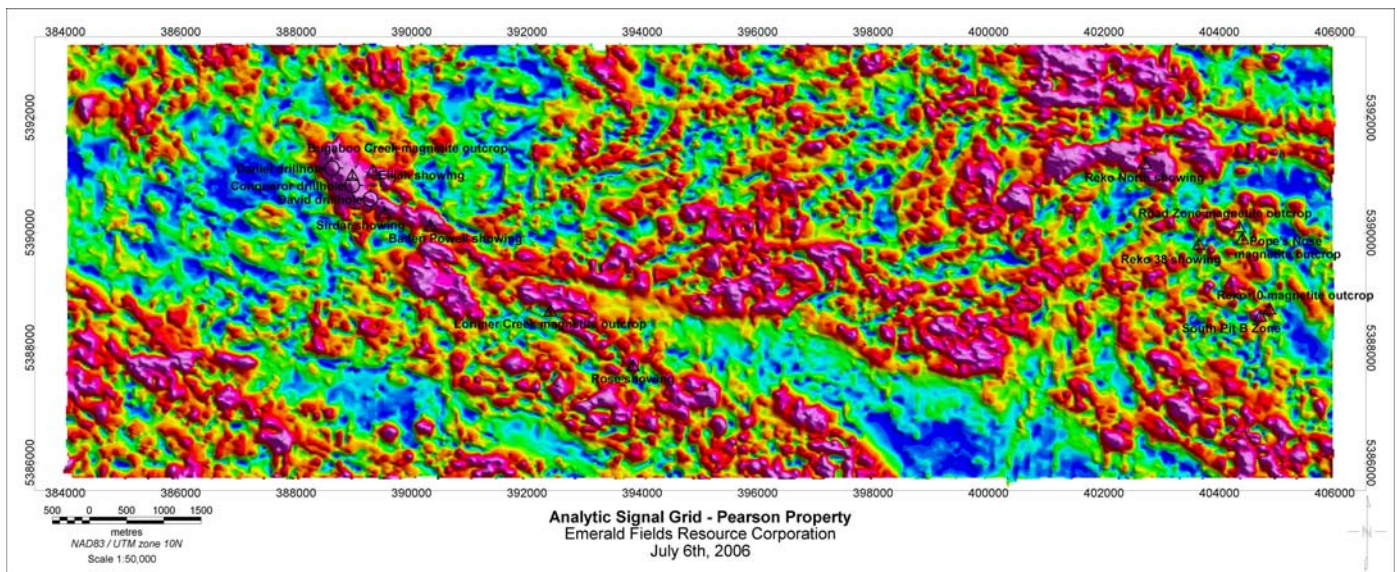


Figure 5. Analytic Signal Grid of 2006 Aeromagnetic Survey

## **5.0 CONCLUSIONS AND RECOMMENDATIONS**

The results of the 2006 exploration program designate zones of interest for further investigation and have proven to be of great benefit in mapping the geology and structure of the Pearson claim block. The airborne geophysical survey has provided good information on the structure and geology of the area of interest resulting in a list of prioritized targets to be pursued with further geological investigations. A high resolution airborne EM survey is recommended to aid in drill-hole selection. The geological studies by D. Canil and Dr. R. Ernst were key in providing insight, information and a deeper understanding of the structure and geology of the Pearson Claim Group. The geological evaluations in conjunction with the geophysical data gathered this year have prompted drill-hole selection and prioritization to follow in 2007.

## **6.0 REFERENCES**

Dobrin, M.B. 1976. Introduction to Geophysical Prospecting. McGraw-Hill Book Co. p.544-545

Massey, N.W.D. 1995. Geology and Mineral Resources of the Cowichan Lake Area, Ministry of Energy, Mines and Petroleum Resources

Sheriff, R. Encyclopedic Dictionary of Exploration Geophysics, SEG

Vacquier, J. 1951. Interpretation of Aeromagnetic Maps, The Geological Society of America Memoir 47.

## **7.0 GEOTECHNICAL SOFTWARE PROGRAMS USED**

Geosoft Oasis Montaj Version 6.2 Standard (SM)

MapInfo

## 8.0 COST STATEMENT

### 8.1.1 Geochemical Sampling

Date	Description	Individual - Job Title	Rate per Unit	No. of Units	Total Cost
Jan. 14 – Aug. 1, 2006	Field Sampling	Gary Pearson - Prospector	\$30.00 / hr	190 hrs	\$ 5700.00
<b>TOTAL</b>					<b>\$ 5,700.00</b>

Table 3: Total Geochemistry Costs (All Claim Blocks).

### 8.1.2 Geophysical Surveying

Date	Description	Individual - Job Title	Rate per Unit	No. of Units	Total Cost
June 12 – 18, 2006	Fugro Aeromagnetic Survey	Fugro Airborne Surveys Corp.	-	-	\$128,000.00
May 1 - 31, 2006	Pearson Project, Vancouver Island: airborne magnetometer survey planning	Monika Sumara - Geophysicist	\$40.00 / hr	13 hours	\$ 520.00
June 1 - 30, 2006	Aeromagnetic Survey QC	Monika Sumara - Geophysicist	\$40.00 / hr	150 hours	\$ 6000.00
July 1 - 31, 2006	Geophysical Interpretation Report and Maps	Monika Sumara - Geophysicist	\$50.00 / hr	54 hours	\$ 2700.00
August 1 – 31, 2006	Geophysical Interpretation Report and Maps	Monika Sumara – Geophysicist	\$50.00 / hr	56 hours	\$ 2800.00
August 1 – 31, 2006	Geophysical / geological maps and reports - hard copies	Zone 14, Winnipeg			\$1,454.18
Sept. 1 – 30, 2006	Geophysical Modelling and Survey Follow-Up	Monika Sumara - Geophysicist	\$50.00 / hr	16 hours	\$ 800.00
November 31, 2006	Geophysical Modelling	Monika Sumara - Geophysicist	\$50.00 / hr	16 hours	\$ 800.00
<b>TOTAL</b>					<b>\$143,074.18</b>

Table 4: Geophysical Analysis Costs (All Claim Blocks).

### 8.1.3 Geological Evaluation

Date	Description	Individual - Job Title	Rate per Unit	No. of Units	Total Cost
Jan. 1 – 30, 2006	Geological field study	Dr. Dante Canil	-	-	\$34,000.00
Aug. 1 – 31, 2006	Field work	Wayne Smith	-	-	\$1,800.00
Aug 23, 2006	Field work	Mike Cedar	-	-	\$80.00
Nov. 7 – 23 <sup>rd</sup> , 2006	Geological assistance	George Owsiacki, geologist	-	-	\$1,500.00
April 28 – Aug. 8, 2006	Geological evaluation	Dr. Richard Ernst	\$600.00 / day	13	\$8,054.18
Sept. 19, 2006	Rock age dating for Dr. Ernst Geological Evaluation report	University of Victoria, School of Earth and Ocean Sciences	-	-	\$3,500.00
<b>TOTAL</b>					<b>\$ 48,934.18</b>

Table 5: Geophysical Analysis Costs (All Claim Blocks).

### 8.1.4 Costs of Preparing Report

Date	Description	Individual - Job Title	Rate per Unit	No. of Units	Total Cost
November , 2005	Pearson Property Claims Assessment Report	Monika Sumara - Geophysicist	\$50.00 / hr	64 hours	\$3200.00
December , 2005	Pearson Property Claims Assessment Report	Monika Sumara - Geophysicist	\$50.00 / hr	97 hours	\$4850.00
<b>TOTAL</b>					<b>\$ 8050.00</b>

Table 6: Assessment Report Costs (All Claim Blocks).

**8.1.5 Administration Costs**

<b>Date</b>	<b>Description</b>	<b>Individual - Job Title</b>	<b>Rate per Unit</b>	<b>No. of Units</b>	<b>Total Cost</b>
May 1 – December 21, 2006	Administration Costs for work pertaining to Pearson claim block exploration program	Emeralds Fields Administration			\$ 20,575.84
<b>TOTAL</b>					<b>\$ 20,575.84</b>

*Table 7: Administration Costs (All Claim Blocks).*

**8.1.6 Costs Allocated to Each Individual Claim Block**

No	Tenure Number	Claim Name/Property	Cost Accrued per Claim
1	358261	GALLEON 8	\$ 2,263.34
2	360704	GALLEON 8-3	\$ 2,263.34
3	361465	GALLEON 50	\$ 2,263.34
4	370610	GALLEON 53	\$ 2,263.34
5	373375	GALLEON 70	\$ 2,263.34
6	373376	GALLEON 71	\$ 2,263.34
7	373716	GALLEON 57	\$ 2,263.34
8	374247	GALLEON 80	\$ 2,263.34
9	374409	OBIN	\$ 2,263.34
10	374714	DAN 1	\$ 2,263.34
11	375070	DAN 4	\$ 2,263.34
12	378446	8-Jan	\$ 2,263.34
13	378447	JACK	\$ 2,263.34
14	378824	DAN 9	\$ 2,263.34
15	378825	DAN 10	\$ 2,263.34
16	378826	DAN 11	\$ 2,263.34
17	379141	ABBEY	\$ 2,263.34
18	379142	PACMIST 4	\$ 2,263.34
19	379144	GHOST	\$ 2,263.34
20	379145	PACMIST 3	\$ 2,263.34
21	379146	OUTHOUSE	\$ 2,263.34
22	379328	PRINCESS	\$ 2,263.34
23	379889	PRINCESS 2	\$ 2,263.34
24	379890	ROCCOD	\$ 2,263.34
25	381142	TIMBER	\$ 2,263.34
26	381143	JAY JAY	\$ 2,263.34
27	385855	WHISTLE 1	\$ 2,263.34
28	386342	WHISTLE 2	\$ 2,263.34
29	390305	COHO 2	\$ 2,263.34
30	390306	COHO 3	\$ 2,263.34
31	390462	COHO #4	\$ 2,263.34
32	390463	COHO #5	\$ 2,263.34
33	390464	COHO #6	\$ 2,263.34
34	394662	GALLEON 8-2	\$ 2,263.34
35	394977	SNUG	\$ 2,263.34
36	394978	HARBOUR	\$ 2,263.34
37	394979	FIFTY-FIVE	\$ 2,263.34
38	408828	NOSE	\$ 2,263.34
39	409241	NOSE 2	\$ 2,263.34
40	414631	GALLEON 54	\$ 2,263.34
41	508322	RENFREW 1	\$ 2,263.34
42	508323	RENFREW 2	\$ 2,263.34
43	508324	RENFREW 3	\$ 2,263.34
44	508325	RENFREW 4	\$ 2,263.34
45	508326	RENFREW 5	\$ 2,263.34
46	508458		\$ 2,263.34
47	508534		\$ 2,263.34
48	508539		\$ 2,263.34
49	508552		\$ 2,263.34

50	508555		\$ 2,263.34
51	508576		\$ 2,263.34
52	508577		\$ 2,263.34
53	508578		\$ 2,263.34
54	508593		\$ 2,263.34
55	508594		\$ 2,263.34
56	508595		\$ 2,263.34
57	508601		\$ 2,263.34
58	508619		\$ 2,263.34
59	508631		\$ 2,263.34
60	508649		\$ 2,263.34
61	508661		\$ 2,263.34
62	508712		\$ 2,263.34
63	508714		\$ 2,263.34
64	508715		\$ 2,263.34
65	508723		\$ 2,263.34
66	508756		\$ 2,263.34
67	508770		\$ 2,263.34
68	515294		\$ 2,263.34
69	515295		\$ 2,263.34
70	515296		\$ 2,263.34
71	515297		\$ 2,263.34
72	515299		\$ 2,263.34
73	515300		\$ 2,263.34
74	515301		\$ 2,263.34
75	515302		\$ 2,263.34
76	515303		\$ 2,263.34
77	519016		\$ 2,263.34
78	519584		\$ 2,263.34
79	519585		\$ 2,263.34
80	519586		\$ 2,263.34
81	519587		\$ 2,263.34
82	519588		\$ 2,263.34
83	519590		\$ 2,263.34
84	519591		\$ 2,263.34
85	520492		\$ 2,263.34
86	520493		\$ 2,263.34
87	520494		\$ 2,263.34
88	520495		\$ 2,263.34
89	520496		\$ 2,263.34
90	520497		\$ 2,263.34
91	520498		\$ 2,263.34
92	520499		\$ 2,263.34
93	520500		\$ 2,263.34
94	520501		\$ 2,263.34
95	520502		\$ 2,263.34
96	520503		\$ 2,263.34
97	520616	THOR	\$ 2,263.34
98	534763		\$ 2,263.34
99	534765		\$ 2,263.34
10	534816		\$ 2,263.34

Table 8. Emerald Fields claim names, tenure numbers and cost allocated per claim.



## 9.0 LIST OF PERSONNEL

### 9.1 Emerald Fields Resource Corporation Personnel

During 2004 – 2005, the following individual participated in exploration activities on the Emerald Fields claims Snug, Harbour, Fifty-Five, and Galleon-4b:

Name	Occupation	Company	Address	City
Gary M. Pearson	Prospector	Emerald Fields Resource Corporation	70 Wickaninnish Road	Port Refrew
Monika Sumara	Geophysicist	Consultant	1303, 933 Seymour St.	Vancouver
Dante Canil	Geologist	University of Victoria	-	Victoria
Wayne Smith	Field worker	-	-	Port Renfrew
Mike Cedar	Field worker	-	-	Port Renfrew
George Owsiaci	Geologist	Consultant	-	Victoria
Dr. Richard Ernst	Geologist	Ernst Geosciences	-	Ottawa

*Table 9. Table of Personnel.*

## 2. SURVEY OPERATIONS

The base of operations for the survey was established at Port Renfrew, BC.

The survey area(s) can be located on NTS map sheets 92C/9,10 (Figure 2).

Table 2-1 lists the corner coordinates of the survey area in NAD 83, UTM Zone 10, and central meridian 123° west.

**Table 2-1**

**Nad83 Utm Zone 10**

Block	Corners	X-UTM (E)	Y-UTM (N)
<b>06051-1</b>	1	384000	5393000
	2	406000	5393000
	3	406000	5386000
	4	384000	5386000

## 10.0 STATEMENT OF QUALIFICATIONS

Monika Sumara  
Consulting Geophysicist  
1303 – 933 Seymour Street, Vancouver, BC  
Phone (604) 737-1371 Cell (778) 866-1313  
Fax (604) 689-8199 Email: monika\_sumara@yahoo.ca

### CERTIFICATE OF AUTHOR

I Monika Sumara am a Geoscientist-in-Training who is employed by Emerald Fields Resource Corporation to complete an assessment report of the Emerald Fields Pearson Group Claims on Vancouver Island.

I am:

- eligible for membership with the Association of Professional Engineers and Geoscientists of British Columbia (APEGBC).

I graduated from the University of Calgary in Alberta with a Bachelor of Science in Geophysics in 2002, and I have practiced my profession continuously since.

My geophysics experience has involved:

- seismic processing and interpretation in the Western Sedimentary basin with Tikal Resources Inc., an oil and gas exploration company of Calgary, Alberta, from 1998 to 2001;
- oil and gas geophysical research with CREWES (Consortium for Research in Elastic Wave Exploration Seismology) at the University of Calgary under the tutelage of Dr. Gary Margrave, involving seismic processing techniques during 2002
- satellite imagery processing with PhotoSat of Vancouver, British Columbia in 2003 involving GIS mapping and rendering;
- diamond exploration with Arctic Star Diamond in Northern Manitoba and the Northwest Territories since 2004; and
- geophysical aeromagnetic surveys with Universal Wing of Vancouver, British Columbia since 2004.

I am presently a Consulting Geophysicist with diamond exploration clients including Arctic Star Diamond Corp. and an aeromagnetic surveying company, Universal Wing Geophysics. Relevant to this report, I acted as Project Geophysicist for Emerald Fields Resource Corporation on the Emerald Fields Pearson Group Claim properties on Vancouver Island, BC.

In 2006, my work included: planning an airborne magnetometer survey, survey data QV, and processing and interpretation of data.

I am not aware of any material fact or material change with respect to the subject matter of this technical report which is not reflected in this report, the omission to disclose which would make this report misleading.

Dated at Vancouver, BC this 21st day of December, 2006.

\_\_\_\_\_  
"MS"  
Monika Sumara

Appendix A. Airborne Magnetometer Survey, Technical Report – Fugro  
Airborne Surveys Corp

Report #06051

**HM1 STINGER MOUNTED  
AEROMAGNETIC SURVEY  
FOR  
EMERALD FIELDS RESOURCE CORP.  
PORT RENFREW, BC**

**NTS: 92C/ 9,10**



Fugro Airborne Surveys Corp.  
Mississauga, Ontario

Igor Sram  
Geophysicist

July 12, 2006

## **SUMMARY**

This report describes the logistics, data acquisition, processing and presentation of results of a magnetic airborne geophysical survey carried out for Emerald Fields Resource Corporation, over a property located near Port Renfrew, British Columbia. Total coverage of the survey block amounted to 1848.9 km. The survey was flown from June 12 to June 18, 2006.

The purpose of the survey was to provide information that could be used to map the geology and structure of the survey area. This was accomplished by using a high sensitivity cesium magnetometer mounted on a stinger in front of the helicopter. The information from this sensor was processed to produce maps that display the magnetic properties of the survey area. A GPS electronic navigation system ensured accurate positioning of the geophysical data with respect to the base map.

The survey data were processed and compiled in the Fugro Airborne Surveys Toronto office. Map products and digital data were provided in accordance with the scales and formats specified in the Survey Agreement.

On review of the survey results areas of interest may be assigned priorities on the basis of supporting geophysical, geochemical and/or geological information. After initial investigations have been carried out, it may be necessary to re-evaluate the remaining anomalies based on information acquired from the follow-up program.

# CONTENTS

1.	INTRODUCTION.....	1.1
2.	SURVEY OPERATIONS.....	2.1
3.	SURVEY EQUIPMENT.....	3.1
	Airborne Magnetometer.....	3.1
	Magnetic Base Station.....	3.2
	Navigation (Global Positioning System).....	3.4
	Radar Altimeter.....	3.5
	Barometric Pressure and Temperature Sensors.....	3.6
	Laser Altimeter.....	3.6
	Digital Data Acquisition System.....	3.7
	Video Flight Path Recording System.....	3.7
4.	QUALITY CONTROL AND IN-FIELD PROCESSING.....	4.1
5.	DATA PROCESSING.....	5.3
	Flight Path Recovery.....	5.3
	Total Magnetic Field.....	5.3
	Calculated Vertical Magnetic Gradient.....	5.4
	Digital Elevation.....	5.4
	Contour, Colour and Shadow Map Displays.....	5.5
6.	PRODUCTS.....	6.1
	Base Maps.....	6.1
	Final Products.....	6.2
7.	SURVEY RESULTS.....	7.1
	General Discussion.....	7.1
8.	CONCLUSIONS AND RECOMMENDATIONS.....	8.1

## **APPENDICES**

- A. List of Personnel
- B. Background Information
- C. Data Archive Description
- D. Data Processing Flowcharts
- E. Tests and Calibrations
- F. Glossary

## 1. INTRODUCTION

A magnetic survey was flown for Emerald Field Resource Corporation, from June 12 to June 18 2006, over a survey block located near Port Renfrew, British Columbia. The survey area can be located on NTS map sheet 92C/9, 10 (Figure 2).

Survey coverage consisted of approximately 1848.9 line-km, including 308 line-km of tie lines. Flight lines were flown in an azimuthal direction of 90°/270° with a line separation of 100 metres. Tie lines were flown orthogonal to the traverse lines with a line separation of 500 metres.

The survey employed a stinger mounted magnetometer, laser, radar and barometric altimeter, video camera, digital recorders, and an electronic navigation system. The instrumentation was installed in an AS350B2 turbine helicopter (Registration C-FDNF) that was provided by Questral Helicopters Ltd. The helicopter flew at an average airspeed of 85 km/h with a sensor height of approximately 60 metres.



Figure 1: Fugro Airborne Surveys Stinger Mag System with AS350-B3

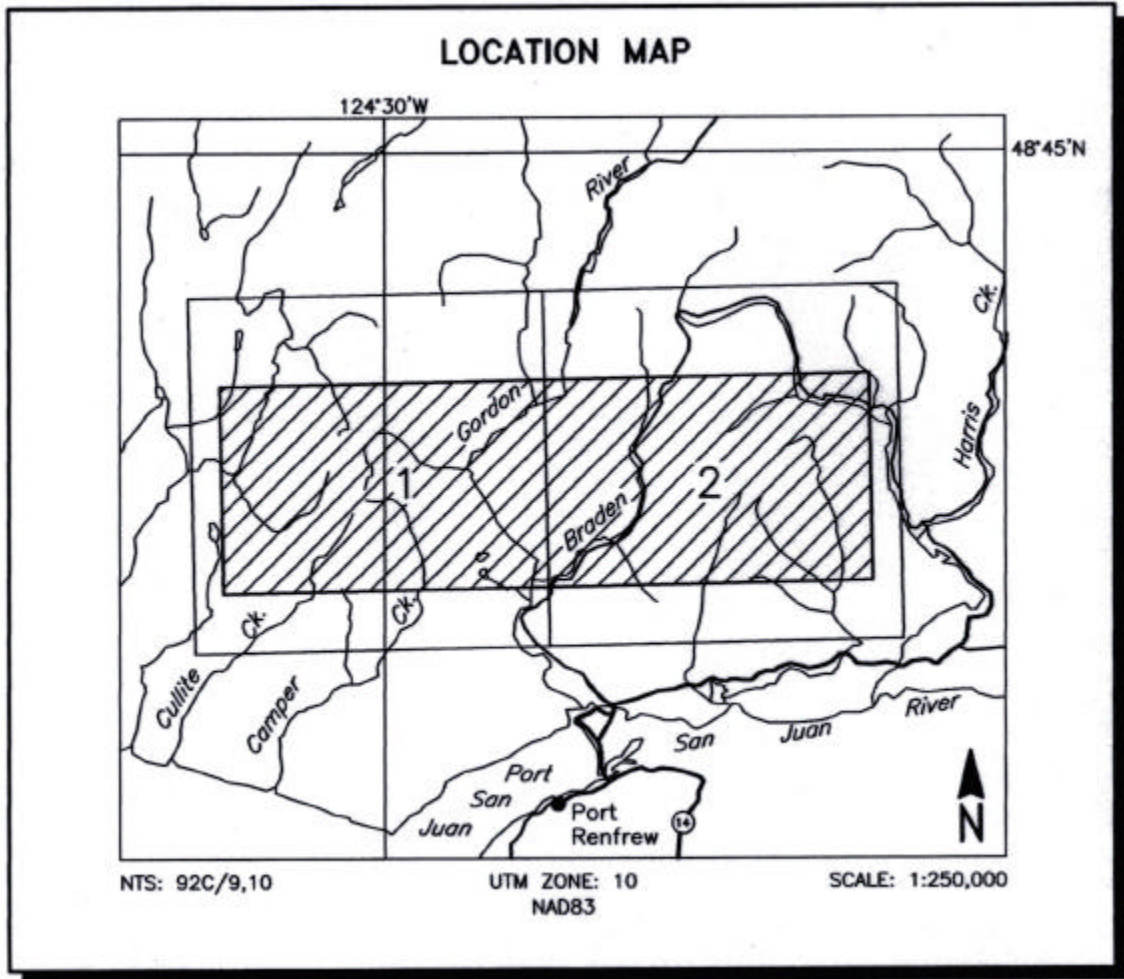


Figure 2  
Location Map and Sheet Layout  
Port Renfrew Survey Area, NTS: 92C/ 9,10

- 2.3 -

Job # 06051

The survey specifications were as follows:

<b>Parameter</b>	<b>Specifications</b>
Traverse line direction	0°/180°
Traverse line spacing	100 m
Tie line direction	90°/270°
Tie line spacing	500 m
Sample interval	10 Hz, 2.5 m @ 85 km/h
Aircraft mean terrain clearance	60 m
EM sensor mean terrain clearance	60 m
Mag sensor mean terrain clearance	60 m
Average speed	85 km/h
Navigation (guidance)	±5 m, Real-time GPS
Post-survey flight path	±2 m, Differential GPS

### 3. SURVEY EQUIPMENT

This section provides a brief description of the geophysical instruments used to acquire the survey data and the calibration procedures employed. The geophysical equipment was installed in an AS350B2 helicopter. This aircraft provides a safe and efficient platform for surveys of this type.

#### **Airborne Magnetometer**

Model:	Scintrex CS2 sensor with FUGRO D1344 magnetic counter
Type:	Optically pumped cesium vapour
Sensitivity:	0.01 nT
Sample rate:	10 per second

The magnetometer sensor is mounted on a boom attached to the skid gear of the helicopter.

## Magnetic Base Station

### Primary

Model: Fugro CF1 base station with timing  
provided by integrated GPS

Sensor type: Geometrics G822 or Scintrex CS-2

Counter specifications: Accuracy:  $\pm 0.1$  nT  
Resolution: 0.01 nT  
Sample rate 1 Hz

GPS specifications: Model: Marconi Allstar  
Type: Code and carrier tracking of L1 band,  
12-channel, C/A code at 1575.42 MHz  
Sensitivity: -90 dBm, 1.0 second update  
Accuracy: Manufacturer's stated accuracy for differential  
corrected GPS is 2 metres

### Environmental

Monitor specifications: Temperature:

- Accuracy:  $\pm 1.5^{\circ}\text{C}$  max
- Resolution:  $0.0305^{\circ}\text{C}$
- Sample rate: 1 Hz
- Range:  $-40^{\circ}\text{C}$  to  $+75^{\circ}\text{C}$

Barometric pressure:

- Model: Motorola MPXA4115A
- Accuracy:  $\pm 3.0^{\circ}$  kPa max ( $-20^{\circ}\text{C}$  to  $105^{\circ}\text{C}$  temp. ranges)
- Resolution: 0.013 kPa
- Sample rate: 1 Hz
- Range: 55 kPa to 108 kPa

### Backup

Model: GEM Systems GSM-19T

Type: Digital recording proton precession  
Sensitivity: 0.10 nT  
Sample rate: 3 second intervals

A digital recorder is operated in conjunction with the base station magnetometer to record the diurnal variations of the earth's magnetic field. The clock of the base station is synchronized with that of the airborne system, using GPS time, to permit subsequent removal of diurnal drift. The Fugro CF1 was the primary magnetic base station. It was located at latitude  $48^{\circ} 33' 14.72891''$  North, longitude  $124^{\circ} 25' 20.23928''$  West at an elevation 6.88 m below the WGS 84 ellipsoid.

## **Navigation (Global Positioning System)**

### Airborne Receiver for Real-time Navigation & Guidance and Flight Path Recovery

Model:	Novatel OEM IV
Type:	Code and carrier tracking of L1 band, 12-channel, dual frequency C/A code at 1575.2 MHz, and L2 P-code 1227 MHz, WAAS enabled for real time correction
Sample rate:	0.5 second update.
Accuracy:	Manufacturer's stated accuracy for differential corrected GPS is better than 1 metre.
Antenna:	Mounted on tail of Aircraft.

### Primary Base Station for Post-Survey Differential Correction

Model:	Novatel OEM IV
Type:	Code and carrier tracking of L1 band, 12-channel, dual frequency C/A code at 1575.2 MHz, and L2 P-code 1227 MHz
Sample rate:	1 second update
Accuracy:	Manufacturer's stated accuracy for differential corrected GPS is better than 1 metre

The Novatel OEM IV is a line of sight, satellite navigation system that utilizes time-coded signals from at least four of forty-eight available satellites. A similar system was used as the primary base station receiver. The mobile and base station raw XYZ data were recorded, thereby permitting post-survey differential corrections for theoretical accuracies

of better than 2 metres. A Marconi Allstar GPS unit, part of the CF-1, was used as a secondary (back-up) base station.

Each base station receiver is able to calculate its own latitude and longitude. For this survey, the primary GPS station was located at latitude 48° 33' 18.3727" N, longitude 124° 25' 14.15893" W at an elevation of 6.88 metres below the ellipsoid. The GPS records data relative to the WGS84 ellipsoid, which is the basis of the revised North American Datum (NAD83). Conversion software is used to transform the WGS84 coordinates to the NAD83 UTM system displayed on the maps.

## **Radar Altimeter**

Manufacturer:	Honeywell/Sperry
Model:	AA 330 or RT220
Type:	Short pulse modulation, 4.3 GHz
Sensitivity:	0.3 m
Sample rate:	2 per second

The radar altimeter measures the vertical distance between the helicopter and the ground.

## Barometric Pressure and Temperature Sensors

Model:	DIGHEM D 1300
Type:	Motorola MPX4115AP analog pressure sensor AD592AN high-impedance remote temperature sensors
Sensitivity:	Pressure: 150 mV/kPa Temperature: 100 mV/°C or 10 mV/°C (selectable)
Sample rate:	10 per second

The D1300 circuit is used in conjunction with one barometric sensor and up to three temperature sensors. Two sensors (baro and temp) are installed in the EM console in the aircraft, to monitor pressure (1KPA) and internal operating temperatures (2TDC).

## Laser Altimeter

Manufacturer:	Optech
Model:	ADMGPA100
Type:	Fixed pulse repetition rate of 2 kHz (First/Last pulse)
Sensitivity:	±5 cm from 10°C to 30°C ±10 cm from -20°C to +50°C
Sample rate:	10 per second

The laser altimeter is mounted on the helicopter, and measures the distance from the aircraft to ground.

## **Digital Data Acquisition System**

Manufacturer: Fugro Airborne Surveys  
Model: HELIDAS  
Recorder: San Disk compact flash card (PCMCIA)

The stored data are downloaded to the field workstation PC at the survey base, for verification, backup and preparation of in-field products.

## **Video Flight Path Recording System**

Type: Sony DXC-101  
Recorder: Panasonic AG 2400 or Panasonic AG-720  
Format: NTSC (VHS)

Fiducial numbers are recorded continuously and are displayed on the margin of each image. This procedure ensures accurate correlation of data with respect to visible features on the ground.



## 4. QUALITY CONTROL AND IN-FIELD PROCESSING

Digital data for each flight were transferred to the field workstation, in order to verify data quality and completeness. A database was created and updated using Geosoft Oasis Montaj and proprietary Fugro Atlas software. This allowed the field personnel to calculate, display and verify both the positional (flight path) and geophysical data on the field computer screen. Records were examined as a preliminary assessment of the data acquired for each flight.

In-field processing of Fugro survey data consists of differential corrections to the airborne GPS data, spike rejection and filtering of all geophysical and ancillary data, verification of flight videos, diurnal correction, and preliminary leveling of magnetic data.

All data, including base station records, were checked on a daily basis, to ensure compliance with the survey contract specifications. Reflights were required if any of the following specifications were not met.

- Navigation - Positional (x,y) accuracy of better than 10 m, with a CEP (circular error of probability) of 95%.
  
- Flight Path - No lines to exceed  $\pm 25\%$  departure from planned flight path over a continuous distance of more than 1 km, except for reasons of safety.

- Clearance - Mean terrain sensor clearance of 60 m, except where precluded by safety considerations, e.g., restricted or populated areas, severe topography, obstructions, tree canopy, aerodynamic limitations, etc.
  
- Airborne Mag - Figure of Merit for the magnetometer not to exceed 2.0 nT. None-normalized 4<sup>th</sup> difference not to exceed 1.6 nT over a continuous distance of 1 km excluding areas where this specification is exceeded due to natural anomalies
  
- Base Mag - Diurnal variations not to exceed 10 nT over a straight line time chord of 1 minute.

## **5. DATA PROCESSING**

### **Flight Path Recovery**

The raw range data from at least four satellites are simultaneously recorded by both the base and mobile GPS units. The geographic positions of both units, relative to the model ellipsoid, are calculated from this information. Differential corrections, which are obtained from the base station, are applied to the mobile unit data to provide a post-flight track of the aircraft, accurate to within 2 m. Speed checks of the flight path are also carried out to determine if there are any spikes or gaps in the data.

The corrected WGS84 latitude/longitude coordinates are transformed to the coordinate system used on the final maps. Images or plots are then created to provide a visual check of the flight path.

### **Total Magnetic Field**

A fourth difference editing routine is applied to the magnetic data to remove any spikes.

The aeromagnetic data is corrected for diurnal variation using the magnetic base station data. The results are then leveled using tie and traverse line intercepts. Manual adjustments are applied to any lines that required leveling, as indicated by shadowed

images of the gridded magnetic data. The manually leveled data are then subjected to a microleveling filter.

## **Calculated Vertical Magnetic Gradient**

The diurnally corrected total magnetic field data is subjected to a processing algorithm that enhances the response of magnetic bodies in the upper 500 m and attenuates the response of deeper bodies. The resulting vertical gradient map provides better definition and resolution of near-surface magnetic units. It also identifies weak magnetic features that may not be evident on the total field map. However, regional magnetic variations and changes in lithology may be better defined on the total magnetic field map.

## **Digital Elevation**

The radar altimeter values (ALTR – aircraft to ground clearance) are subtracted from the differentially corrected and de-spiked GPS-Z values to produce profiles of the height above the ellipsoid along the survey lines. These values are gridded to produce contour maps showing approximate elevations within the survey area. The calculated digital terrain data are then tie-line leveled and adjusted to mean sea level. Any remaining subtle

line-to-line discrepancies are manually removed. After the manual corrections are applied, the digital terrain data are filtered with a microleveling algorithm.

The accuracy of the elevation calculation is directly dependent on the accuracy of the two input parameters, ALTR and GPS-Z. The ALTR value may be erroneous in areas of heavy tree cover, where the altimeter reflects the distance to the tree canopy rather than the ground. The GPS-Z value is primarily dependent on the number of available satellites.

Although post-processing of GPS data will yield X and Y accuracies in the order of 1-2 metres, the accuracy of the Z value is usually much less, sometimes in the  $\pm 10$  metre range. Further inaccuracies may be introduced during the interpolation and gridding process.

Because of the inherent inaccuracies of this method, no guarantee is made or implied that the information displayed is a true representation of the height above sea level. Although this product may be of some use as a general reference, THIS PRODUCT MUST NOT BE USED FOR NAVIGATION PURPOSES.

## **Contour, Colour and Shadow Map Displays**

The geophysical data are interpolated onto a regular grid using a modified Akima spline technique. The resulting grid is suitable for image processing and generation of contour maps. The grid cell size is 20% of the line interval.

Colour maps are produced by interpolating the grid down to the pixel size. The parameter is then incremented with respect to specific amplitude ranges to provide colour "contour" maps.

Monochromatic shadow maps or images are generated by employing an artificial sun to cast shadows on a surface defined by the geophysical grid. There are many variations in the shadowing technique. These techniques can be applied to total field or enhanced magnetic data, magnetic derivatives, resistivity, etc. The shadowing technique is also used as a quality control method to detect subtle changes between lines.



## 6. PRODUCTS

This section lists the final maps and products that have been provided under the terms of the survey agreement. Other products can be prepared from the existing dataset, if requested.

### Base Maps

Base maps of the survey area were produced (from digital topography (.dxf files) supplied by Fugro Airborne Surveys by scanning published topographic maps to a bitmap (.bmp) format. This process provides a relatively accurate, distortion-free base that facilitates correlation of the navigation data to the map coordinate system. The topographic files were combined with geophysical data for plotting the final maps. All maps were created using the following parameters:

#### Projection Description:

Datum:	NAD 83
Ellipsoid:	GRS 1980
Projection:	UTM (Zone: 10 N)
Central Meridian:	123° W
False Northing:	0
False Easting:	500000
Scale Factor:	0.9996
WGS84 to Local Conversion:	Molodensky
Datum Shifts:	DX: 0    DY: 0    DZ: 0

The following parameters are presented on 1 map sheet at a scale of 1:20 000. All maps

include flight lines and topography, unless otherwise indicated. Preliminary products are not listed.

## Final Products

	No. of Map Sets		
	Mylar	Blackline	Colour
Total Magnetic Field			2
Calculated Vertical Magnetic Gradient			2

### Additional Products

Digital Archive (see Archive Description)  
Survey Report  
Flight Path Video (VHS)

1 CD-ROM  
2 paper copies, 1 PDF  
5 VHS cassettes

## **7. SURVEY RESULTS**

### **General Discussion**

A Fugro CF-1 cesium vapour magnetometer was operated at the survey base to record diurnal variations of the earth's magnetic field. The clock of the base station was synchronized with that of the airborne system to permit subsequent removal of diurnal drift. Base level of 54640 nT was used for diurnal removal processing.

The total magnetic field data have been presented as contours on the base map using a contour interval of 5 nT where gradients permit. (Enhanced total magnetic field maps have also been prepared, using the measured horizontal gradient.) The map(s) show(s) the magnetic properties of the rock units underlying the survey area(s).

The total magnetic field data have been subjected to a processing algorithm to produce maps of the calculated vertical gradient. This procedure enhances near-surface magnetic units and suppresses regional gradients. It also provides better definition and resolution of magnetic units and displays weak magnetic features that may not be clearly evident on the total field maps.

There is some evidence on the magnetic map(s) that suggests that the survey area(s) has (have) been subjected to deformation and/or alteration. These structural complexities are

evident on the contour maps as variations in magnetic intensity, irregular patterns, and as offsets or changes in strike direction.

If a specific magnetic intensity can be assigned to the rock type that is believed to host the target mineralization, it may be possible to select areas of higher priority on the basis of the total field magnetic data. This is based on the assumption that the magnetite content of the host rocks will give rise to a limited range of contour values that will permit differentiation of various lithological units.

The magnetic results, in conjunction with the other geophysical parameters, have provided valuable information that can be used to effectively map the geology and structure in the survey area(s).

## **8. CONCLUSIONS AND RECOMMENDATIONS**

This report provides a very brief description of the survey results and describes the equipment, data processing procedures and logistics of the survey.

It is also recommended that image processing of existing geophysical data be considered, in order to extract the maximum amount of information from the survey results. Current software and imaging techniques often provide valuable information on structure and lithology, which may not be clearly evident on the contour and colour maps. These techniques can yield images that define subtle, but significant, structural details.

Respectfully submitted,

**FUGRO AIRBORNE SURVEYS CORP.**

Igor Sram  
Geophysicist

IS/sdp

R06051JUL.06

## APPENDIX A

### LIST OF PERSONNEL

The following personnel were involved in the acquisition, processing, interpretation and presentation of data, relating to a HM1 airborne geophysical survey carried out for Emerald Fields Resource Corp., near Port Renfrew, British Columbia.

David Miles	Manager, Helicopter Operations
Emily Farquhar	Manager, Data Processing and Interpretation
Amit Praharaj	Geophysical Operator
Sheli Droszio	Field Geophysicist
Terry Thomson	Helicopter Pilot
Ed Howell	Helicopter AME
Amir H. Soltanzadeh	Geophysical Data Processor
Igor Sram	Geophysical Data Processor
Lyn Vanderstarren	Drafting Supervisor
Susan Pothiah	Word Processing Operator
Albina Tonello	Secretary/Expeditior

The survey consisted of 1848.9 km of coverage, flown from June 12 to June 18, 2006.

All personnel are employees of Fugro Airborne Surveys, except for the pilot and engineer who are employees of Questral Helicopters Ltd.

---

**APPENDIX B**

**BACKGROUND INFORMATION**

---

## BACKGROUND INFORMATION

### Electromagnetics

Fugro electromagnetic responses fall into two general classes, discrete and broad. The discrete class consists of sharp, well-defined anomalies from discrete conductors such as sulphide lenses and steeply dipping sheets of graphite and sulphides. The broad class consists of wide anomalies from conductors having a large horizontal surface such as flatly dipping graphite or sulphide sheets, saline water-saturated sedimentary formations, conductive overburden and rock, kimberlite pipes and geothermal zones. A vertical conductive slab with a width of 200 m would straddle these two classes.

The vertical sheet (half plane) is the most common model used for the analysis of discrete conductors. All anomalies plotted on the geophysical maps are analyzed according to this model. The following section entitled **Discrete Conductor Analysis** describes this model in detail, including the effect of using it on anomalies caused by broad conductors such as conductive overburden.

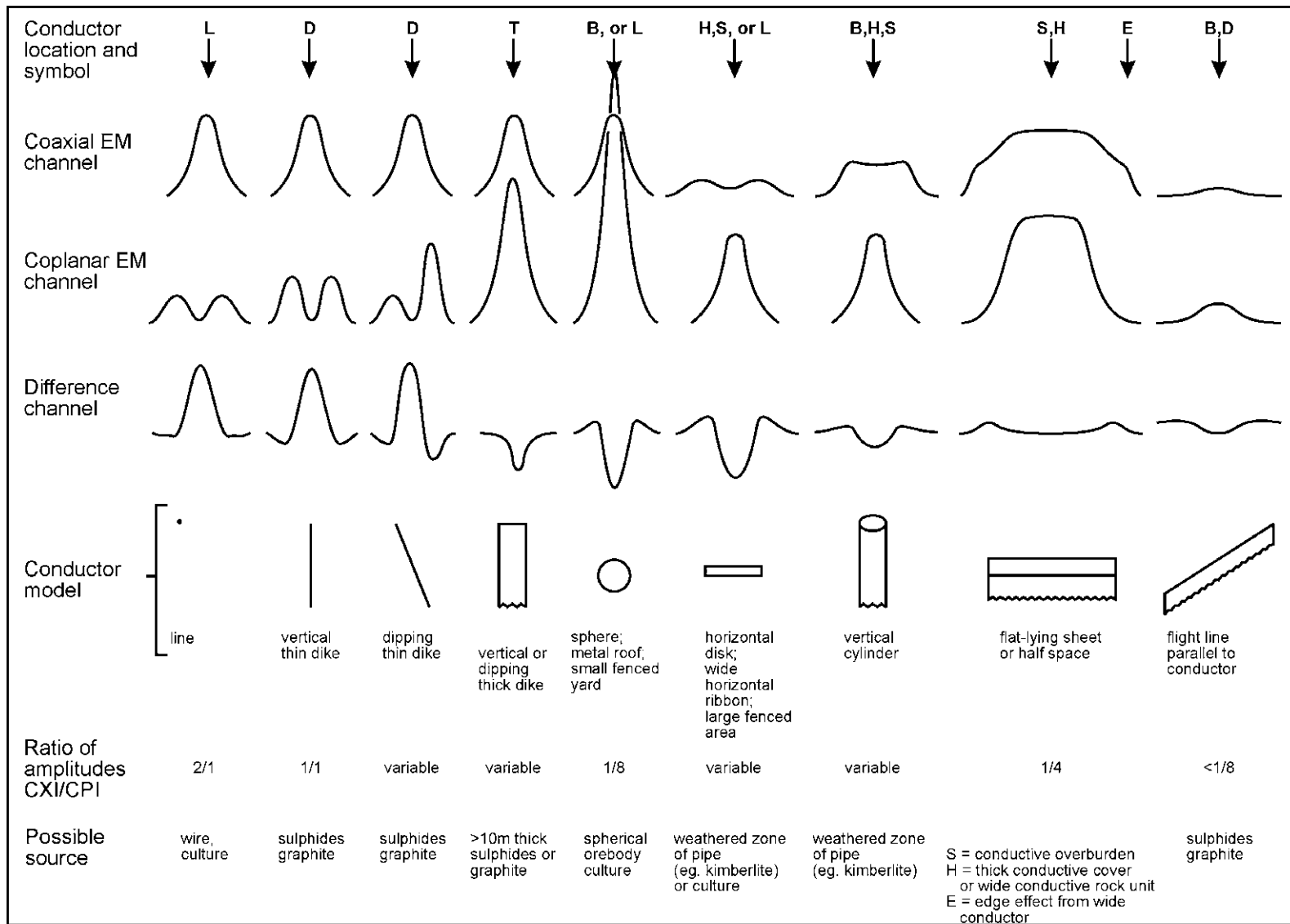
The conductive earth (half-space) model is suitable for broad conductors. Resistivity contour maps result from the use of this model. A later section entitled **Resistivity Mapping** describes the method further, including the effect of using it on anomalies caused by discrete conductors such as sulphide bodies.

### Geometric Interpretation

The geophysical interpreter attempts to determine the geometric shape and dip of the conductor. Figure C-1 shows typical HEM anomaly shapes which are used to guide the geometric interpretation.

### Discrete Conductor Analysis

The EM anomalies appearing on the electromagnetic map are analyzed by computer to give the conductance (i.e., conductivity-thickness product) in siemens (mhos) of a vertical sheet model. This is done regardless of the interpreted geometric shape of the conductor. This is not an unreasonable procedure, because the computed conductance increases as the electrical quality of the conductor increases, regardless of its true shape. DIGHEM anomalies are divided into seven grades of conductance, as shown in Table C-1. The conductance in siemens (mhos) is the reciprocal of resistance in ohms.



Typical HEM anomaly shapes

Figure C-1

- Appendix B.3 -

The conductance value is a geological parameter because it is a characteristic of the conductor alone. It generally is independent of frequency, flying height or depth of burial, apart from the averaging over a greater portion of the conductor as height increases. Small anomalies from deeply buried strong conductors are not confused with small anomalies from shallow weak conductors because the former will have larger conductance values.

**Table C-1. EM Anomaly Grades**

Anomaly Grade	Siemens
7	> 100
6	50 - 100
5	20 - 50
4	10 - 20
3	5 - 10
2	1 - 5
1	< 1

Conductive overburden generally produces broad EM responses which may not be shown as anomalies on the geophysical maps. However, patchy conductive overburden in otherwise resistive areas can yield discrete anomalies with a conductance grade (cf. Table C-1) of 1, 2 or even 3 for conducting clays which have resistivities as low as 50 ohm-m. In areas where ground resistivities are below 10 ohm-m, anomalies caused by weathering variations and similar causes can have any conductance grade. The anomaly shapes from the multiple coils often allow such conductors to be recognized, and these are indicated by the letters S, H, and sometimes E on the geophysical maps (see EM legend on maps).

For bedrock conductors, the higher anomaly grades indicate increasingly higher conductances. Examples: the New Inco copper discovery (Noranda, Canada) yielded a grade 5 anomaly, as did the neighbouring copper-zinc Magusi River ore body; Mattabi (copper-zinc, Sturgeon Lake, Canada) and Whistle (nickel, Sudbury, Canada) gave grade 6; and the Montcalm nickel-copper discovery (Timmins, Canada) yielded a grade 7 anomaly. Graphite and sulphides can span all grades but, in any particular survey area, field work may show that the different grades indicate different types of conductors.

Strong conductors (i.e., grades 6 and 7) are characteristic of massive sulphides or graphite. Moderate conductors (grades 4 and 5) typically reflect graphite or sulphides of a less massive character, while weak bedrock conductors (grades 1 to 3) can signify poorly connected graphite or heavily disseminated sulphides. Grades 1 and 2 conductors may not respond to ground EM equipment using frequencies less than 2000 Hz.

The presence of sphalerite or gangue can result in ore deposits having weak to moderate conductances. As an example, the three million ton lead-zinc deposit of Restigouche

- Appendix B.4 -

Mining Corporation near Bathurst, Canada, yielded a well-defined grade 2 conductor. The 10 percent by volume of sphalerite occurs as a coating around the fine grained massive pyrite, thereby inhibiting electrical conduction. Faults, fractures and shear zones may produce anomalies that typically have low conductances (e.g., grades 1 to 3). Conductive rock formations can yield anomalies of any conductance grade. The conductive materials in such rock formations can be salt water, weathered products such as clays, original depositional clays, and carbonaceous material.

For each interpreted electromagnetic anomaly on the geophysical maps, a letter identifier and an interpretive symbol are plotted beside the EM grade symbol. The horizontal rows of dots, under the interpretive symbol, indicate the anomaly amplitude on the flight record. The vertical column of dots, under the anomaly letter, gives the estimated depth. In areas where anomalies are crowded, the letter identifiers, interpretive symbols and dots may be obliterated. The EM grade symbols, however, will always be discernible, and the obliterated information can be obtained from the anomaly listing appended to this report.

The purpose of indicating the anomaly amplitude by dots is to provide an estimate of the reliability of the conductance calculation. Thus, a conductance value obtained from a large ppm anomaly (3 or 4 dots) will tend to be accurate whereas one obtained from a small ppm anomaly (no dots) could be quite inaccurate. The absence of amplitude dots indicates that the anomaly from the coaxial coil-pair is 5 ppm or less on both the in-phase and quadrature channels. Such small anomalies could reflect a weak conductor at the surface or a stronger conductor at depth. The conductance grade and depth estimate illustrates which of these possibilities fits the recorded data best.

The conductance measurement is considered more reliable than the depth estimate. There are a number of factors that can produce an error in the depth estimate, including the averaging of topographic variations by the altimeter, overlying conductive overburden, and the location and attitude of the conductor relative to the flight line. Conductor location and attitude can provide an erroneous depth estimate because the stronger part of the conductor may be deeper or to one side of the flight line, or because it has a shallow dip. A heavy tree cover can also produce errors in depth estimates. This is because the depth estimate is computed as the distance of bird from conductor, minus the altimeter reading. The altimeter can lock onto the top of a dense forest canopy. This situation yields an erroneously large depth estimate but does not affect the conductance estimate.

Dip symbols are used to indicate the direction of dip of conductors. These symbols are used only when the anomaly shapes are unambiguous, which usually requires a fairly resistive environment.

A further interpretation is presented on the EM map by means of the line-to-line correlation of bedrock anomalies, which is based on a comparison of anomaly shapes on adjacent lines. This provides conductor axes that may define the geological structure over portions of the survey area. The absence of conductor axes in an area implies that anomalies could not be correlated from line to line with reasonable confidence.

## - Appendix B.5 -

The electromagnetic anomalies are designed to provide a correct impression of conductor quality by means of the conductance grade symbols. The symbols can stand alone with geology when planning a follow-up program. The actual conductance values are printed in the attached anomaly list for those who wish quantitative data. The anomaly ppm and depth are indicated by inconspicuous dots which should not distract from the conductor patterns, while being helpful to those who wish this information. The map provides an interpretation of conductors in terms of length, strike and dip, geometric shape, conductance, depth, and thickness. The accuracy is comparable to an interpretation from a high quality ground EM survey having the same line spacing.

The appended EM anomaly list provides a tabulation of anomalies in ppm, conductance, and depth for the vertical sheet model. No conductance or depth estimates are shown for weak anomalous responses that are not of sufficient amplitude to yield reliable calculations.

Since discrete bodies normally are the targets of EM surveys, local base (or zero) levels are used to compute local anomaly amplitudes. This contrasts with the use of true zero levels which are used to compute true EM amplitudes. Local anomaly amplitudes are shown in the EM anomaly list and these are used to compute the vertical sheet parameters of conductance and depth.

### **Questionable Anomalies**

The EM maps may contain anomalous responses that are displayed as asterisks (\*). These responses denote weak anomalies of indeterminate conductance, which may reflect one of the following: a weak conductor near the surface, a strong conductor at depth (e.g., 100 to 120 m below surface) or to one side of the flight line, or aerodynamic noise. Those responses that have the appearance of valid bedrock anomalies on the flight profiles are indicated by appropriate interpretive symbols (see EM legend on maps). The others probably do not warrant further investigation unless their locations are of considerable geological interest.

### **The Thickness Parameter**

A comparison of coaxial and coplanar shapes can provide an indication of the thickness of a steeply dipping conductor. The amplitude of the coplanar anomaly (e.g., CPI channel) increases relative to the coaxial anomaly (e.g., CXI) as the apparent thickness increases, i.e., the thickness in the horizontal plane. (The thickness is equal to the conductor width if the conductor dips at 90 degrees and strikes at right angles to the flight line.) This report refers to a conductor as thin when the thickness is likely to be less than 3 m, and thick when in excess of 10 m. Thick conductors are indicated on the EM map by parentheses "( )". For base metal exploration in steeply dipping geology, thick conductors can be high priority targets because many massive sulphide ore bodies are thick. The system cannot

sense the thickness when the strike of the conductor is subparallel to the flight line, when the conductor has a shallow dip, when the anomaly amplitudes are small, or when the resistivity of the environment is below 100 ohm-m.

## Resistivity Mapping

Resistivity mapping is useful in areas where broad or flat lying conductive units are of interest. One example of this is the clay alteration which is associated with Carlin-type deposits in the south west United States. The resistivity parameter was able to identify the clay alteration zone over the Cove deposit. The alteration zone appeared as a strong resistivity low on the 900 Hz resistivity parameter. The 7,200 Hz and 56,000 Hz resistivities showed more detail in the covering sediments, and delineated a range front fault. This is typical in many areas of the south west United States, where conductive near surface sediments, which may sometimes be alkalic, attenuate the higher frequencies.

Resistivity mapping has proven successful for locating diatremes in diamond exploration. Weathering products from relatively soft kimberlite pipes produce a resistivity contrast with the unaltered host rock. In many cases weathered kimberlite pipes were associated with thick conductive layers that contrasted with overlying or adjacent relatively thin layers of lake bottom sediments or overburden.

Areas of widespread conductivity are commonly encountered during surveys. These conductive zones may reflect alteration zones, shallow-dipping sulphide or graphite-rich units, saline ground water, or conductive overburden. In such areas, EM amplitude changes can be generated by decreases of only 5 m in survey altitude, as well as by increases in conductivity. The typical flight record in conductive areas is characterized by in-phase and quadrature channels that are continuously active. Local EM peaks reflect either increases in conductivity of the earth or decreases in survey altitude. For such conductive areas, apparent resistivity profiles and contour maps are necessary for the correct interpretation of the airborne data. The advantage of the resistivity parameter is that anomalies caused by altitude changes are virtually eliminated, so the resistivity data reflect only those anomalies caused by conductivity changes. The resistivity analysis also helps the interpreter to differentiate between conductive bedrock and conductive overburden. For example, discrete conductors will generally appear as narrow lows on the contour map and broad conductors (e.g., overburden) will appear as wide lows.

The apparent resistivity is calculated using the pseudo-layer (or buried) half-space model defined by Fraser (1978)<sup>1</sup>. This model consists of a resistive layer overlying a conductive

---

<sup>1</sup> Resistivity mapping with an airborne multicoil electromagnetic system: Geophysics, v. 43, p.144-172

## - Appendix B.7 -

half-space. The depth channels give the apparent depth below surface of the conductive material. The apparent depth is simply the apparent thickness of the overlying resistive layer. The apparent depth (or thickness) parameter will be positive when the upper layer is more resistive than the underlying material, in which case the apparent depth may be quite close to the true depth.

The apparent depth will be negative when the upper layer is more conductive than the underlying material, and will be zero when a homogeneous half-space exists. The apparent depth parameter must be interpreted cautiously because it will contain any errors that might exist in the measured altitude of the EM bird (e.g., as caused by a dense tree cover). The inputs to the resistivity algorithm are the in-phase and quadrature components of the coplanar coil-pair. The outputs are the apparent resistivity of the conductive half-space (the source) and the sensor-source distance. The flying height is not an input variable, and the output resistivity and sensor-source distance are independent of the flying height when the conductivity of the measured material is sufficient to yield significant in-phase as well as quadrature responses. The apparent depth, discussed above, is simply the sensor-source distance minus the measured altitude or flying height. Consequently, errors in the measured altitude will affect the apparent depth parameter but not the apparent resistivity parameter.

The apparent depth parameter is a useful indicator of simple layering in areas lacking a heavy tree cover. Depth information has been used for permafrost mapping, where positive apparent depths were used as a measure of permafrost thickness. However, little quantitative use has been made of negative apparent depths because the absolute value of the negative depth is not a measure of the thickness of the conductive upper layer and, therefore, is not meaningful physically. Qualitatively, a negative apparent depth estimate usually shows that the EM anomaly is caused by conductive overburden. Consequently, the apparent depth channel can be of significant help in distinguishing between overburden and bedrock conductors.

### **Interpretation in Conductive Environments**

Environments having low background resistivities (e.g., below 30 ohm-m for a 900 Hz system) yield very large responses from the conductive ground. This usually prohibits the recognition of discrete bedrock conductors. However, Fugro data processing techniques produce three parameters that contribute significantly to the recognition of bedrock conductors in conductive environments. These are the in-phase and quadrature difference channels (DIFI and DIFQ, which are available only on systems with "common" frequencies on orthogonal coil pairs), and the resistivity and depth channels (RES and DEP) for each coplanar frequency.

The EM difference channels (DIFI and DIFQ) eliminate most of the responses from conductive ground, leaving responses from bedrock conductors, cultural features (e.g., telephone lines, fences, etc.) and edge effects. Edge effects often occur near the

perimeter of broad conductive zones. This can be a source of geologic noise. While edge effects yield anomalies on the EM difference channels, they do not produce resistivity anomalies. Consequently, the resistivity channel aids in eliminating anomalies due to edge effects. On the other hand, resistivity anomalies will coincide with the most highly conductive sections of conductive ground, and this is another source of geologic noise. The recognition of a bedrock conductor in a conductive environment therefore is based on the anomalous responses of the two difference channels (DIFI and DIFQ) and the resistivity channels (RES). The most favourable situation is where anomalies coincide on all channels.

The DEP channels, which give the apparent depth to the conductive material, also help to determine whether a conductive response arises from surficial material or from a conductive zone in the bedrock. When these channels ride above the zero level on the depth profiles (i.e., depth is negative), it implies that the EM and resistivity profiles are responding primarily to a conductive upper layer, i.e., conductive overburden. If the DEP channels are below the zero level, it indicates that a resistive upper layer exists, and this usually implies the existence of a bedrock conductor. If the low frequency DEP channel is below the zero level and the high frequency DEP is above, this suggests that a bedrock conductor occurs beneath conductive cover.

## **Reduction of Geologic Noise**

Geologic noise refers to unwanted geophysical responses. For purposes of airborne EM surveying, geologic noise refers to EM responses caused by conductive overburden and magnetic permeability. It was mentioned previously that the EM difference channels (i.e., channel DIFI for in-phase and DIFQ for quadrature) tend to eliminate the response of conductive overburden.

Magnetite produces a form of geological noise on the in-phase channels. Rocks containing less than 1% magnetite can yield negative in-phase anomalies caused by magnetic permeability. When magnetite is widely distributed throughout a survey area, the in-phase EM channels may continuously rise and fall, reflecting variations in the magnetite percentage, flying height, and overburden thickness. This can lead to difficulties in recognizing deeply buried bedrock conductors, particularly if conductive overburden also exists. However, the response of broadly distributed magnetite generally vanishes on the in-phase difference channel DIFI. This feature can be a significant aid in the recognition of conductors that occur in rocks containing accessory magnetite.

## **EM Magnetite Mapping**

The information content of HEM data consists of a combination of conductive eddy current responses and magnetic permeability responses. The secondary field resulting from conductive eddy current flow is frequency-dependent and consists of both in-phase and quadrature components, which are positive in sign. On the other hand, the secondary field

resulting from magnetic permeability is independent of frequency and consists of only an in-phase component which is negative in sign. When magnetic permeability manifests itself by decreasing the measured amount of positive in-phase, its presence may be difficult to recognize. However, when it manifests itself by yielding a negative in-phase anomaly (e.g., in the absence of eddy current flow), its presence is assured. In this latter case, the negative component can be used to estimate the percent magnetite content.

A magnetite mapping technique, based on the low frequency coplanar data, can be complementary to magnetometer mapping in certain cases. Compared to magnetometry, it is far less sensitive but is more able to resolve closely spaced magnetite zones, as well as providing an estimate of the amount of magnetite in the rock. The method is sensitive to 1/4% magnetite by weight when the EM sensor is at a height of 30 m above a magnetitic half-space. It can individually resolve steep dipping narrow magnetite-rich bands which are separated by 60 m. Unlike magnetometry, the EM magnetite method is unaffected by remanent magnetism or magnetic latitude.

The EM magnetite mapping technique provides estimates of magnetite content which are usually correct within a factor of 2 when the magnetite is fairly uniformly distributed. EM magnetite maps can be generated when magnetic permeability is evident as negative in-phase responses on the data profiles.

Like magnetometry, the EM magnetite method maps only bedrock features, provided that the overburden is characterized by a general lack of magnetite. This contrasts with resistivity mapping which portrays the combined effect of bedrock and overburden.

## **The Susceptibility Effect**

When the host rock is conductive, the positive conductivity response will usually dominate the secondary field, and the susceptibility effect<sup>2</sup> will appear as a reduction in the in-phase, rather than as a negative value. The in-phase response will be lower than would be predicted by a model using zero susceptibility. At higher frequencies the in-phase conductivity response also gets larger, so a negative magnetite effect observed on the low frequency might not be observable on the higher frequencies, over the same body. The susceptibility effect is most obvious over discrete magnetite-rich zones, but also occurs over uniform geology such as a homogeneous half-space.

---

<sup>2</sup> Magnetic susceptibility and permeability are two measures of the same physical property. Permeability is generally given as relative permeability,  $\mu_r$ , which is the permeability of the substance divided by the permeability of free space ( $4 \pi \times 10^{-7}$ ). Magnetic susceptibility  $k$  is related to permeability by  $k = \mu_r - 1$ . Susceptibility is a unitless measurement, and is usually reported in units of  $10^{-6}$ . The typical range of susceptibilities is  $-1$  for quartz,  $130$  for pyrite, and up to  $5 \times 10^5$  for magnetite, in  $10^{-6}$  units (Telford et al, 1986).

High magnetic susceptibility will affect the calculated apparent resistivity, if only conductivity is considered. Standard apparent resistivity algorithms use a homogeneous half-space model, with zero susceptibility. For these algorithms, the reduced in-phase response will, in most cases, make the apparent resistivity higher than it should be. It is important to note that there is nothing wrong with the data, nor is there anything wrong with the processing algorithms. The apparent difference results from the fact that the simple geological model used in processing does not match the complex geology.

## **Measuring and Correcting the Magnetite Effect**

Theoretically, it is possible to calculate (forward model) the combined effect of electrical conductivity and magnetic susceptibility on an EM response in all environments. The difficulty lies, however, in separating out the susceptibility effect from other geological effects when deriving resistivity and susceptibility from EM data.

Over a homogeneous half-space, there is a precise relationship between in-phase, quadrature, and altitude. These are often resolved as phase angle, amplitude, and altitude. Within a reasonable range, any two of these three parameters can be used to calculate the half space resistivity. If the rock has a positive magnetic susceptibility, the in-phase component will be reduced and this departure can be recognized by comparison to the other parameters.

The algorithm used to calculate apparent susceptibility and apparent resistivity from HEM data, uses a homogeneous half-space geological model. Non half-space geology, such as horizontal layers or dipping sources, can also distort the perfect half-space relationship of the three data parameters. While it may be possible to use more complex models to calculate both rock parameters, this procedure becomes very complex and time-consuming. For basic HEM data processing, it is most practical to stick to the simplest geological model.

Magnetite reversals (reversed in-phase anomalies) have been used for many years to calculate an "FeO" or magnetite response from HEM data (Fraser, 1981). However, this technique could only be applied to data where the in-phase was observed to be negative, which happens when susceptibility is high and conductivity is low.

## **Applying Susceptibility Corrections**

Resistivity calculations done with susceptibility correction may change the apparent resistivity. High-susceptibility conductors, that were previously masked by the susceptibility effect in standard resistivity algorithms, may become evident. In this case the susceptibility corrected apparent resistivity is a better measure of the actual resistivity of the earth. However, other geological variations, such as a deep resistive layer, can also reduce the in-phase by the same amount. In this case, susceptibility correction would not be the best method. Different geological models can apply in different areas of the same

data set. The effects of susceptibility, and other effects that can create a similar response, must be considered when selecting the resistivity algorithm.

## Susceptibility from EM vs Magnetic Field Data

The response of the EM system to magnetite may not match that from a magnetometer survey. First, HEM-derived susceptibility is a rock property measurement, like resistivity. Magnetic data show the total magnetic field, a measure of the potential field, not the rock property. Secondly, the shape of an anomaly depends on the shape and direction of the source magnetic field. The electromagnetic field of HEM is much different in shape from the earth's magnetic field. Total field magnetic anomalies are different at different magnetic latitudes; HEM susceptibility anomalies have the same shape regardless of their location on the earth.

In far northern latitudes, where the magnetic field is nearly vertical, the total magnetic field measurement over a thin vertical dike is very similar in shape to the anomaly from the HEM-derived susceptibility (a sharp peak over the body). The same vertical dike at the magnetic equator would yield a negative magnetic anomaly, but the HEM susceptibility anomaly would show a positive susceptibility peak.

## Effects of Permeability and Dielectric Permittivity

Resistivity algorithms that assume free-space magnetic permeability and dielectric permittivity, do not yield reliable values in highly magnetic or highly resistive areas. Both magnetic polarization and displacement currents cause a decrease in the in-phase component, often resulting in negative values that yield erroneously high apparent resistivities. The effects of magnetite occur at all frequencies, but are most evident at the lowest frequency. Conversely, the negative effects of dielectric permittivity are most evident at the higher frequencies, in resistive areas.

The table below shows the effects of varying permittivity over a resistive (10,000 ohm-m) half space, at frequencies of 56,000 Hz (DIGHEM<sup>V</sup>) and 102,000 Hz (RESOLVE).

### Apparent Resistivity Calculations Effects of Permittivity on In-phase/Quadrature/Resistivity

Freq (Hz)	Coil	Sep (m)	Thres (ppm)	Alt (m)	In Phase	Quad Phase	App Res	App Depth (m)	Permittivity
56,000	CP	6.3	0.1	30	7.3	35.3	10118	-1.0	1 Air
56,000	CP	6.3	0.1	30	3.6	36.6	19838	-13.2	5 Quartz
56,000	CP	6.3	0.1	30	-1.1	38.3	81832	-25.7	10 Epidote
56,000	CP	6.3	0.1	30	-10.4	42.3	76620	-25.8	20 Granite
56,000	CP	6.3	0.1	30	-19.7	46.9	71550	-26.0	30 Diabase

- Appendix B.12 -

56,000	CP	6.3	0.1	30	-28.7	52.0	66787	-26.1	40 Gabbro
102,000	CP	7.86	0.1	30	32.5	117.2	9409	-0.3	1 Air
102,000	CP	7.86	0.1	30	11.7	127.2	25956	-16.8	5 Quartz
102,000	CP	7.86	0.1	30	-14.0	141.6	97064	-26.5	10 Epidote
102,000	CP	7.86	0.1	30	-62.9	176.0	83995	-26.8	20 Granite
102,000	CP	7.86	0.1	30	-107.5	215.8	73320	-27.0	30 Diabase
102,000	CP	7.86	0.1	30	-147.1	259.2	64875	-27.2	40 Gabbro

Methods have been developed (Huang and Fraser, 2000, 2001) to correct apparent resistivities for the effects of permittivity and permeability. The corrected resistivities yield more credible values than if the effects of permittivity and permeability are disregarded.

### Recognition of Culture

Cultural responses include all EM anomalies caused by man-made metallic objects. Such anomalies may be caused by inductive coupling or current gathering. The concern of the interpreter is to recognize when an EM response is due to culture. Points of consideration used by the interpreter, when coaxial and coplanar coil-pairs are operated at a common frequency, are as follows:

1. Channels CXPL and CPPL monitor 60 Hz radiation. An anomaly on these channels shows that the conductor is radiating power. Such an indication is normally a guarantee that the conductor is cultural. However, care must be taken to ensure that the conductor is not a geologic body that strikes across a power line, carrying leakage currents.
2. A flight that crosses a "line" (e.g., fence, telephone line, etc.) yields a centre-peaked coaxial anomaly and an m-shaped coplanar anomaly.<sup>3</sup> When the flight crosses the cultural line at a high angle of intersection, the amplitude ratio of coaxial/coplanar response is 2. Such an EM anomaly can only be caused by a line. The geologic body that yields anomalies most closely resembling a line is the vertically dipping thin dike. Such a body, however, yields an amplitude ratio of 1 rather than 2. Consequently, an m-shaped coplanar anomaly with a CXI/CPI amplitude ratio of 2 is virtually a guarantee that the source is a cultural line.
3. A flight that crosses a sphere or horizontal disk yields centre-peaked coaxial and coplanar anomalies with a CXI/CPI amplitude ratio (i.e., coaxial/coplanar) of 1/8. In the absence of geologic bodies of this geometry, the most likely conductor is a

---

<sup>3</sup> See Figure C-1 presented earlier.

## - Appendix B.13 -

metal roof or small fenced yard.<sup>4</sup> Anomalies of this type are virtually certain to be cultural if they occur in an area of culture.

4. A flight that crosses a horizontal rectangular body or wide ribbon yields an m-shaped coaxial anomaly and a centre-peaked coplanar anomaly. In the absence of geologic bodies of this geometry, the most likely conductor is a large fenced area.<sup>5</sup> Anomalies of this type are virtually certain to be cultural if they occur in an area of culture.
5. EM anomalies that coincide with culture, as seen on the camera film or video display, are usually caused by culture. However, care is taken with such coincidences because a geologic conductor could occur beneath a fence, for example. In this example, the fence would be expected to yield an m-shaped coplanar anomaly as in case #2 above. If, instead, a centre-peaked coplanar anomaly occurred, there would be concern that a thick geologic conductor coincided with the cultural line.
6. The above description of anomaly shapes is valid when the culture is not conductively coupled to the environment. In this case, the anomalies arise from inductive coupling to the EM transmitter. However, when the environment is quite conductive (e.g., less than 100 ohm-m at 900 Hz), the cultural conductor may be conductively coupled to the environment. In this latter case, the anomaly shapes tend to be governed by current gathering. Current gathering can completely distort the anomaly shapes, thereby complicating the identification of cultural anomalies. In such circumstances, the interpreter can only rely on the radiation channels and on the camera film or video records.

## Magnetic Responses

The measured total magnetic field provides information on the magnetic properties of the earth materials in the survey area. The information can be used to locate magnetic bodies of direct interest for exploration, and for structural and lithological mapping.

The total magnetic field response reflects the abundance of magnetic material in the source. Magnetite is the most common magnetic mineral. Other minerals such as ilmenite, pyrrhotite, franklinite, chromite, hematite, arsenopyrite, limonite and pyrite are also magnetic, but to a lesser extent than magnetite on average.

---

<sup>4</sup> It is a characteristic of EM that geometrically similar anomalies are obtained from: (1) a planar conductor, and (2) a wire which forms a loop having dimensions identical to the perimeter of the equivalent planar conductor.

## - Appendix B.14 -

In some geological environments, an EM anomaly with magnetic correlation has a greater likelihood of being produced by sulphides than one which is non-magnetic. However, sulphide ore bodies may be non-magnetic (e.g., the Kidd Creek deposit near Timmins, Canada) as well as magnetic (e.g., the Mattabi deposit near Sturgeon Lake, Canada).

Iron ore deposits will be anomalously magnetic in comparison to surrounding rock due to the concentration of iron minerals such as magnetite, ilmenite and hematite.

Changes in magnetic susceptibility often allow rock units to be differentiated based on the total field magnetic response. Geophysical classifications may differ from geological classifications if various magnetite levels exist within one general geological classification. Geometric considerations of the source such as shape, dip and depth, inclination of the earth's field and remanent magnetization will complicate such an analysis.

In general, mafic lithologies contain more magnetite and are therefore more magnetic than many sediments which tend to be weakly magnetic. Metamorphism and alteration can also increase or decrease the magnetization of a rock unit.

Textural differences on a total field magnetic contour, colour or shadow map due to the frequency of activity of the magnetic parameter resulting from inhomogeneities in the distribution of magnetite within the rock, may define certain lithologies. For example, near surface volcanics may display highly complex contour patterns with little line-to-line correlation.

Rock units may be differentiated based on the plan shapes of their total field magnetic responses. Mafic intrusive plugs can appear as isolated "bulls-eye" anomalies. Granitic intrusives appear as sub-circular zones, and may have contrasting rings due to contact metamorphism. Generally, granitic terrain will lack a pronounced strike direction, although granite gneiss may display strike.

Linear north-south units are theoretically not well-defined on total field magnetic maps in equatorial regions due to the low inclination of the earth's magnetic field. However, most stratigraphic units will have variations in composition along strike that will cause the units to appear as a series of alternating magnetic highs and lows.

Faults and shear zones may be characterized by alteration that causes destruction of magnetite (e.g., weathering) that produces a contrast with surrounding rock. Structural breaks may be filled by magnetite-rich, fracture filling material as is the case with diabase dikes, or by non-magnetic felsic material.

Faulting can also be identified by patterns in the magnetic total field contours or colours. Faults and dikes tend to appear as lineaments and often have strike lengths of several kilometres. Offsets in narrow, magnetic, stratigraphic trends also delineate structure. Sharp contrasts in magnetic lithologies may arise due to large displacements along strike-slip or dip-slip faults.

## **Gamma Ray Spectrometry**

Radioelement concentrations are measures of the abundance of radioactive elements in the rock. The original abundance of the radioelements in any rock can be altered by the subsequent processes of metamorphism and weathering.

Gamma radiation in the range that is measured in the thorium, potassium, uranium and total count windows is strongly attenuated by rock, overburden and water. Almost all of the total radiation measured from rock and overburden originates in the upper .5 metres. Moisture in soil and bodies of water will mask the radioactivity from underlying rock. Weathered rock materials that have been displaced by glacial, water or wind action will not reflect the general composition of the underlying bedrock. Where residual soils exist, they may reflect the composition of underlying rock except where equilibrium does not exist between the original radioelement and the products in its decay series.

Radioelement counts (expressed as counts per second) are the rates of detection of the gamma radiation from specific decaying particles corresponding to products in each radioelements decay series. The radiation source for uranium is bismuth (Bi-214), for thorium it is thallium (Tl-208) and for potassium it is potassium (K-40).

The uranium and thorium radioelement concentrations are dependent on a state of equilibrium between the parent and daughter products in the decay series. Some daughter products in the uranium decay are long lived and could be removed by processes such as leaching. One product in the series, radon (Rn-222), is a gas which can easily escape. Both of these factors can affect the degree to which the calculated uranium concentrations reflect the actual composition of the source rock. Because the daughter products of thorium are relatively short lived, there is more likelihood that the thorium decay series is in equilibrium.

Lithological discrimination can be based on the measured relative concentrations and total, combined, radioactivity of the radioelements. Feldspar and mica contain potassium. Zircon, sphene and apatite are accessory minerals in igneous rocks that are sources of uranium and thorium. Monazite, thorianite, thorite, uraninite and uranothorite are also sources of uranium and thorium which are found in granites and pegmatites.

In general, the abundance of uranium, thorium and potassium in igneous rock increases with acidity. Pegmatites commonly have elevated concentrations of uranium relative to thorium. Sedimentary rocks derived from igneous rocks may have characteristic signatures that are influenced by their parent rocks, but these will have been altered by subsequent weathering and alteration.

Metamorphism and alteration will cause variations in the abundance of certain radioelements relative to each other. For example, alternative processes may cause

- Appendix B.16 -

uranium enrichment to the extent that a rock will be of economic interest. Uranium anomalies are more likely to be economically significant if they consist of an increase in the uranium relative to thorium and potassium, rather than a sympathetic increase in all three radioelements.

Faults can exhibit radioactive highs due to increased permeability which allows radon migration, or as lows due to structural control of drainage and fluvial sediments which attenuate gamma radiation from the underlying rocks. Faults can also be recognized by sharp contrasts in radiometric lithologies due to large strike-slip or dip-slip displacements. Changes in relative radioelement concentrations due to alteration will also define faults.

Similar to magnetics, certain rock types can be identified by their plan shapes if they also produce a radiometric contrast with surrounding rock. For example, granite intrusions will appear as sub-circular bodies, and may display concentric zonations. They will tend to lack a prominent strike direction. Offsets of narrow, continuous, stratigraphic units with contrasting radiometric signatures can identify faulting, and folding of stratigraphic trends will also be apparent.

---

**APPENDIX C**

**DATA ARCHIVE DESCRIPTION**

---

## APPENDIX C

### ARCHIVE DESCRIPTION

This CD-ROM contains final data archives of an airborne survey conducted by Fugro Airborne Surveys on behalf of Emerald Fields Resource Corp. in the Port Renfrew area, British Columbia from June 12 to June 18, 2006.

Fugro Job # 06051

The archives contain 3 directories.

1. XYZ: XYZ data in Geosoft format, along with format description.
2. Grids: Grids in Geosoft format for the following parameters:
  1. Total Magnetic Total Field
  2. Calculated Vertical Gradient
3. Report in PDF format

#### Projection Description:

Datum:	NAD 83
Ellipsoid:	GRS 1980
Projection:	UTM (Zone: 10 N)
Central Meridian:	123 ° West
False Northing:	0
False Easting:	500000
Scale Factor:	0.9996
WGS84-Local Conversion:	Molodensky
Datum Shifts:	DX: 0 DY: 0 DZ: 0

---

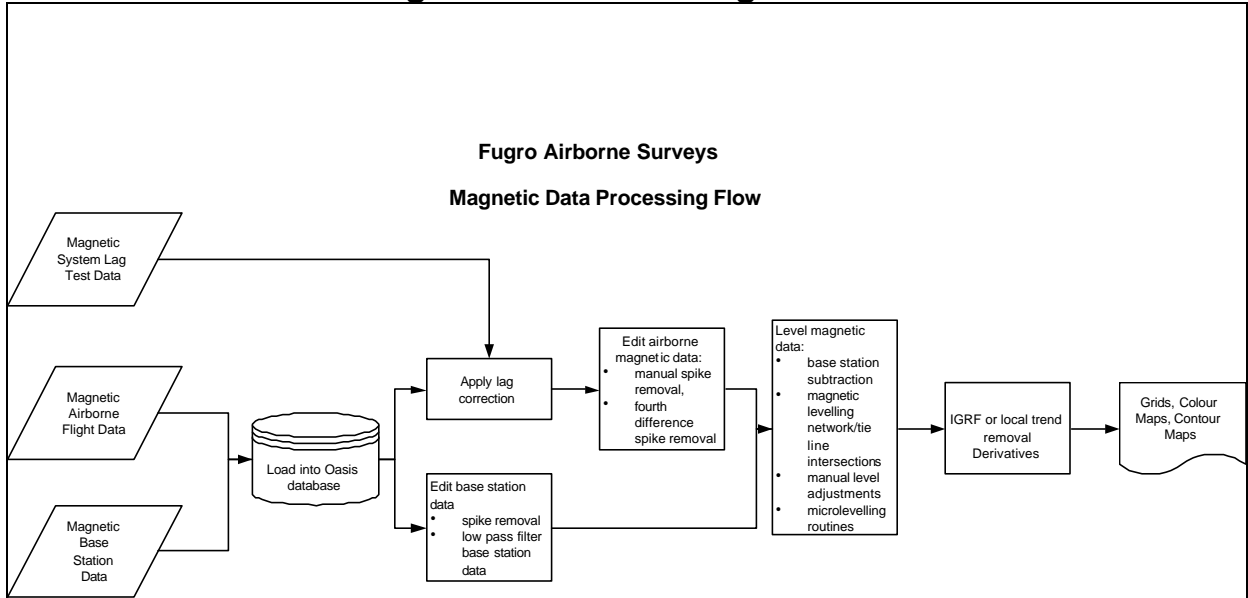
**APPENDIX D**

**DATA PROCESSING  
FLOWCHARTS**

---

# APPENDIX D

## Processing Flow Chart - Magnetic Data



---

**APPENDIX E**

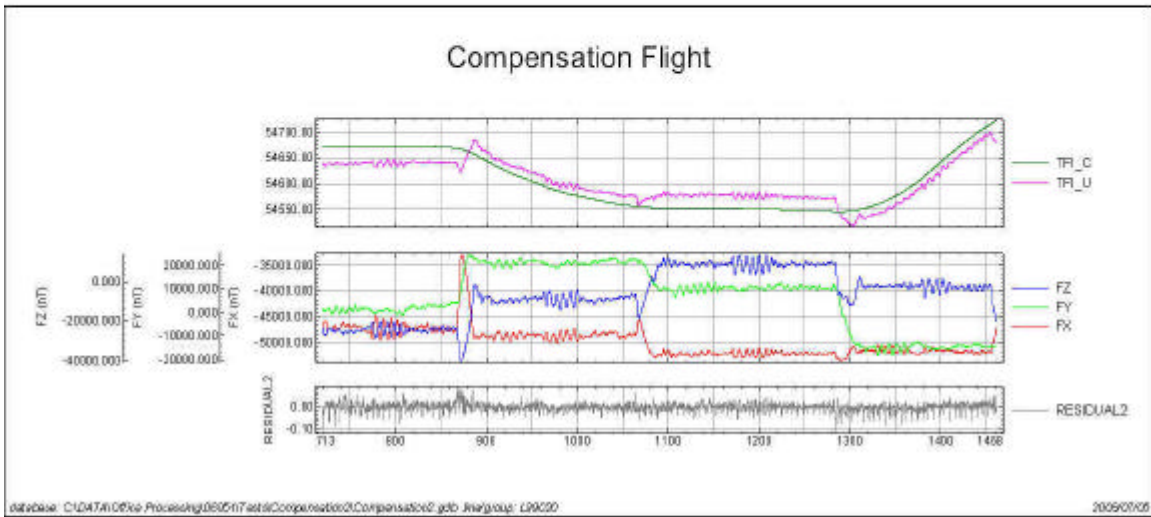
**TESTS AND CALIBRATIONS**

---

## Compensation Flight

Date Performed: June 11, 2006

Compensation flight was performed to determine compensation on the magnetic sensor due to the aircraft movement. By using this compensation, the magnetic effects from helicopter are removed. The Figure of Merit (FOM) is calculated by summing the amplitude of residual for each maneuver in all 4 directions of the survey. A value of 1.02 nT was calculated from the FOM and is acceptable. A graph of residual, fluxgate, compensated and un-compensated total magnetic field from the compensation flight is shown below.



---

**APPENDIX F**

**GLOSSARY**

---

## APPENDIX F

### GLOSSARY OF AIRBORNE GEOPHYSICAL TERMS

Note: The definitions given in this glossary refer to the common terminology as used in airborne geophysics.

**altitude attenuation:** the absorption of gamma rays by the atmosphere between the earth and the detector. The number of gamma rays detected by a system decreases as the altitude increases.

**apparent- :** the *physical parameters* of the earth measured by a geophysical system are normally expressed as apparent, as in “apparent *resistivity*”. This means that the measurement is limited by assumptions made about the geology in calculating the response measured by the geophysical system. Apparent resistivity calculated with *HEM*, for example, generally assumes that the earth is a *homogeneous half-space* – not layered.

**amplitude:** The strength of the total electromagnetic field. In *frequency domain* it is most often the sum of the squares of *in-phase* and *quadrature* components. In multi-component electromagnetic surveys it is generally the sum of the squares of all three directional components.

**analytic signal:** The total amplitude of all the directions of magnetic *gradient*. Calculated as the sum of the squares.

**anisotropy:** Having different *physical parameters* in different directions. This can be caused by layering or fabric in the geology. Note that a unit can be anisotropic, but still **homogeneous**.

**anomaly:** A localized change in the geophysical data characteristic of a discrete source, such as a conductive or magnetic body: something locally different from the **background**.

**B-field:** In time-domain **electromagnetic** surveys, the magnetic field component of the (electromagnetic) **field**. This can be measured directly, although more commonly it is calculated by integrating the time rate of change of the magnetic field **dB/dt**, as measured with a receiver coil.

**background:** The “normal” response in the geophysical data – that response observed over most of the survey area. **Anomalies** are usually measured relative to the background. In airborne gamma-ray spectrometric surveys the term defines the **cosmic**, radon, and aircraft responses in the absence of a signal from the ground.

**base-level:** The measured values in a geophysical system in the absence of any outside signal. All geophysical data are measured relative to the system base level.

- Appendix F.2 -

**base frequency:** The frequency of the pulse repetition for a *time-domain electromagnetic* system. Measured between subsequent positive pulses.

**bird:** A common name for the pod towed beneath or behind an aircraft, carrying the geophysical sensor array.

**bucking:** The process of removing the strong *signal* from the *primary field* at the *receiver* from the data, to measure the *secondary field*. It can be done electronically or mathematically. This is done in *frequency-domain EM*, and to measure *on-time* in *time-domain EM*.

**calibration coil:** A wire coil of known size and dipole moment, which is used to generate a field of known *amplitude* and *phase* in the receiver, for system calibration. Calibration coils can be external, or internal to the system. Internal coils may be called Q-coils.

**coaxial coils:** [CX] Coaxial coils in an HEM system are in the vertical plane, with their axes horizontal and collinear in the flight direction. These are most sensitive to vertical conductive objects in the ground, such as thin, steeply dipping conductors perpendicular to the flight direction. Coaxial coils generally give the sharpest anomalies over localized conductors. (See also *coplanar coils*)

**coil:** A multi-turn wire loop used to transmit or detect electromagnetic fields. Time varying *electromagnetic* fields through a coil induce a voltage proportional to the strength of the field and the rate of change over time.

**compensation:** Correction of airborne geophysical data for the changing effect of the aircraft. This process is generally used to correct data in *fixed-wing time-domain electromagnetic* surveys (where the transmitter is on the aircraft and the receiver is moving), and magnetic surveys (where the sensor is on the aircraft, turning in the earth's magnetic field).

**component:** In *frequency domain electromagnetic* surveys this is one of the two *phase* measurements – *in-phase or quadrature*. In “multi-component” electromagnetic surveys it is also used to define the measurement in one geometric direction (vertical, horizontal in-line and horizontal transverse – the Z, X and Y components).

**Compton scattering:** gamma ray photons will bounce off electrons as they pass through the earth and atmosphere, reducing their energy and then being detected by *radiometric* sensors at lower energy levels. See also *stripping*.

**conductance:** See *conductivity thickness*

**conductivity:** [s] The facility with which the earth or a geological formation conducts electricity. Conductivity is usually measured in milli-Siemens per metre (mS/m). It is the reciprocal of *resistivity*.

**conductivity-depth imaging:** see **conductivity-depth transform**.

**conductivity-depth transform:** A process for converting electromagnetic measurements to an approximation of the conductivity distribution vertically in the earth, assuming a **layered earth**. (Macnae and Lamontagne, 1987; Wolfgram and Karlik, 1995)

**conductivity thickness:** [st] The product of the **conductivity**, and thickness of a large, tabular body. (It is also called the “conductivity-thickness product”) In electromagnetic geophysics, the response of a thin plate-like conductor is proportional to the conductivity multiplied by thickness. For example a 10 metre thickness of 20 Siemens/m mineralization will be equivalent to 5 metres of 40 S/m; both have 200 S conductivity thickness. Sometimes referred to as conductance.

**conductor:** Used to describe anything in the ground more conductive than the surrounding geology. Conductors are most often clays or graphite, or hopefully some type of mineralization, but may also be man-made objects, such as fences or pipelines.

**coplanar coils: [CP]** In HEM, the coplanar coils lie in the horizontal plane with their axes vertical, and parallel. These coils are most sensitive to massive conductive bodies, horizontal layers, and the **halfspace**.

**cosmic ray:** High energy sub-atomic particles from outer space that collide with the earth’s atmosphere to produce a shower of gamma rays (and other particles) at high energies.

**counts (per second):** The number of **gamma-rays** detected by a gamma-ray **spectrometer**. The rate depends on the geology, but also on the size and sensitivity of the detector.

**culture:** A term commonly used to denote any man-made object that creates a geophysical anomaly. Includes, but not limited to, power lines, pipelines, fences, and buildings.

**current channelling:** See current gathering.

**current gathering:** The tendency of electrical currents in the ground to channel into a conductive formation. This is particularly noticeable at higher frequencies or early time channels when the formation is long and parallel to the direction of current flow. This tends to enhance anomalies relative to inductive currents (see also **induction**). Also known as current channelling.

**daughter products:** The radioactive natural sources of gamma-rays decay from the original “parent” element (commonly potassium, uranium, and thorium) to one or more lower-energy “daughter” elements. Some of these lower energy elements are also

- Appendix F.4 -

radioactive and decay further. **Gamma-ray spectrometry** surveys may measure the gamma rays given off by the original element or by the decay of the daughter products.

**$\frac{dB}{dt}$ :** As the **secondary electromagnetic field** changes with time, the magnetic field [**B**] component induces a voltage in the receiving **coil**, which is proportional to the rate of change of the magnetic field over time.

**decay:** In **time-domain electromagnetic** theory, the weakening over time of the **eddy currents** in the ground, and hence the **secondary field** after the **primary field** electromagnetic pulse is turned off. In **gamma-ray spectrometry**, the radioactive breakdown of an element, generally potassium, uranium, thorium, or one of their **daughter** products.

**decay constant:** see time constant.

**decay series:** In **gamma-ray spectrometry**, a series of progressively lower energy **daughter products** produced by the radioactive breakdown of uranium or thorium.

**depth of exploration:** The maximum depth at which the geophysical system can detect the target. The depth of exploration depends very strongly on the type and size of the target, the contrast of the target with the surrounding geology, the homogeneity of the surrounding geology, and the type of geophysical system. One measure of the maximum depth of exploration for an electromagnetic system is the depth at which it can detect the strongest conductive target – generally a highly conductive horizontal layer.

**differential resistivity:** A process of transforming **apparent resistivity** to an approximation of layer resistivity at each depth. The method uses multi-frequency HEM data and approximates the effect of shallow layer **conductance** determined from higher frequencies to estimate the deeper conductivities (Huang and Fraser, 1996)

**dipole moment:** [NIA] For a transmitter, the product of the area of a **coil**, the number of turns of wire, and the current flowing in the coil. At a distance significantly larger than the size of the coil, the magnetic field from a coil will be the same if the dipole moment product is the same. For a receiver coil, this is the product of the area and the number of turns. The sensitivity to a magnetic field (assuming the source is far away) will be the same if the dipole moment is the same.

**diurnal:** The daily variation in a natural field, normally used to describe the natural fluctuations (over hours and days) of the earth's magnetic field.

**dielectric permittivity:** [**e**] The capacity of a material to store electrical charge, this is most often measured as the relative permittivity [ $\epsilon_r$ ], or ratio of the material dielectric to that of free space. The effect of high permittivity may be seen in HEM data at high frequencies over highly resistive geology as a reduced or negative **in-phase**, and higher **quadrature** data.

- Appendix F.5 -

**drape:** To fly a survey following the terrain contours, maintaining a constant altitude above the local ground surface. Also applied to re-processing data collected at varying altitudes above ground to simulate a survey flown at constant altitude.

**drift:** Long-time variations in the base-level or calibration of an instrument.

**eddy currents:** The electrical currents induced in the ground, or other conductors, by a time-varying **electromagnetic field** (usually the **primary field**). Eddy currents are also induced in the aircraft's metal frame and skin; a source of **noise** in EM surveys.

**electromagnetic: [EM]** Comprised of a time-varying electrical and magnetic field. Radio waves are common electromagnetic fields. In geophysics, an electromagnetic system is one which transmits a time-varying **primary field** to induce **eddy currents** in the ground, and then measures the **secondary field** emitted by those eddy currents.

**energy window:** A broad spectrum of **gamma-ray** energies measured by a spectrometric survey. The energy of each gamma-ray is measured and divided up into numerous discrete energy levels, called windows.

**equivalent (thorium or uranium):** The amount of radioelement calculated to be present, based on the gamma-rays measured from a **daughter** element. This assumes that the **decay series** is in equilibrium – progressing normally.

**exposure rate:** in radiometric surveys, a calculation of the total exposure rate due to gamma rays at the ground surface. It is used as a measurement of the concentration of all the **radioelements** at the surface. See also: **natural exposure rate**.

**fiducial, or fid:** Timing mark on a survey record. Originally these were timing marks on a profile or film; now the term is generally used to describe 1-second interval timing records in digital data, and on maps or profiles.

**Figure of Merit: (FOM)** A sum of the 12 distinct magnetic noise variations measured by each of four flight directions, and executing three aircraft attitude variations (yaw, pitch, and roll) for each direction. The flight directions are generally parallel and perpendicular to planned survey flight directions. The FOM is used as a measure of the **manoeuvre noise** before and after **compensation**.

**fixed-wing:** Aircraft with wings, as opposed to “rotary wing” helicopters.

**footprint:** This is a measure of the area of sensitivity under the aircraft of an airborne geophysical system. The footprint of an **electromagnetic** system is dependent on the altitude of the system, the orientation of the transmitter and receiver and the separation between the receiver and transmitter, and the conductivity of the ground. The footprint of

- Appendix F.6 -

a **gamma-ray spectrometer** depends mostly on the altitude. For all geophysical systems, the footprint also depends on the strength of the contrasting **anomaly**.

**frequency domain:** An **electromagnetic** system which transmits a **primary field** that oscillates smoothly over time (sinusoidal), inducing a similarly varying electrical current in the ground. These systems generally measure the changes in the **amplitude** and **phase** of the **secondary field** from the ground at different frequencies by measuring the **in-phase** and **quadrature** phase components. See also **time-domain**.

**full-stream data:** Data collected and recorded continuously at the highest possible sampling rate. Normal data are stacked (see **stacking**) over some time interval before recording.

**gamma-ray:** A very high-energy photon, emitted from the nucleus of an atom as it undergoes a change in energy levels.

**gamma-ray spectrometry:** Measurement of the number and energy of natural (and sometimes man-made) gamma-rays across a range of photon energies.

**gradient:** In magnetic surveys, the gradient is the change of the magnetic field over a distance, either vertically or horizontally in either of two directions. Gradient data is often measured, or calculated from the total magnetic field data because it changes more quickly over distance than the **total magnetic field**, and so may provide a more precise measure of the location of a source. See also **analytic signal**.

**ground effect:** The response from the earth. A common calibration procedure in many geophysical surveys is to fly to altitude high enough to be beyond any measurable response from the ground, and there establish **base levels** or **backgrounds**.

**half-space:** A mathematical model used to describe the earth – as infinite in width, length, and depth below the surface. The most common halfspace models are **homogeneous** and **layered earth**.

**heading error:** A slight change in the magnetic field measured when flying in opposite directions.

**HEM:** Helicopter ElectroMagnetic, This designation is most commonly used for helicopter-borne, **frequency-domain** electromagnetic systems. At present, the transmitter and receivers are normally mounted in a **bird** carried on a sling line beneath the helicopter.

**herringbone pattern:** A pattern created in geophysical data by an asymmetric system, where the **anomaly** may be extended to either side of the source, in the direction of flight. Appears like fish bones, or like the teeth of a comb, extending either side of centre, each tooth an alternate flight line.

- Appendix F.7 -

**homogeneous:** This is a geological unit that has the same *physical parameters* throughout its volume. This unit will create the same response to an HEM system anywhere, and the HEM system will measure the same apparent *resistivity* anywhere. The response may change with system direction (see *anisotropy*).

**HTEM:** Helicopter Time-domain ElectroMagnetic, This designation is used for the new generation of helicopter-borne, *time-domain* electromagnetic systems.

**in-phase:** the component of the measured *secondary field* that has the same phase as the transmitter and the *primary field*. The in-phase component is stronger than the *quadrature* phase over relatively higher *conductivity*.

**induction:** Any time-varying electromagnetic field will induce (cause) electrical currents to flow in any object with non-zero *conductivity*. (see *eddy currents*)

**induction number:** also called the “response parameter”, this number combines many of the most significant parameters affecting the *EM* response into one parameter against which to compare responses. For a *layered earth* the response parameter is  $\mu w s h^2$  and for a large, flat, *conductor* it is  $\mu w s t h$ , where  $\mu$  is the *magnetic permeability*,  $w$  is the angular *frequency*,  $s$  is the *conductivity*,  $t$  is the thickness (for the flat conductor) and  $h$  is the height of the system above the conductor.

**inductive limit:** When the frequency of an EM system is very high, or the *conductivity* of the target is very high, the response measured will be entirely *in-phase* with no *quadrature* (*phase* angle =0). The in-phase response will remain constant with further increase in conductivity or frequency. The system can no longer detect changes in conductivity of the target.

**infinite:** In geophysical terms, an “infinite” dimension is one much greater than the *footprint* of the system, so that the system does not detect changes at the edges of the object.

**International Geomagnetic Reference Field: [IGRF]** An approximation of the smooth magnetic field of the earth, in the absence of variations due to local geology. Once the IGRF is subtracted from the measured magnetic total field data, any remaining variations are assumed to be due to local geology. The IGRF also predicts the slow changes of the field up to five years in the future.

**inversion, or inverse modeling:** A process of converting geophysical data to an earth model, which compares theoretical models of the response of the earth to the data measured, and refines the model until the response closely fits the measured data (Huang and Palacky, 1991)

- Appendix F.8 -

**layered earth:** A common geophysical model which assumes that the earth is horizontally layered – the **physical parameters** are constant to **infinite** distance horizontally, but change vertically.

**magnetic permeability:** [ $\mu$ ] This is defined as the ratio of magnetic induction to the inducing magnetic field. The relative magnetic permeability [ $\mu_r$ ] is often quoted, which is the ratio of the rock permeability to the permeability of free space. In geology and geophysics, the **magnetic susceptibility** is more commonly used to describe rocks.

**magnetic susceptibility:** [ $k$ ] A measure of the degree to which a body is magnetized. In SI units this is related to relative **magnetic permeability** by  $k = \mu_r - 1$ , and is a dimensionless unit. For most geological material, susceptibility is influenced primarily by the percentage of magnetite. It is most often quoted in units of  $10^{-6}$ . In HEM data this is most often apparent as a negative **in-phase** component over high susceptibility, high **resistivity** geology such as diabase dikes.

**manoeuvre noise:** variations in the magnetic field measured caused by changes in the relative positions of the magnetic sensor and magnetic objects or electrical currents in the aircraft. This type of noise is generally corrected by magnetic **compensation**.

**model:** Geophysical theory and applications generally have to assume that the geology of the earth has a form that can be easily defined mathematically, called the model. For example steeply dipping **conductors** are generally modeled as being **infinite** in horizontal and depth extent, and very thin. The earth is generally modeled as horizontally layered, each layer infinite in extent and uniform in characteristic. These models make the mathematics to describe the response of the (normally very complex) earth practical. As theory advances, and computers become more powerful, the useful models can become more complex.

**natural exposure rate:** in radiometric surveys, a calculation of the total exposure rate due to natural-source gamma rays at the ground surface. It is used as a measurement of the concentration of all the natural **radioelements** at the surface. See also: **exposure rate**.

**noise:** That part of a geophysical measurement that the user does not want. Typically this includes electronic interference from the system, the atmosphere (**sferics**), and man-made sources. This can be a subjective judgment, as it may include the response from geology other than the target of interest. Commonly the term is used to refer to high frequency (short period) interference. See also **drift**.

**Occam's inversion:** an **inversion** process that matches the measured **electromagnetic** data to a theoretical model of many, thin layers with constant thickness and varying resistivity (Constable et al, 1987).

**off-time:** In a **time-domain electromagnetic** survey, the time after the end of the **primary field pulse**, and before the start of the next pulse.

- Appendix F.9 -

**on-time:** In a *time-domain electromagnetic* survey, the time during the *primary field pulse*.

**overburden:** In engineering and mineral exploration terms, this most often means the soil on top of the unweathered bedrock. It may be sand, glacial till, or weathered rock.

**Phase, phase angle:** The angular difference in time between a measured sinusoidal electromagnetic field and a reference – normally the primary field. The phase is calculated from  $\tan^{-1}(\textit{in-phase} / \textit{quadrature})$ .

**physical parameters:** These are the characteristics of a geological unit. For electromagnetic surveys, the important parameters are *conductivity*, *magnetic permeability* (or *susceptibility*) and *dielectric permittivity*; for magnetic surveys the parameter is magnetic susceptibility, and for gamma ray spectrometric surveys it is the concentration of the major radioactive elements: potassium, uranium, and thorium.

**permittivity:** see *dielectric permittivity*.

**permeability:** see *magnetic permeability*.

**primary field:** the EM field emitted by a transmitter. This field induces *eddy currents* in (energizes) the conductors in the ground, which then create their own *secondary fields*.

**pulse:** In time-domain EM surveys, the short period of intense *primary* field transmission. Most measurements (the *off-time*) are measured after the pulse. **On-time** measurements may be made during the pulse.

**quadrature:** that component of the measured *secondary field* that is phase-shifted 90° from the *primary field*. The quadrature component tends to be stronger than the *in-phase* over relatively weaker *conductivity*.

**Q-coils:** see *calibration coil*.

**radioelements:** This normally refers to the common, naturally-occurring radioactive elements: potassium (K), uranium (U), and thorium (Th). It can also refer to man-made radioelements, most often cobalt (Co) and cesium (Cs)

**radiometric:** Commonly used to refer to *gamma ray* spectrometry.

**radon:** A radioactive daughter product of uranium and thorium, radon is a gas which can leak into the atmosphere, adding to the non-geological background of a gamma-ray spectrometric survey.

- Appendix F.10 -

**receiver:** the *signal* detector of a geophysical system. This term is most often used in active geophysical systems – systems that transmit some kind of signal. In airborne *electromagnetic* surveys it is most often a *coil*. (see also, *transmitter*)

**resistivity:** [ $\rho$ ] The strength with which the earth or a geological formation resists the flow of electricity, typically the flow induced by the *primary field* of the electromagnetic transmitter. Normally expressed in ohm-metres, it is the reciprocal of *conductivity*.

**resistivity-depth transforms:** similar to *conductivity depth transforms*, but the calculated *conductivity* has been converted to *resistivity*.

**resistivity section:** an approximate vertical section of the resistivity of the layers in the earth. The resistivities can be derived from the *apparent resistivity*, the *differential resistivities*, *resistivity-depth transforms*, or *inversions*.

**Response parameter:** another name for the *induction number*.

**secondary field:** The field created by conductors in the ground, as a result of electrical currents induced by the *primary field* from the *electromagnetic* transmitter. Airborne *electromagnetic* systems are designed to create and measure a secondary field.

**Sengpiel section:** a *resistivity section* derived using the *apparent resistivity* and an approximation of the depth of maximum sensitivity for each frequency.

**sferic:** Lightning, or the *electromagnetic* signal from lightning, it is an abbreviation of “atmospheric discharge”. These appear to magnetic and electromagnetic sensors as sharp “spikes” in the data. Under some conditions lightning storms can be detected from hundreds of kilometres away. (see *noise*)

**signal:** That component of a measurement that the user wants to see – the response from the targets, from the earth, etc. (See also *noise*)

**skin depth:** A measure of the depth of penetration of an electromagnetic field into a material. It is defined as the depth at which the primary field decreases to 1/e of the field at the surface. It is calculated by approximately  $503 \times \sqrt{(\text{resistivity}/\text{frequency})}$ . Note that depth of penetration is greater at higher *resistivity* and/or lower *frequency*.

**spectrometry:** Measurement across a range of energies, where *amplitude* and energy are defined for each measurement. In gamma-ray spectrometry, the number of gamma rays are measured for each energy *window*, to define the *spectrum*.

**spectrum:** In *gamma ray spectrometry*, the continuous range of energy over which gamma rays are measured. In *time-domain electromagnetic* surveys, the spectrum is the energy of the *pulse* distributed across an equivalent, continuous range of frequencies.

**spheric:** see *sferic*.

**stacking:** Summing repeat measurements over time to enhance the repeating *signal*, and minimize the random *noise*.

**stripping:** Estimation and correction for the gamma ray photons of higher and lower energy that are observed in a particular *energy window*. See also *Compton scattering*.

**susceptibility:** See *magnetic susceptibility*.

**tau:** [ $t$ ] Often used as a name for the *time constant*.

**TDEM:** *time domain electromagnetic*.

**thin sheet:** A standard model for electromagnetic geophysical theory. It is usually defined as a thin, flat-lying conductive sheet, *infinite* in both horizontal directions. (see also *vertical plate*)

**tie-line:** A survey line flown across most of the *traverse lines*, generally perpendicular to them, to assist in measuring *drift* and *diurnal* variation. In the short time required to fly a tie-line it is assumed that the drift and/or diurnal will be minimal, or at least changing at a constant rate.

**time constant:** The time required for an *electromagnetic* field to decay to a value of  $1/e$  of the original value. In *time-domain* electromagnetic data, the time constant is proportional to the size and *conductance* of a tabular conductive body. Also called the decay constant.

**Time channel:** In *time-domain electromagnetic* surveys the decaying *secondary field* is measured over a period of time, and the divided up into a series of consecutive discrete measurements over that time.

**time-domain:** *Electromagnetic* system which transmits a pulsed, or stepped *electromagnetic* field. These systems induce an electrical current (*eddy current*) in the ground that persists after the *primary field* is turned off, and measure the change over time of the *secondary field* created as the currents *decay*. See also *frequency-domain*.

**total energy envelope:** The sum of the squares of the three *components* of the *time-domain electromagnetic secondary field*. Equivalent to the *amplitude* of the secondary field.

**transient:** Time-varying. Usually used to describe a very short period pulse of *electromagnetic* field.

- Appendix F.12 -

**transmitter:** The source of the **signal** to be measured in a geophysical survey. In airborne **EM** it is most often a **coil** carrying a time-varying electrical current, transmitting the **primary field**. (see also **receiver**)

**traverse line:** A normal geophysical survey line. Normally parallel traverse lines are flown across the property in spacing of 50 m to 500 m, and generally perpendicular to the target geology.

**vertical plate:** A standard model for electromagnetic geophysical theory. It is usually defined as thin conductive sheet, **infinite** in horizontal dimension and depth extent. (see also **thin sheet**)

**waveform:** The shape of the **electromagnetic pulse** from a **time-domain** electromagnetic transmitter.

**window:** A discrete portion of a **gamma-ray spectrum** or **time-domain electromagnetic decay**. The continuous energy spectrum or **full-stream** data are grouped into windows to reduce the number of samples, and reduce **noise**.

Version 1.5, November 29, 2005  
Greg Hodges,  
Chief Geophysicist  
Fugro Airborne Surveys, Toronto

### Common Symbols and Acronyms

<b>k</b>	Magnetic susceptibility
<b>e</b>	Dielectric permittivity
<b>m, m<sub>r</sub></b>	Magnetic permeability, relative permeability
<b>r, r<sub>a</sub></b>	Resistivity, apparent resistivity
<b>s, s<sub>a</sub></b>	Conductivity, apparent conductivity
<b>st</b>	Conductivity thickness
<b>t</b>	Tau, or time constant
<b>Wm</b>	ohm-metres, units of resistivity
<b>AGS</b>	Airborne gamma ray spectrometry.
<b>CDT</b>	Conductivity-depth transform, conductivity-depth imaging (Macnae and Lamontagne, 1987; Wolfgram and Karlik, 1995)
<b>CPI, CPQ</b>	Coplanar in-phase, quadrature
<b>CPS</b>	Counts per second
<b>CTP</b>	Conductivity thickness product
<b>CXI, CXQ</b>	Coaxial, in-phase, quadrature
<b>FOM</b>	Figure of Merit
<b>fT</b>	femtoteslas, normal unit for measurement of B-Field
<b>EM</b>	Electromagnetic
<b>keV</b>	kilo electron volts – a measure of gamma-ray energy
<b>MeV</b>	mega electron volts – a measure of gamma-ray energy 1MeV = 1000keV
<b>NIA</b>	dipole moment: turns x current x Area
<b>nT</b>	nanotesla, a measure of the strength of a magnetic field
<b>nG/h</b>	nanoGreys/hour – gamma ray dose rate at ground level
<b>ppm</b>	parts per million – a measure of secondary field or noise relative to the primary or radioelement concentration.
<b>pT/s</b>	picoteslas per second: Units of decay of secondary field, dB/dt
<b>S</b>	siemens – a unit of conductance
<b>x:</b>	the horizontal component of an EM field parallel to the direction of flight.
<b>y:</b>	the horizontal component of an EM field perpendicular to the direction of flight.
<b>z:</b>	the vertical component of an EM field.

**References:**

Constable, S.C., Parker, R.L., And Constable, C.G., 1987, Occam's inversion: a practical algorithm for generating smooth models from electromagnetic sounding data: *Geophysics*, 52, 289-300

Huang, H. and Fraser, D.C, 1996. The differential parameter method for multifrequency airborne resistivity mapping. *Geophysics*, 55, 1327-1337

Huang, H. and Palacky, G.J., 1991, Damped least-squares inversion of time-domain airborne EM data based on singular value decomposition: *Geophysical Prospecting*, v.39, 827-844

Macnae, J. and Lamontagne, Y., 1987, Imaging quasi-layered conductive structures by simple processing of transient electromagnetic data: *Geophysics*, v52, 4, 545-554.

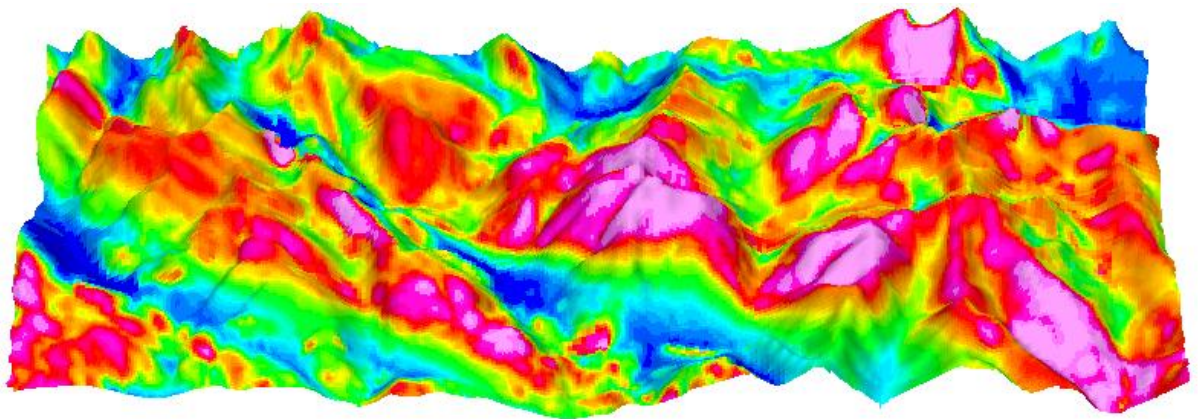
Sengpiel, K.P. 1988, Approximate inversion of airborne EM data from a multi-layered ground. *Geophysical Prospecting*, 36, 446-459

Wolfgram, P. and Karlik, G., 1995, Conductivity-depth transform of GEOTEM data: *Exploration Geophysics*, 26, 179-185.

Yin, C. and Fraser, D.C. (2002), The effect of the electrical anisotropy on the responses of helicopter-borne frequency domain electromagnetic systems, Submitted to *Geophysical Prospecting*

Appendix B. Review of Aeromagnetic Data over the Pearson Property – M.  
Sumara

**REVIEW  
OF  
AEROMAGNETIC DATA  
OVER THE  
PEARSON PROPERTY  
ON BEHALF OF  
EMERALD FIELDS RESOURCE CORPORATION**



**REPORT BY  
MONIKA SUMARA**

August 25<sup>th</sup>, 2006

Monika Sumara

1303, 933 Seymour Street  
Vancouver, British Columbia  
V6B 6L6

Tel: 604.737.1371  
Fax: 604.689.8199

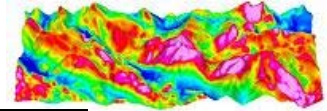


**Table of Contents**

***INTRODUCTION*.....4**

***MAGNETIC SURVEY*.....4**

    Survey Specification.....4

    Altitude.....4

    Magnetic Noise.....4

***SURVEY LOCATION* .....4**

***MAGNETIC MAPS* .....5**

***DATA PROCESSING AND PRESENTATION* .....5**

***DISCUSSION AND RECOMMENDATIONS*.....6**

    Anomaly P1 .....6

    Anomaly P2 .....7

    Anomaly P4 .....8

    Anomaly P9 .....9

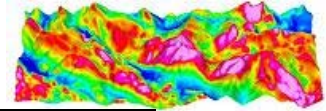
    Anomaly P12 .....10

    Anomaly P13 .....11

***FOLLOW-UP CONSIDERATIONS* .....12**

***APPENDIX A – geophysical images and figures*.....13**

***STATEMENT OF QUALIFICATIONS*.....26**



## **INTRODUCTION**

This report describes the data obtained from the airborne magnetometer survey as pertaining to the geology of the Pearson claim block for Emerald Field Resource Corporation on Southwestern Vancouver Island, BC. In June 2006, Fugro was contracted to fly a low altitude, magnetometer survey with their helicopter based, stinger mounted single sensor system over the key area of interest on the Pearson property.

## **MAGNETIC SURVEY**

### **Survey Specification**

The helicopter based magnetometer survey was flown by Fugro and was completed over a period spanning between Jun 12, 2006 and June 20, 2006. The grid measured 22km by 7km and consisted of N-S lines at 100m spacing and E-W tie lines at 500m spacing for a total distance of 1972 line kilometers.

### **Altitude**

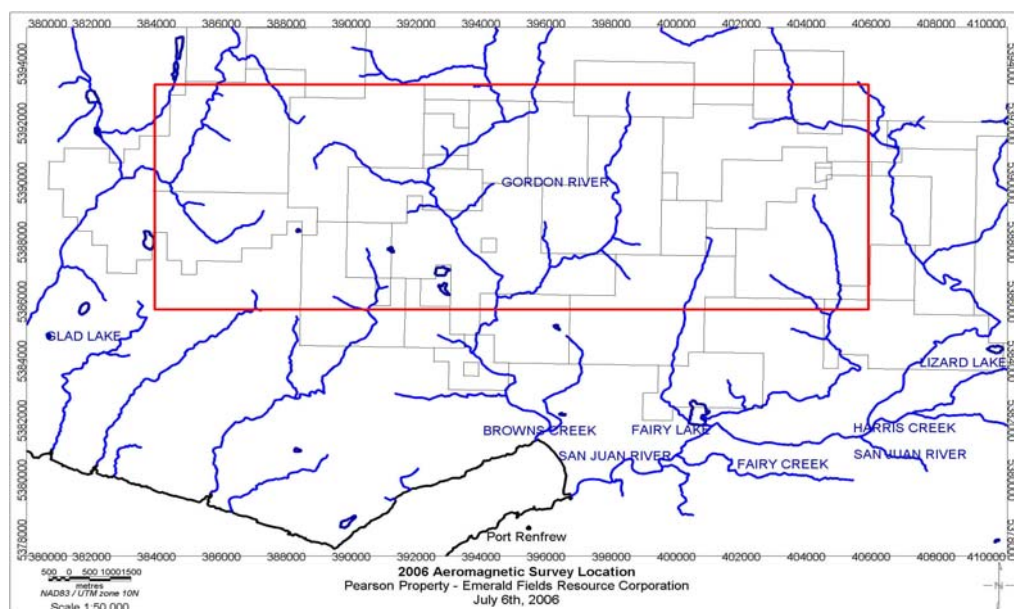
Altitude control was accomplished via onboard helicopter altimeter. The target elevation of 60m average altitude was achieved with a mean variation of 15m. This was deemed acceptable for the rugged terrain of the southern part of Vancouver Island.

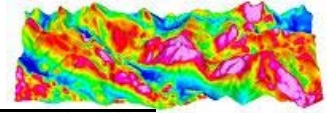
### **Magnetic Noise**

A fourth difference filter was applied to the diurnally corrected data to inspect the level of noise. The noise envelope was at an acceptable level well below 0.1nT, and overall the magnetic data was very clean.

## **SURVEY LOCATION**

The 2006 Aeromagnetic survey was flown over a portion of the Pearson claim block located on SW Vancouver Island, BC, as seen on the map below.





## **MAGNETIC MAPS**

A total magnetic field map was made over the entire survey area and contoured at an interval of 100nT. Also provided are the vertical derivative and the analytic signal grids showing the locations of historical drillholes and mineral showings. Where magnetic anomalies of interest were noted, further zoomed images of the area of interest were created. These maps and figures are included as an appendix to this report.

## **DATA PROCESSING AND PRESENTATION**

All data was collected and processed in the NAD 83, Zone 10 projection. A standard sequence of geophysical processing was applied to the aeromagnetic data as described in the steps below.

The aeromagnetic data was gridded using the bi-directional method with a 25m cell size, and a Total Magnetic Field image was created. In addition, two other grids were created which included the Vertical Derivative and Analytics Signal in order to investigate the magnetic characteristics of the geology in this area.

The Vertical Derivative is commonly applied to total magnetic field data to enhance the shallowest geological sources. Isolating short wavelength magnetic features enhances the response of near surface features at the expense of deeper sources and provides a more direct correlation between magnetic anomalies and geological map units.

The Analytic Signal grid is a valuable geophysical interpretation tool in locating the edges of magnetic source bodies, particularly where remanence complicates interpretation. The analytic signal is the square root of the sum of the squares of the derivatives in the x, y, and z directions.

### **Diurnal Corrections**

Basemag readings were carried out by Fugro as was the diurnal correction of the raw data.

### **Lag Correction**

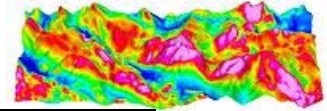
A lag shift of -5 fiducial was used in the lag correction.

### **Heading Correction**

Heading corrections were performed by the survey data acquisition system as part of the aircraft compensation system. The correction parameters were determined by a heading test flight at the start of the survey.

### **Statistical Leveling of Total Magnetic Field**

A statistical leveling of the magnetic data was done first on the tie lines, and then a full level was done on all lines. A least-squares trend line was calculated through an error channel to derive a trend error curve, which was then added to the channel to be leveled. The trend curve was then saved for later inspection.



## **DISCUSSION AND RECOMMENDATIONS**

The detailed 2006 aeromagnetic data reveals a great deal of structural variety as compared to the widespread high level magnetic response visible on a regional scale. The geology consists mainly of the metamorphic Westcoast Complex which includes: gneiss, amphibolite, migmatite, and quartz diorite. These Paleozoic and Mesozoic age rocks are characterized by a moderately strong magnetic response, with NW trending, linear, magnetically low structures. The prominent geological features within the survey area are the two groups of intrusive rocks which consist of the early to middle Jurassic Island Plutonic Suite and are signified by a higher magnetic domain.

The geological map, MINFILE Occurrence MAP 092C, Cape Flattery, Ministry of Energy, Mines and Petroleum Resources, BC, was used in the geophysical interpretation.

A compilation of anomalies throughout the survey block is summarized in Table 1 of the Appendix. The interpreted anomalies were analyzed and prioritized based on signal strength, structure, size as well as any evidence of mineral showings or drillhole results. The information provided by the magnetics suggests six significant anomalies of interest, however, further geological follow-up and investigation is strongly recommended, particularly over anomalies where there is only magnetic data available.

### **Anomaly P1**

The western section of the survey area includes the Daniel, Conqueror and David drillholes as well as a number of mineral showings and magnetite outcrops potentially associated with skarns formed as volcanics of the Island Suite intruded into overlying carbonates. The structure that hosts all three drillholes has the strongest magnetic response (anomaly P1) of the survey block at a magnitude of approximately 2500nT. This is a very broad and intense response that would be characteristic of an intrabasement source of the anomaly. The size and shape of the profiles suggest that this source is a near vertical dike (Figure 7 in the Appendix) however, it is possible that there is more than one source of the signal (ie. two or more magnetic bodies overlaying each other) which would affect the profiles.

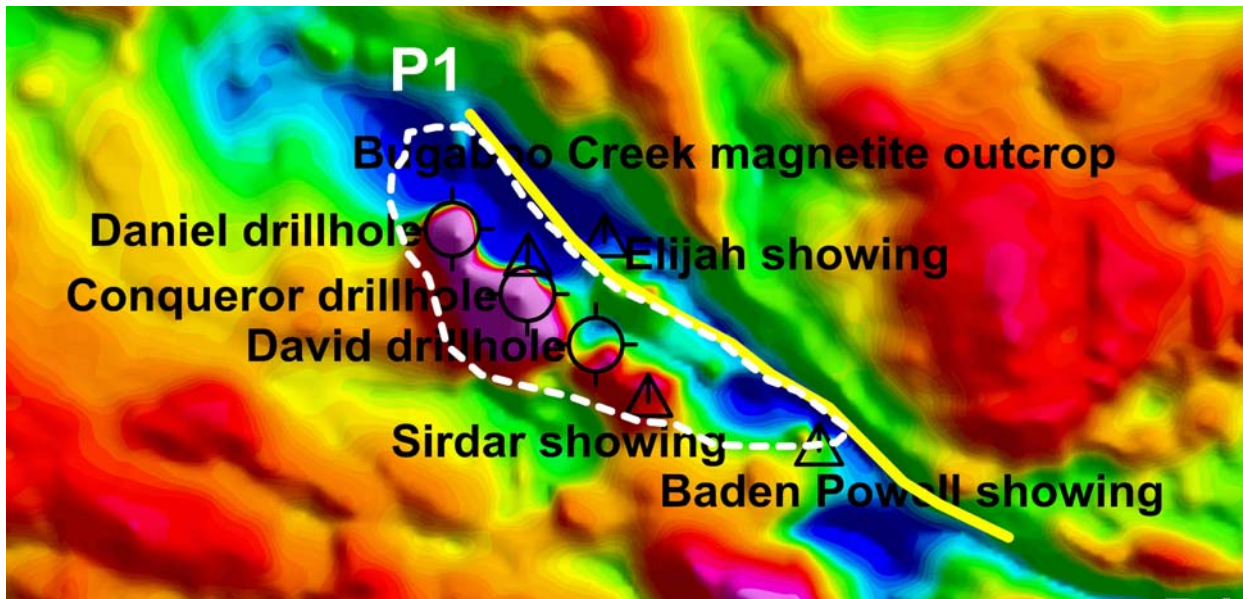
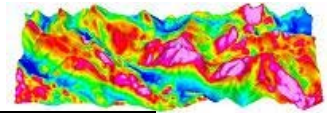


Figure 1: Anomaly P1 Image

Under the assumption that the anomaly is caused by vertical contacts, the analytic signal can be used to estimate depth (using an amplitude half-width rule) which would give a value of approximately 160m for



anomaly P1. The anomaly itself appears to be 2500m in length by 700m in width at its widest point. There appears to be a contact zone to the NE of this anomaly which is marked by a sharp change in amplitude and as well as a change in magnetic texture.

### Anomaly P2

Anomaly P2 is an elongate, NW trending mag high that measure roughly 1900m in length by 900m at its widest point. It is roughly located between the Baden Powell showing and the Lorimer Creek magnetite outcrop. The depth to the source is estimated to be 200m. Given the strength of the signal of this anomaly and the fact that it falls in line with the structure that holds the P1 anomaly it merits further exploration in the way of geological investigation. The structure between anomalies P1 and P2 may well be linked.

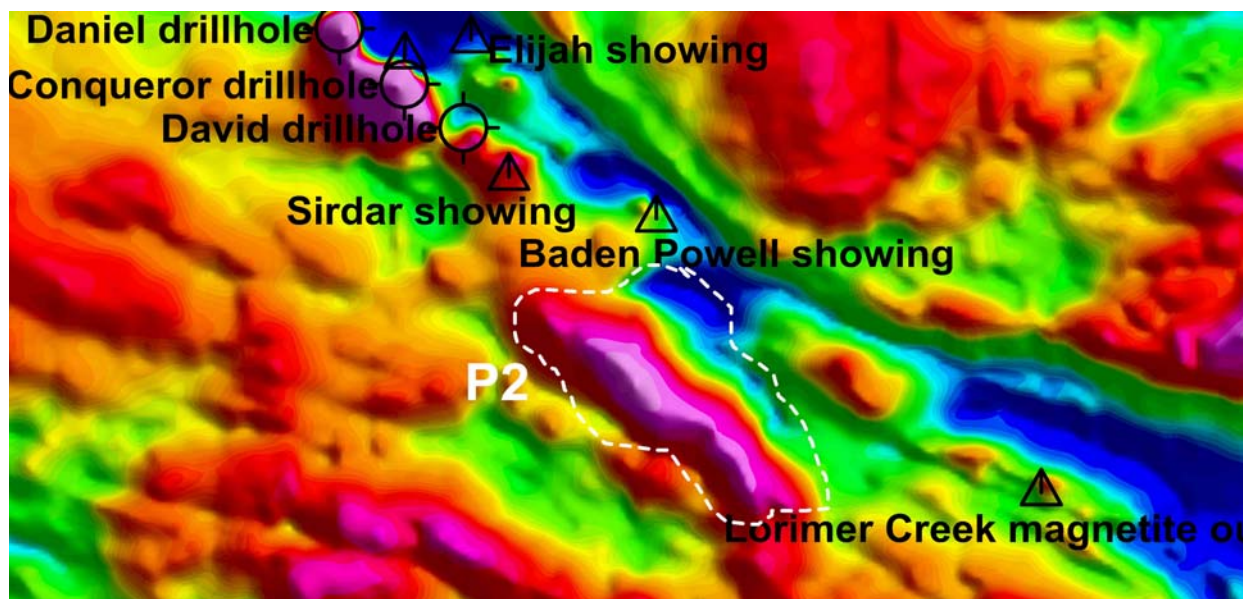
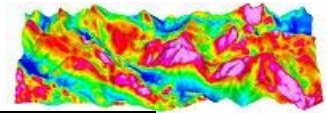


Figure 2: Anomaly P2 Image



### Anomaly P4

Anomaly P4 appears as a dipole in the Total Magnetic Field grid and the structure holds together nicely in the Analytic Signal grid. It is located over the Lorimer Creek magnetite outcrop and is of moderate strength at 500nT. As with the previous two anomalies it falls in line with the NW trending structure and is approximately 1300m by 270m in dimension. The source has an estimated burial depth of 100m. To gain more information on the shape and size of this structure, a ground magnetometer survey is recommended. Anomaly P4 is an order of magnitude smaller than P1 which may indicate a shallow source at this location.

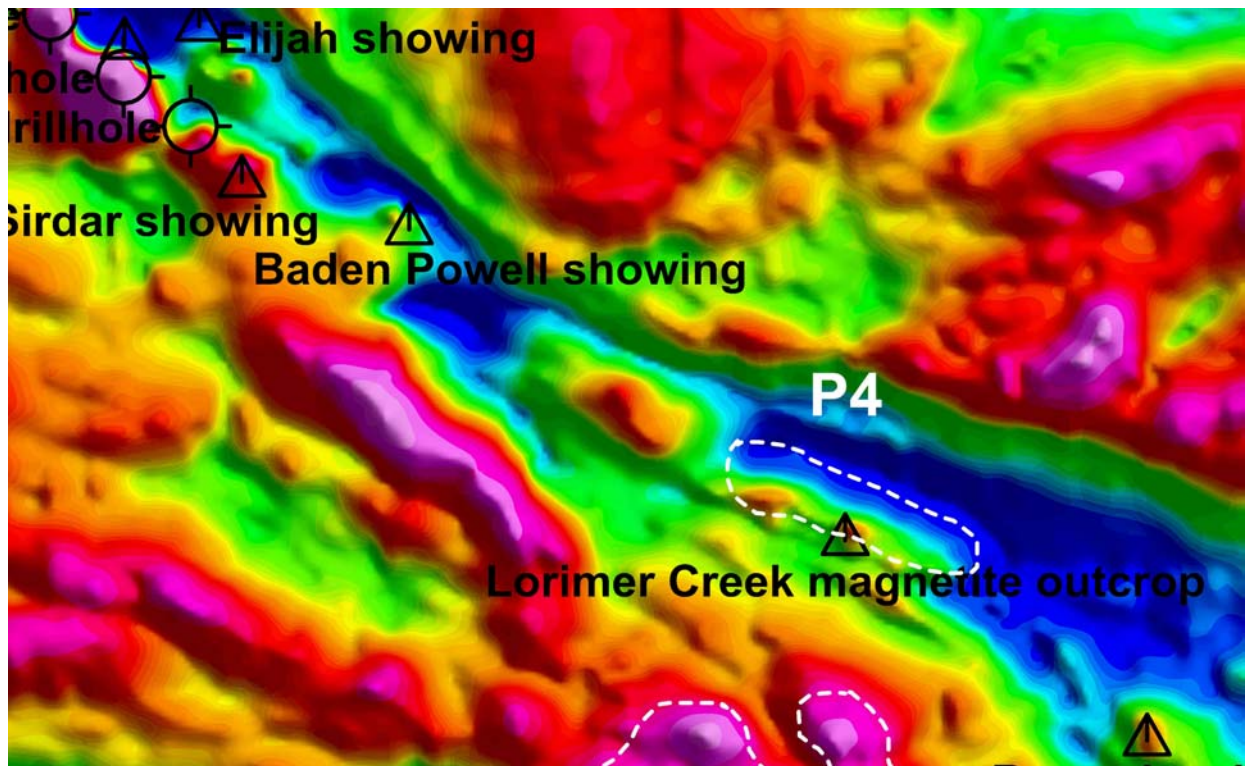
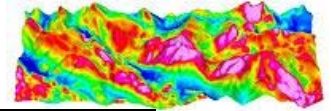


Figure 3: Anomaly P4 Image



### Anomaly P9

Anomaly P9 is located in the central region of the survey area along a larger magnetic high that trends NW. At 1500nT it is the strongest anomaly this central region and it measures approximately 2000m in length by 500m in width. Further geological recon is recommended to ascertain the source of this signal which is estimated to have a burial depth of approximately 170m.

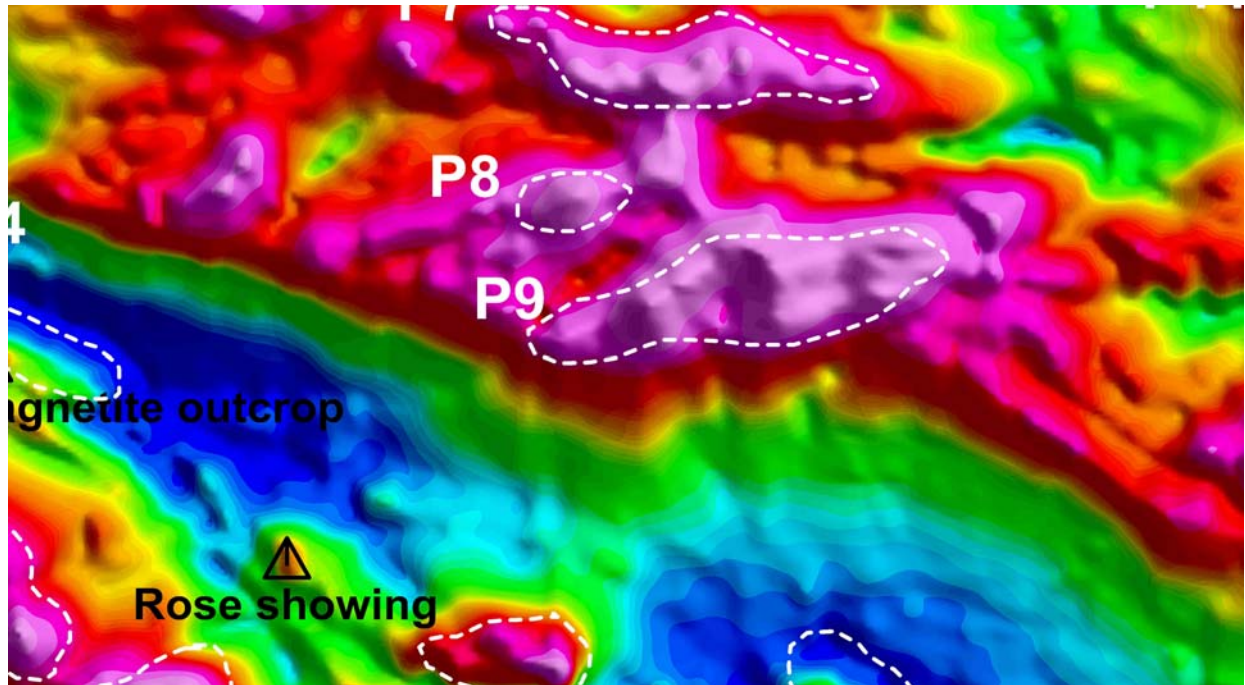
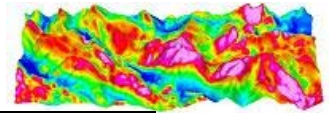


Figure 4: Anomaly P9 Image



### Anomaly P12

The most prominent anomaly (P12) in the east section of the survey has a magnitude of 1275nT and encompasses the Reko North showing (as seen in Figure 9 of the Appendix.) This anomaly is an EW trending structure measuring approximately 300m by 900m in diameter, and an estimated depth of 150m at it's deepest (the southern part of the structure where the anomaly is strongest ). The amplitude of the (Total Magnetic Field) profiles suggests that this is one structure, although the strongest response is in the southern portion. A ground magnetometer survey over this anomaly is recommended to map out the extent of the structure.

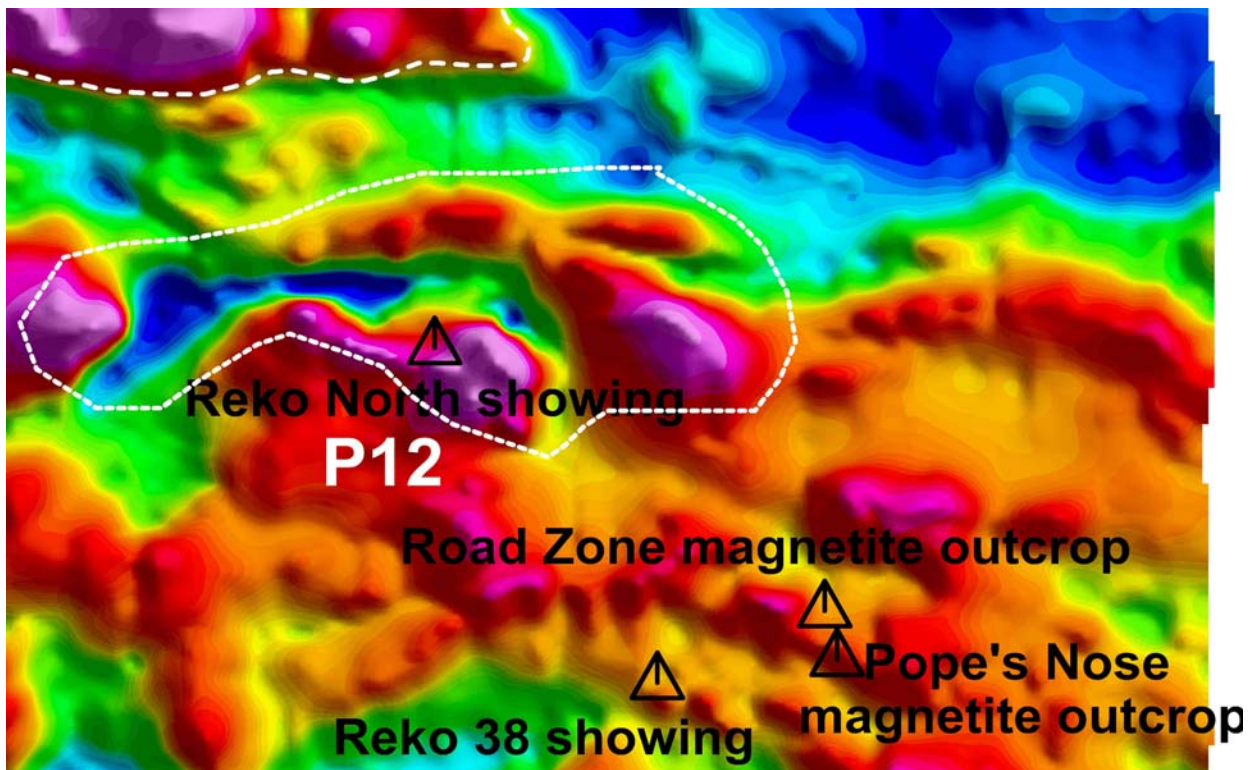
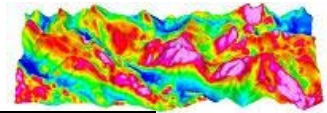


Figure 5: Anomaly P12 Image



### Anomaly P13

Anomaly P13 is located at the NE end of the survey block and has a very strong response at 1400nT. It's approximately 3000m by 830m in dimension and trends NW though not as strongly as the previous anomalies. Based on the large size and strength of the magnetic response, this anomaly merits further exploration. EM and geological recon are recommended.

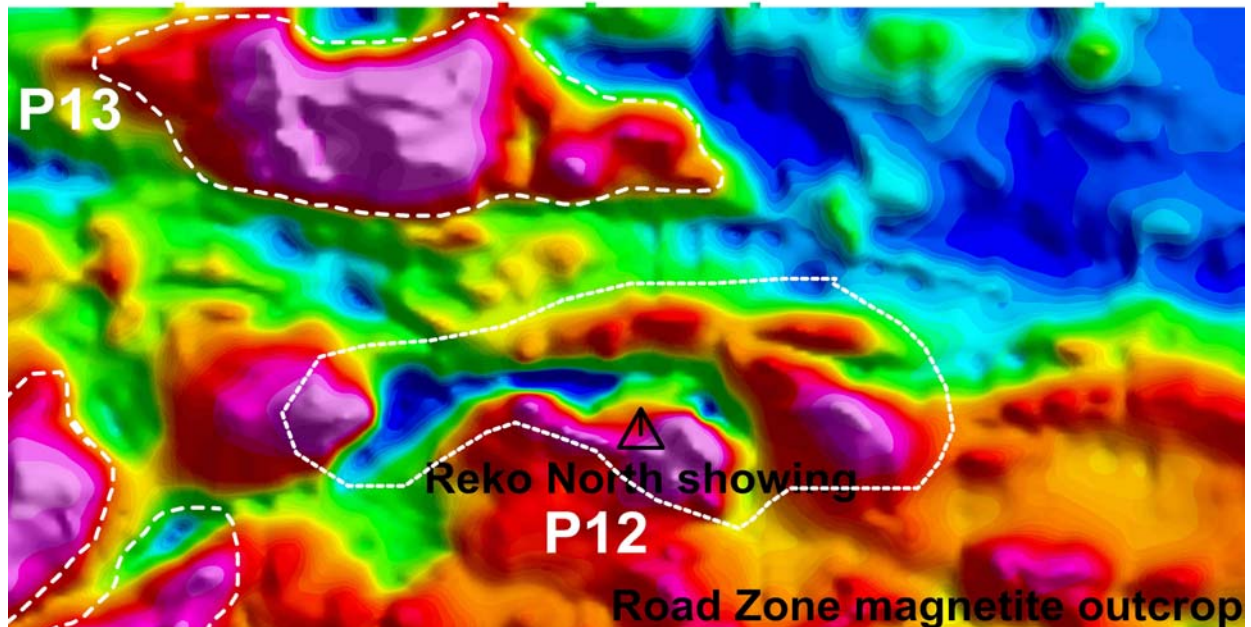
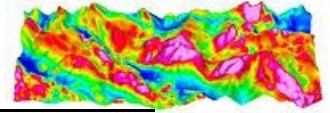


Figure 6: Anomaly P13 Image

The source of the other mineral showings in the eastern section of the survey including the Road Zone magnetite outcrop, Pope's Nose Zone magnetite outcrop, Reko 38 showing and Reko 10 magnetite outcrop, do not appear to have very deep sources as shown in the vertical derivative and analytic signal grids, and therefore show less potential as economic ore bodies.

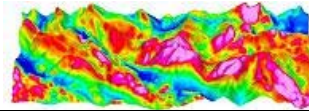


### ***FOLLOW-UP CONSIDERATIONS***

For anomalies at both the east and west end of the 2006 survey block, follow up investigation should include a high resolution, horizontal loop electromagnetic HLEM survey to detect and map out any associated conductivity and define further the geological structure.

For the eastern section of the property in particular, gravity surveying as well as further geological mapping would be beneficial in delineating the structure of the area. The West Zone is significantly more promising a target compared to the East Zone due to the size and depth of the potential structure. Ground magnetics should be conducted at all high priority anomaly locations to pin-point potential drill targets.

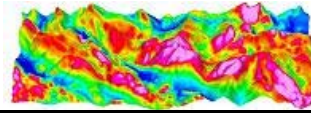
The 2006 aeromagnetic survey offers a detailed insight into the geological structure of the area and positive enforcement as to the presence of a large iron bearing structure. And as this survey covers just a portion of the Emerald Field claims on Southern Vancouver Island, it leaves much for future exploration and potential development.



**APPENDIX A – GEOPHYSICAL IMAGES AND FIGURES**

*Table 1: Anomaly Classification*

<i>Anomaly</i>	<i>Xnad83</i>	<i>Ynad83</i>	<i>Amplitude (nT)</i>	<i>Dimension (m)</i>	<i>Comments</i>
P1	388908	5390803	2500	2500 x 700	Strongest mag high in the survey area
P2	390184	5389236	1200	1900 x 900	South of the Baden Powell showing, substantial mag high
P3	393023	5386974	1380	900 x 560	Mag high structure South of Rose showing
P4	392429	5388667	500	1300 x 270	Anomaly over the Lorimer Creek magnetite outcrop, dipole
P5	392550	5387326	900	820 x 300	West of Rose showing, same response as anomaly P6 directly west, size decreases in analytic signal
P6	391731	5387702	900	800 x 500	West of Rose showing, same response as anomaly P5 directly east, size decreases in analytic signal
P7	395639	5390002	1100	1850 x 370	Structures decreases in size significantly in analytic signal, further geological recon recommended
P8	395236	5389442	1200	520 x 250	Structures decreases in size significantly in analytic signal, further geological recon recommended
P9	395592	5388916	1500	2000 x 500	Strongest anomaly of the P7, P8 and P9 cluster, further geological recon recommended



P10	384366	5392158	900	900 x 350	Small mag high at the far western end of the survey block, further geological recon recommended
P11	385649	5387371	700	980 x 300	Moderate mag high in the southwestern corner of the survey block, requires further geological recon
P12	402919	5391192	1275	3100 x 900	large E-W trending structure that encompasses Reko North showing
P13	401507	5392669	1400	3000 x 830	large E-W trending structure, strong mag high, requires further geological recon
P14	399722	5390962	900	1660 x 730	Moderate mag high, analytic signal indicates the source is many small parts rather than one large structure
P15	399843	5387885	1600	1880 x 1300	Strong anomaly, further geological recon recommended
P16	403327	5386898	1300	2700 x 1200	Broad anomaly, analytic signal indicates the source is many small parts rather than one large structure
P17	400592	5390486	700	1130 x 500	Moderate mag high, N-E trending structure, further geological recon recommended
P18	395115	5387159	900	770 x 340	Moderate mag high southeast of Rose showing, further geological recon recommended
P19	396947	5386722	500	1100 x 440	S-E trending mag high further geological recon recommended

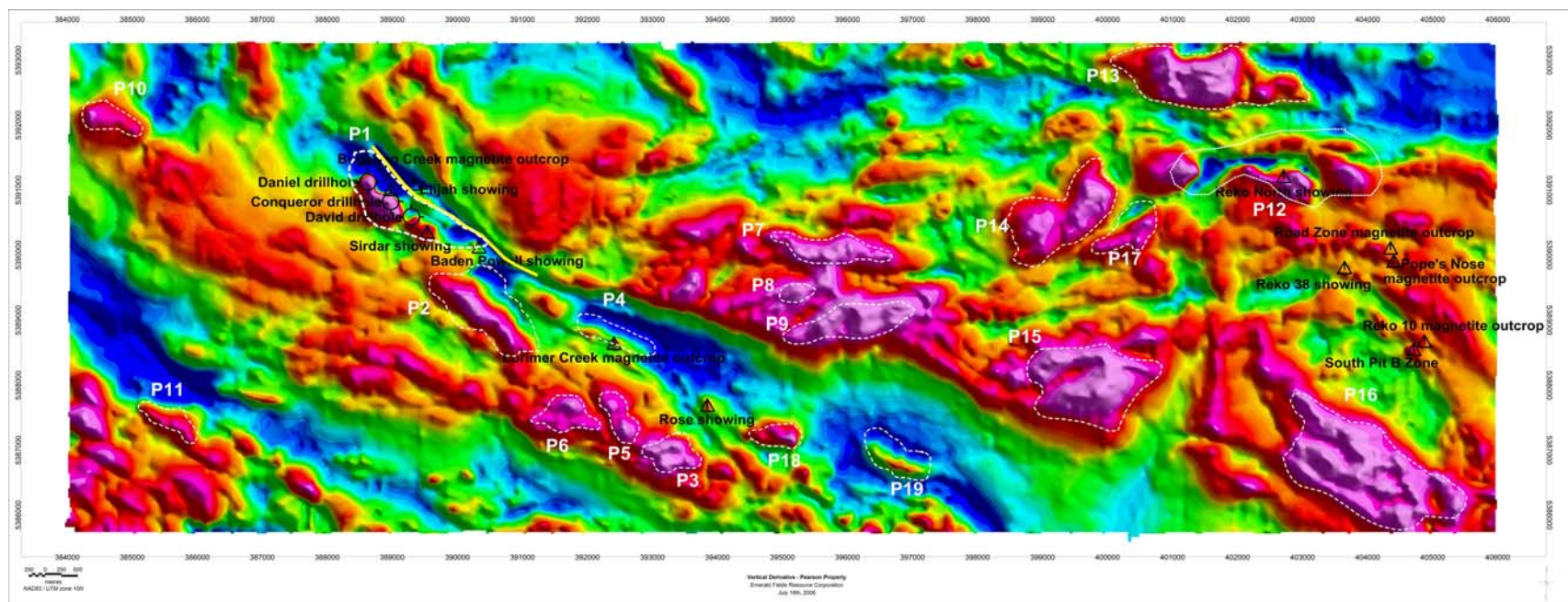
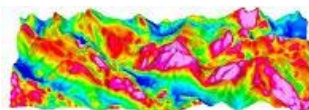


Figure 7: Summary Anomaly Map of 2006 Aeromagnetic Survey

Pearson Project - Emerald Fields Resource Corporation  
Aeromagnetic Interpretation Report

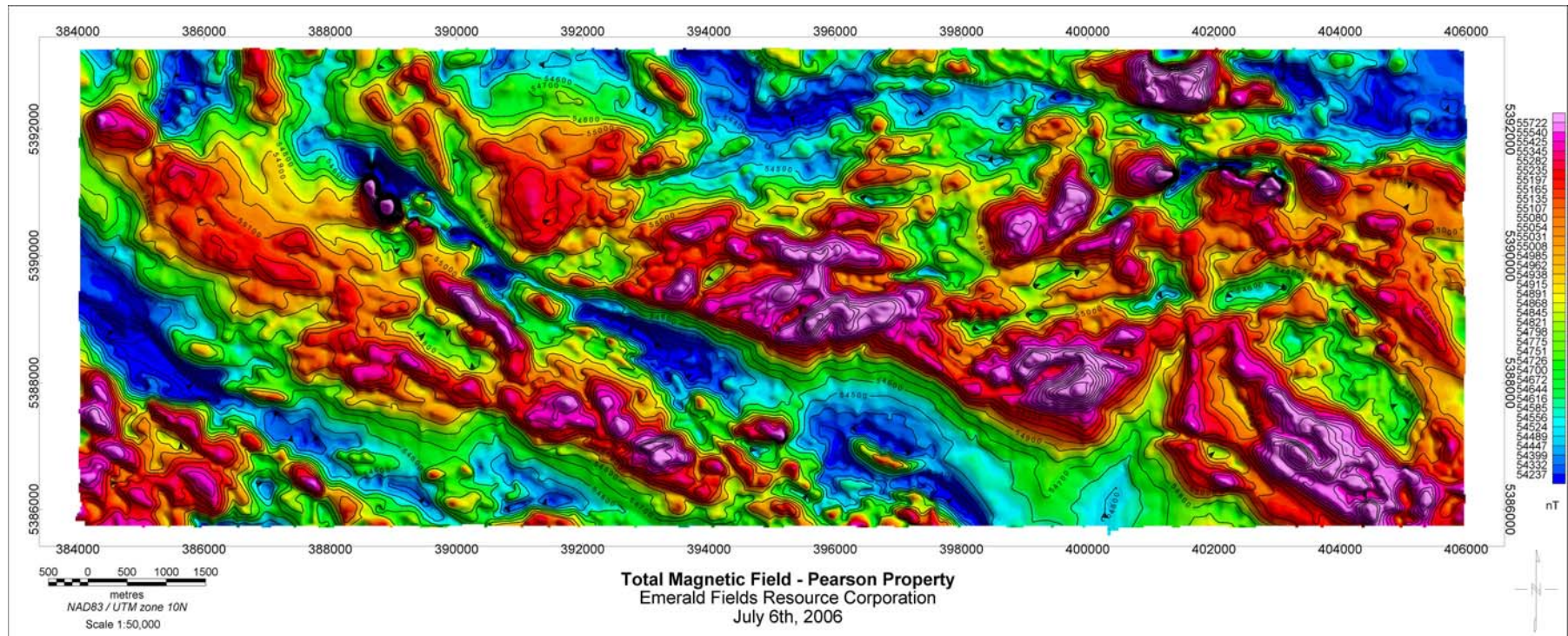
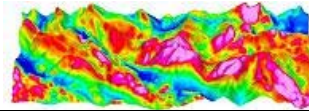


Figure 8: Total Magnetic Field Map of 2006 Aeromagnetic Survey.

Pearson Project - Emerald Fields Resource Corporation  
Aeromagnetic Interpretation Report

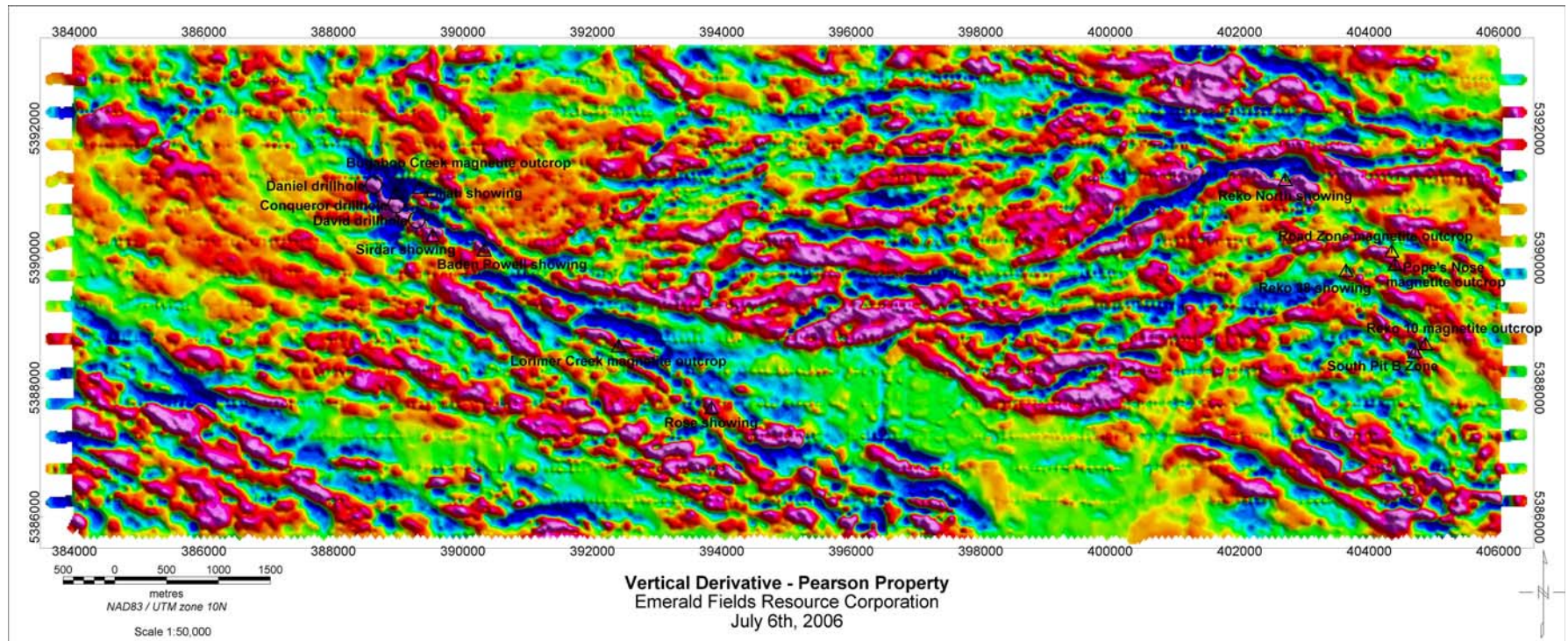
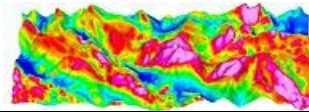


Figure 9: Vertical Derivative Grid 2006 Aeromagnetic Survey with showings and drillholes.

Pearson Project - Emerald Fields Resource Corporation  
Aeromagnetic Interpretation Report

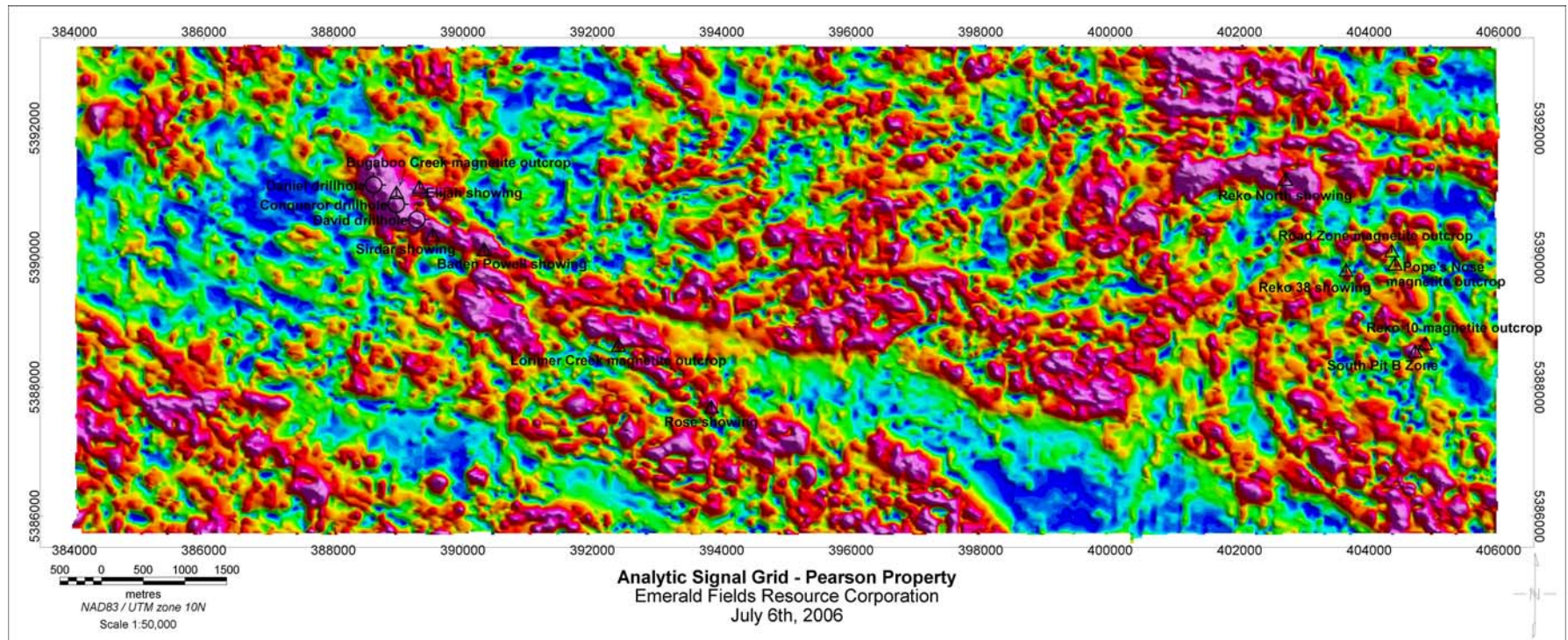
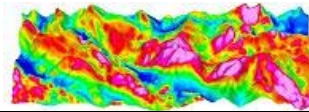


Figure 10: Analytic Signal Grid of 2006 Aeromagnetic Survey with showings and drillholes.

Pearson Project - Emerald Fields Resource Corporation  
 Aeromagnetic Interpretation Report

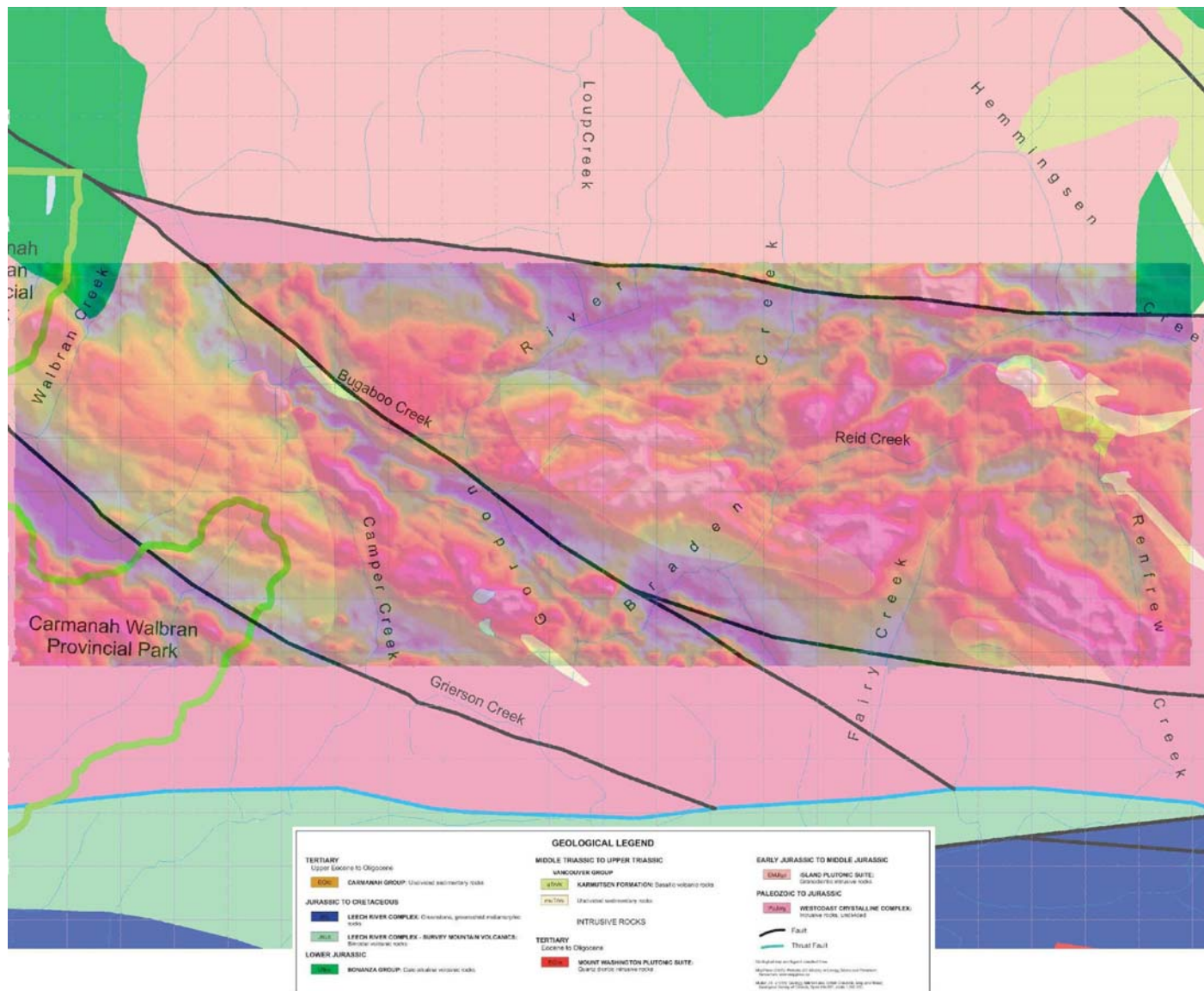
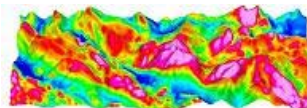


Figure 11: Overlay of Regional Geology and Total Magnetic Field.

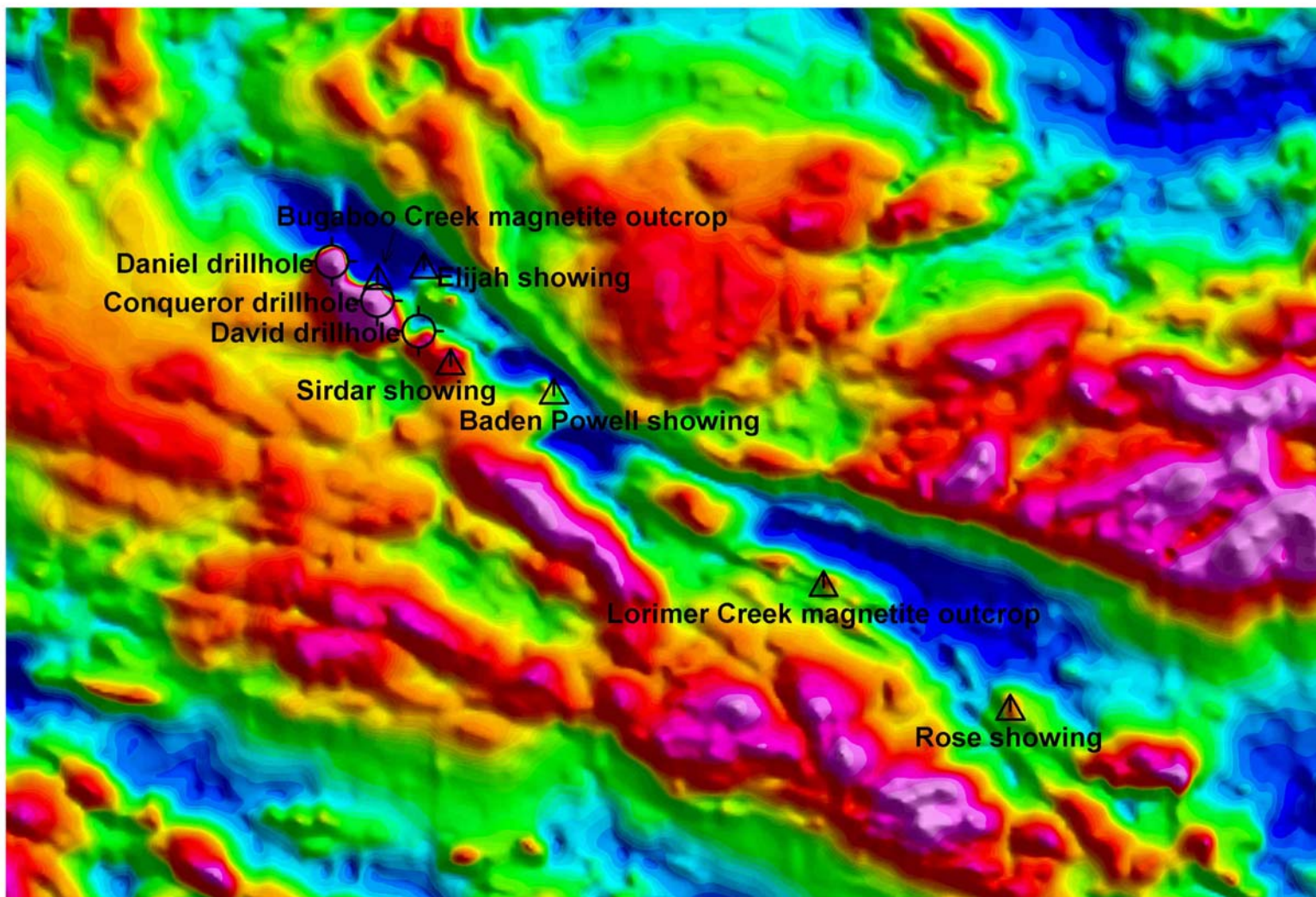
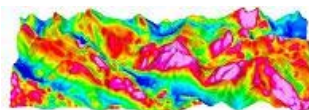


Figure 12: West Side of Property - Total Magnetic Field with showing and drillholes.

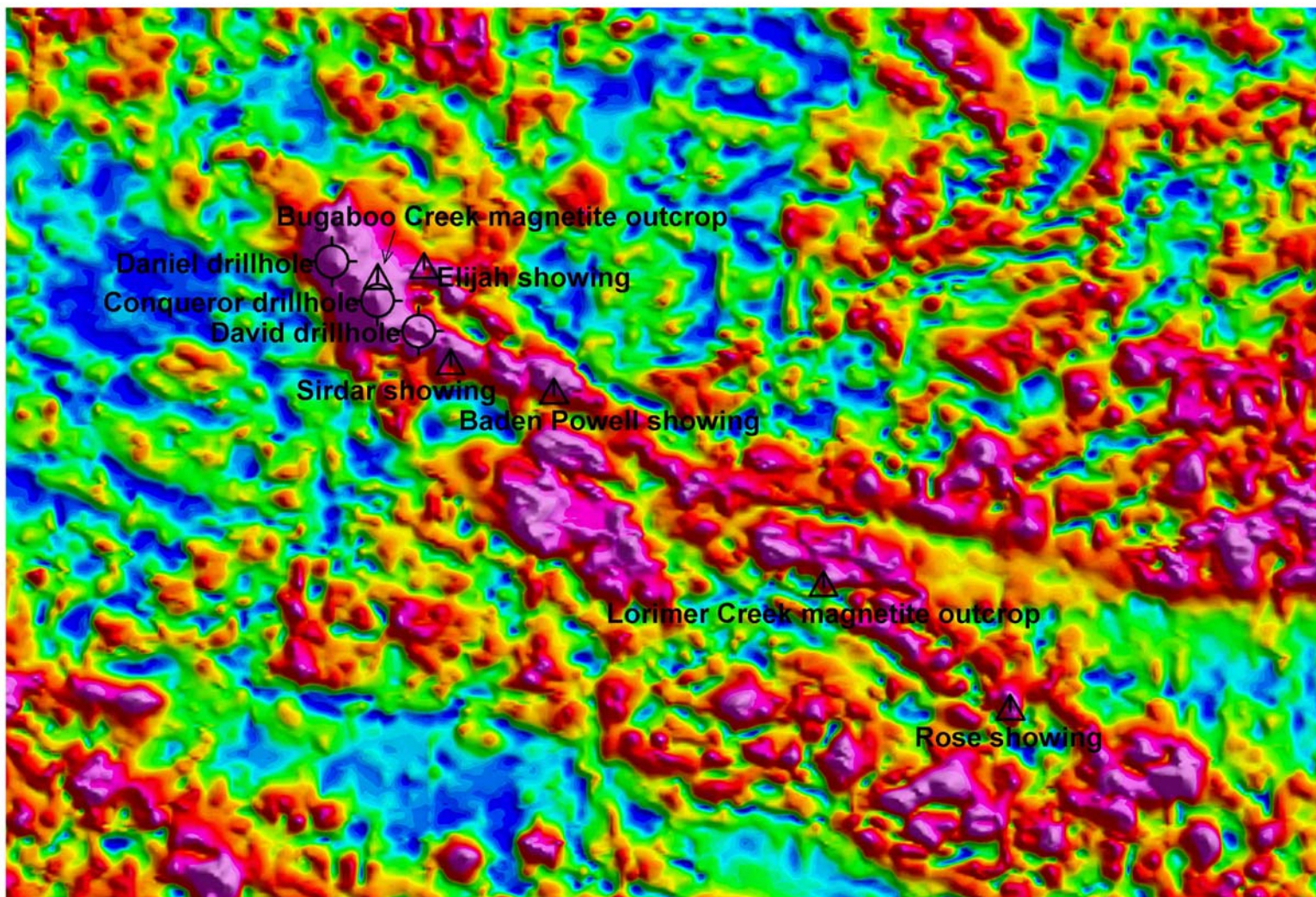
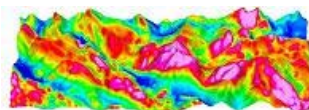
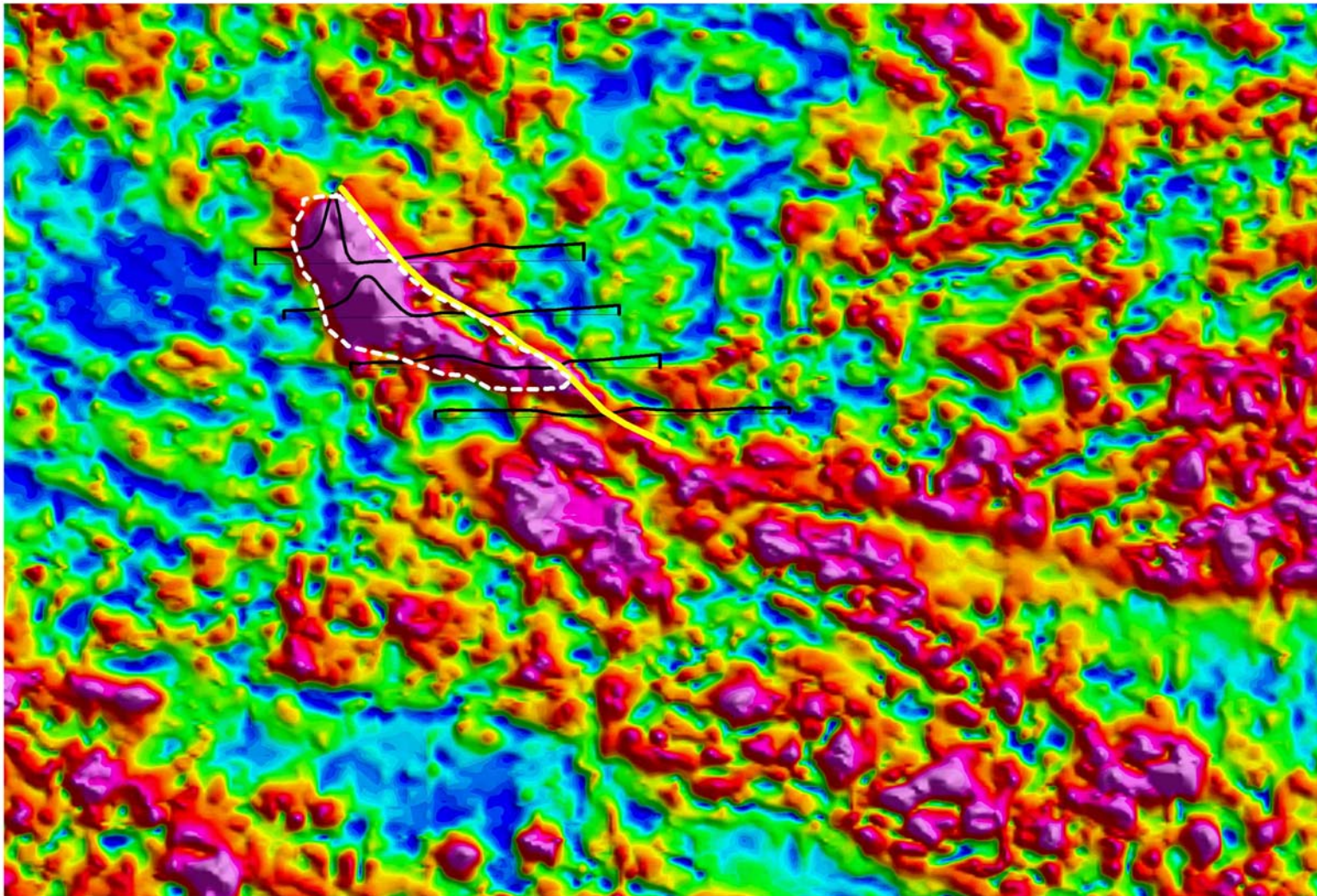
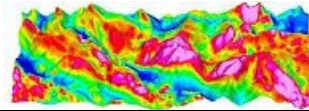


Figure 13: West Side of Property – Analytic Signal with showing and drillhole locations.



*Figure 14: West Zone Analytic Signal with Total Magnetic Field Profiles: A possible contact is marked with the yellow line where there is a change in amplitude of the profiles. A white line marks the outline of the structure which has with the highest magnetic response in this section of the property. The geophysical signature is consistent with that of a highly magnetic body.*

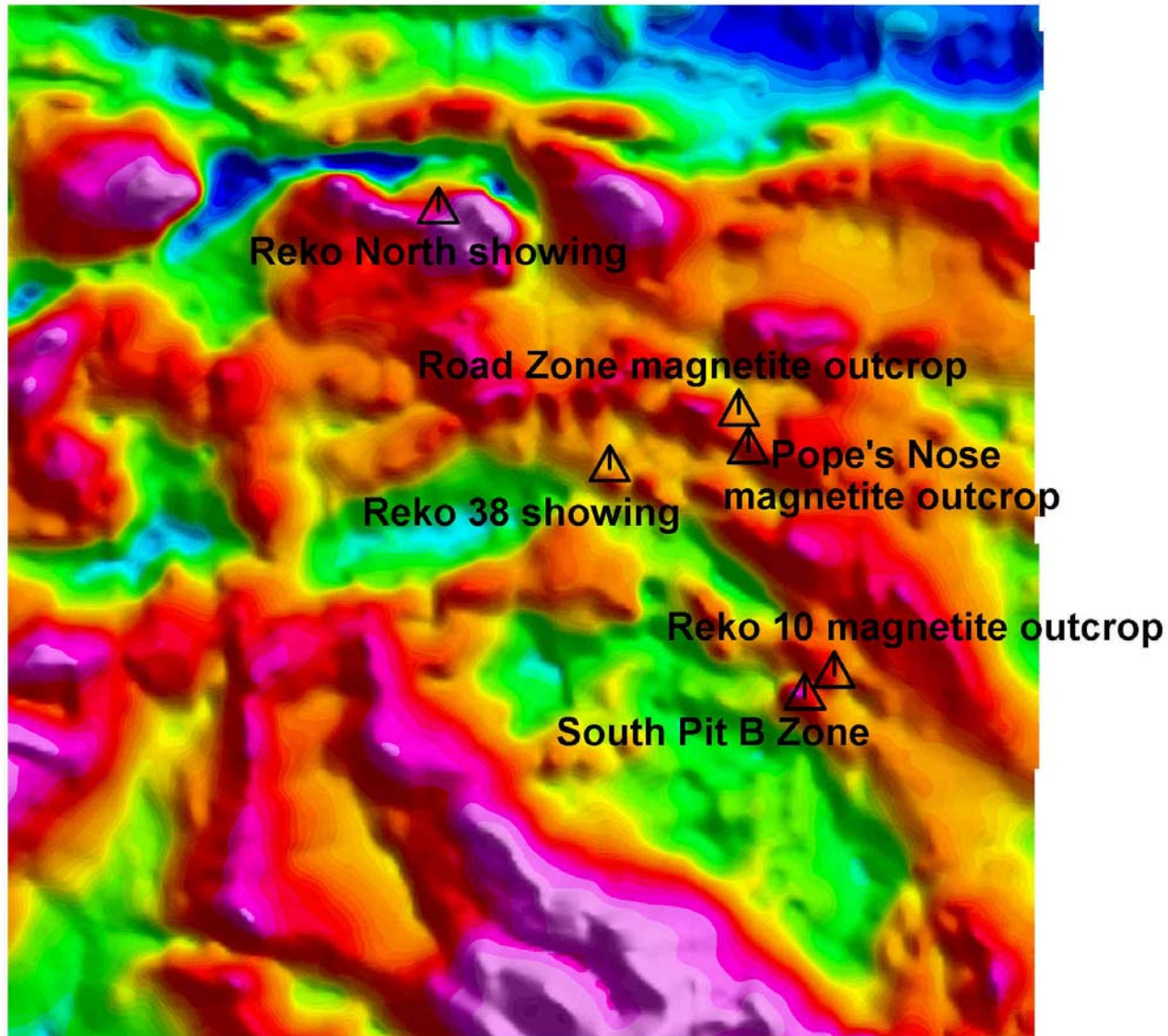
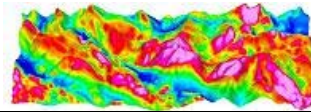


Figure 15: East Side of Property – Total Magnetic Field.

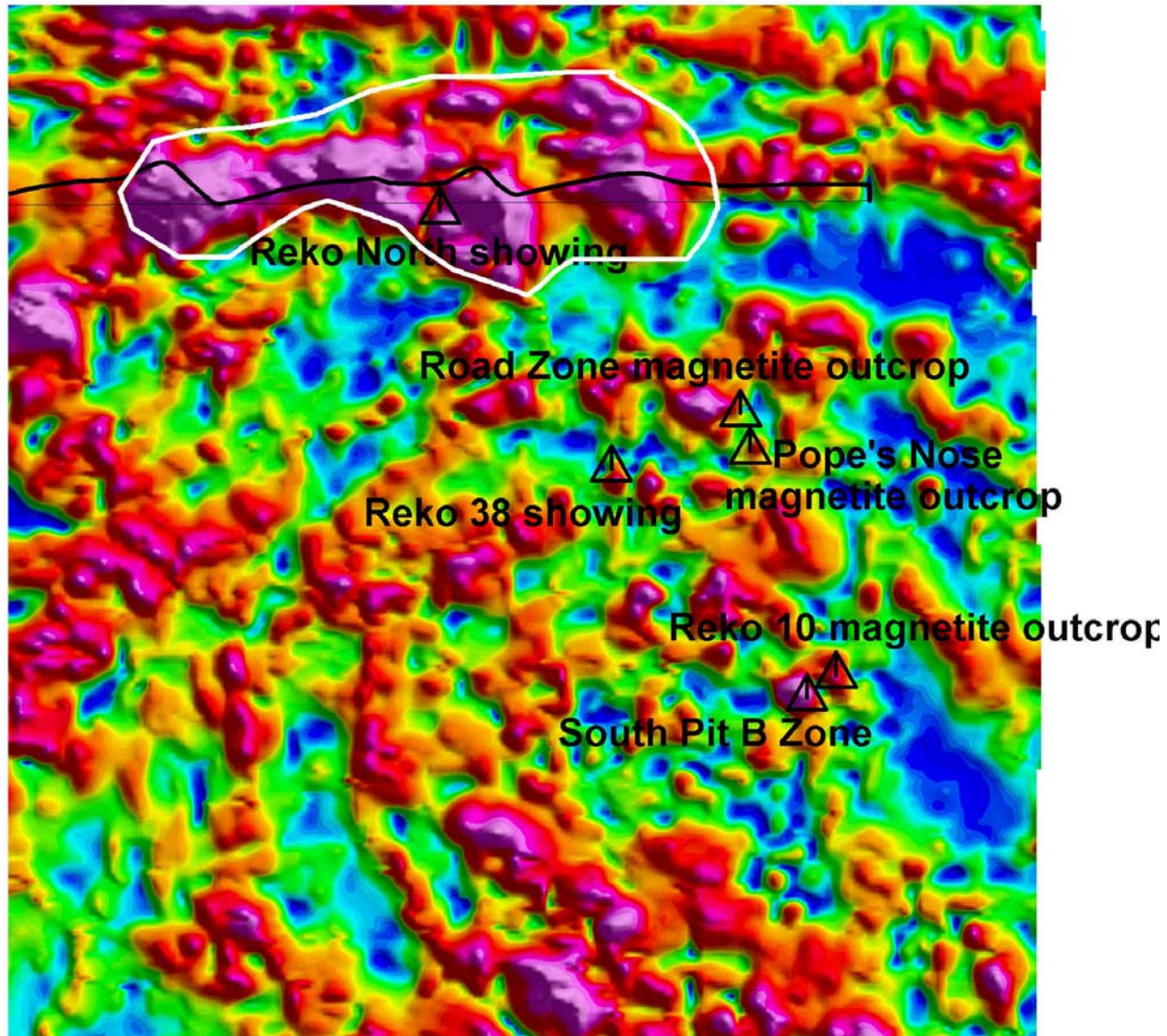
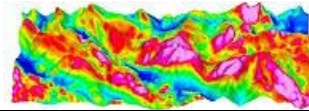


Figure 16: Analytic Signal Grid of the East Section of the survey. The structure (marked by a white line) is the strongest anomaly in this part of the survey, and reflects a broad and deep source. Total Magnetic Field profile through the anomaly (black) shows the highest magnetic response.

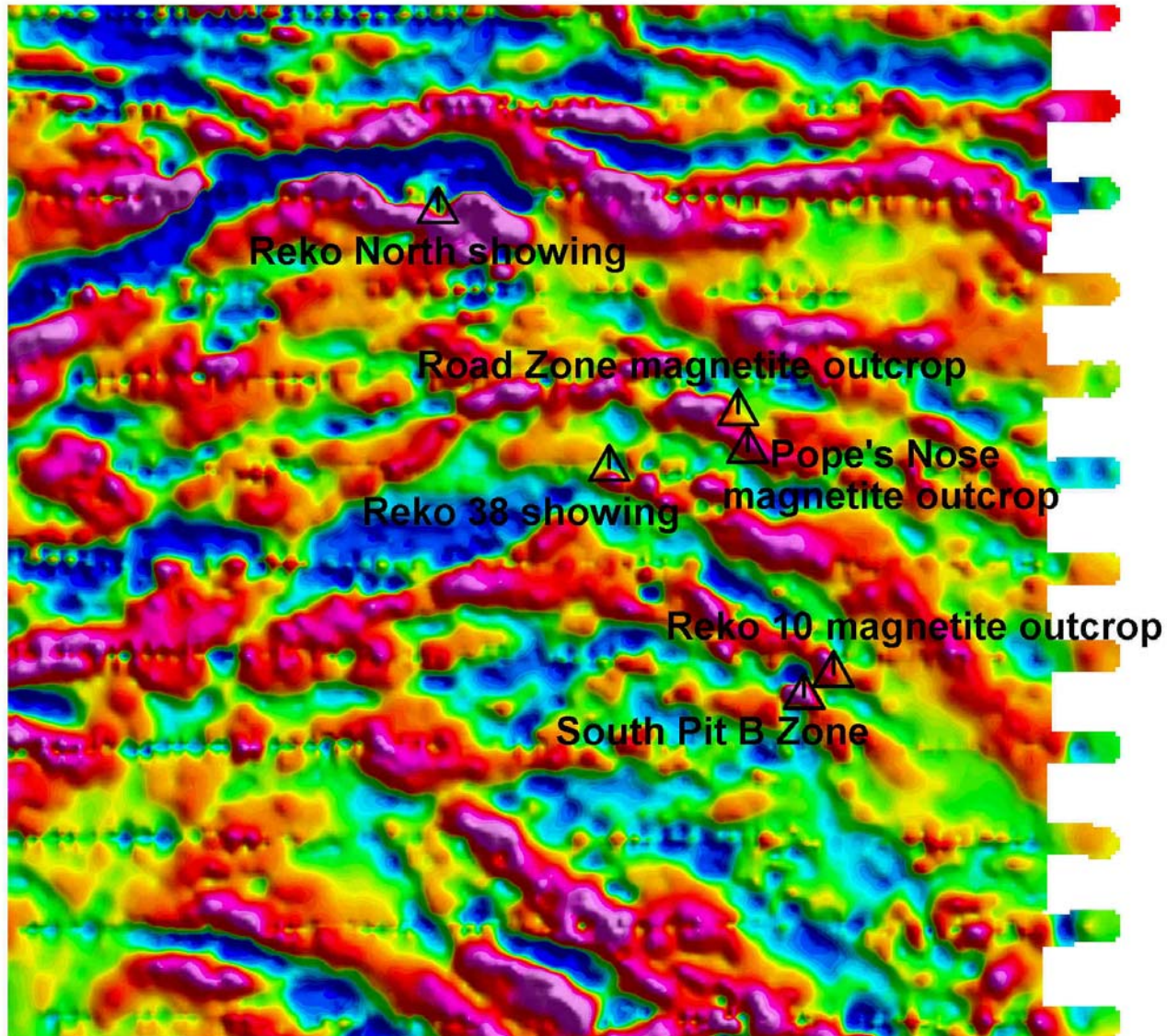
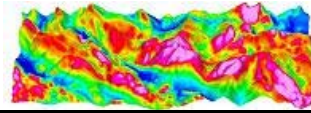
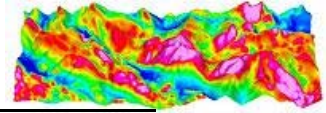


Figure 17: East Side of Property – Vertical Derivative Grid.



---

**STATEMENT OF QUALIFICATIONS**

Monika Sumara

I, Monika Sumara am a Consulting Geophysicist who is employed by Emerald Fields Resource Corporation to analyze, interpret and provide follow-up recommendations regarding geophysical data of the Pearson Property on southwest Vancouver Island. I have completed a field visit to the property.

I am:

- Eligible for membership with the Association of Professional Engineers and Geoscientists of British Columbia (APEGBC).

I graduated from the University of Calgary in Alberta with a Bachelor of Science in Geophysics in 2002, and I have practiced my profession continuously since.

My geophysics experience has involved:

- diamond exploration with Arctic Star Diamond in Northern Manitoba, Ontario and the Northwest Territories since 2004;
- geophysical aeromagnetic surveys with Universal Wing of Vancouver, British Columbia since 2004;
- satellite imagery processing with PhotoSat of Vancouver, British Columbia in 2003 involving GIS mapping and rendering;
- oil and gas geophysical research with CREWES (Consortium for Research in Elastic Wave Exploration Seismology) at the University of Calgary under the tutelage of Dr. Gary Margrave, involving seismic processing techniques during 2002;
- seismic survey planning, processing and interpretation in the Western Sedimentary basin with Tikal Resources Inc., an oil and gas exploration company of Calgary, Alberta, from 1998 to 2001.

I am not aware of any material fact or material change with respect to the subject matter of this technical report which is not reflected in this report, the omission to disclose which would make this report misleading.

Dated at Vancouver, BC this 8th day of July, 2006.

"Monika Sumara"

July, 2006

Appendix C. Preliminary Review of Ultramafic Rock Occurrences Near Port  
Renfrew, Southern Vancouver Island – D. Canil

**Preliminary Review of Ultramafic Rock Occurrences  
near Port Renfrew, southern Vancouver Island**

Submitted by

D. Canil  
School of Earth and Ocean Sciences  
University of Victoria  
3800 Finnerty Rd.  
Victoria, BC V8W 3P6

Submitted Dec. 12, 2006

## **Introduction**

Recently, several isolated bodies of ultramafic rock were recognized in the Port Renfrew area by Gary Pearson, a local prospector. During the summer of 2006, a field mapping study jointly funded by Geoscience BC and Emeralds fields Resources was conducted to ascertain the extent of the ultramafic bodies and to determine their relationship to other rocks of southern Vancouver Island.

## **Field Area**

The field area on southern Vancouver Island (NTS092C,F,G,B) is bordered by the San Juan River in the south, Cowichan Lake in the north, Lake Nitinat to the west, and the Fleet River to the east (Figure 1). Overall, rock exposures are mainly concentrated along active logging roads. Exposure is best in elevated areas that have recently been logged. Remote mountaintops with overgrown logging roads are accessible only by helicopter.

## **Regional Geology**

Previous geologic maps in the area were done at 1:100 000 scale and compiled to 1:250 000 (Mueller, 1977). Most of the area is underlain by rocks of Wrangellia. The Devonian Sicker Group forms the basement to Wrangellia on Vancouver Island, and consists of mafic and felsic volcanics and volcanoclastics, overlain by epiclastic and carbonate sediments of the Permian Buttle Lake Group. Overlying the Sicker Group are the Triassic Karmutsen basalts. Conformably overlying the Karmutsen basalts is the Quatsino Formation, a thin (< 75 m) sequence of micritic limestone, which is itself conformably overlain by the Parsons Bay Formation, a 35 m thick sequence of thinly bedded argillaceous mudstone, limestone, siltstone, and sandstone. The Jurassic Bonanza Arc intrudes, as well as unconformably overlies, older units of Wrangellia. clastic sediments of the Oligocene Carmanah group unconformably overly all older units long the western coast of the island.

## **Jurassic Bonanza Arc**

In the field area, rocks of the Bonanza arc are separated from the Jurassic-Cretaceous Pacific Rim Terrane to the south by the San Juan fault, and from the Sicker Group to the north by the Cowichan Fault. The Jurassic-aged rocks of Wrangellia include, from base to top, the West Coast Crystalline complex, the Island Plutonic Suite, and the Bonanza Group volcanics. These rocks have undergone zeolite to locally greenschist facies metamorphism, but original igneous lithologies are used in their description.

***West Coast Complex*** - The West Coast Complex has been interpreted as the deepest preserved structural level, and is dominantly quartz diorite and gabbro with varying amounts of hornblende, biotite, orthopyroxene and clinopyroxene with accessory pyrite, pyrhotite. Grain sizes vary locally from fine grained to pegmatitic. Weakly concordant diabase bodies are found locally in the West Coast Complex in the field area, southwest of the Gordon River. Directly to the north, two distinct bands of light grey marble occur as screens or septa in the diorite. Similar marble outcrops are found in the eastern part of the field area, although these are more irregular in outcrop pattern. Minor magnetite-rich skarn bodies, with variably-developed diopside-garnet and magnetite-chacopyrite

assemblages, are found at the contact of diorite or diabase with the marble. Due to the metamorphosed nature of these carbonate rocks, they are here suggested to represent fragments and/or faulted slices of the Buttle Lake formation.

Regional-scale aeromagnetic data available for Southern Vancouver Island shows a prominent magnetic high, running parallel to, and extending north from the San Juan fault. At this resolution, the magnetic anomaly appears to roughly correspond with areas underlain by West Coast Complex rocks, but deviations from this general trend exist.

***Island Plutonic Suite*** - The Island Plutonic Suite occurs as a roughly northwest-southeast aligned series of plutons ranging from quartz diorite to alkali feldspar granite. The Island Plutonic Suite most commonly intrudes the Triassic Karmutsen basalts, and, are distinguished from plutons of similar composition of the West Coast Complex by lacking any foliation. The contact between the Island Plutonic Suite and the West Coast Complex is not well defined. In the field area, rocks of the Island Plutonic Suite mainly occur in the northern and eastern parts of the field area, separated from the West Coast Complex to the southwest by intervals of Karmutsen basalt and Quatsino limestone.

***Bonanza volcanics*** - The Bonanza volcanics are only very weakly metamorphosed, displaying assemblages indicative of the zeolite facies and vary from aphanitic basalt, through plagioclase-, pyroxene-, and/or hornblende-phyric andesite, to minor dacite, and lesser pyroclastic deposits. The lateral extent and continuity of these deposits is obscured by vegetation and overburden.

## **Ultramafic Rocks**

Ultramafic rocks occur as discrete bodies within the West Coast Complex diorite, ranging in size from a meter to several tens of meters. Although obscured by overburden, there is some lateral continuity or concentration of the ultramafic bodies, over distances of up to 1 km. Contact relationships between the ultramafic bodies and the West Coast Complex diorite are quite variable. Smaller bodies, which tend to be more olivine-rich, have either abrupt, undeformed contacts with their host, or are present as sheared pods. Larger bodies, which are mostly olivine gabbro, grade into the diorites of the West Coast Complex. In several locations, the association of olivine pyroxenite and pegmatitic hornblende diorite has been noted.

In outcrop, peridotite and olivine pyroxenite outcrops weather to dun or chocolate brown, and have fresh surfaces that are dark grey to black, often with large oikocrysts of amphibole and pyroxene enclosing subhedral olivine. The gabbroic outcrops weather to a dark brown/dun colour, and are better preserved than their olivine-rich counterparts. In thin section, the peridotites and olivine pyroxenites consist of variably serpentinized cumulus olivine with inclusions of euhedral spinel, poikilolitically enclosed by either orthopyroxene, amphibole, or more rarely, clinopyroxene. Orthopyroxene and clinopyroxene coexist in several samples. Weakly to strongly altered plagioclase is present as an intercumulus phase in some samples. In these samples, olivine is never directly in contact with plagioclase, and is always mantled by a corona of pyroxene. Where present, amphibole appears as the result of reaction with pyroxene, along grain boundaries or along exsolution lamellae. Igneous phlogopite is also present as a minor phase in some samples.

Gabbro and gabbronorite display cumulus plagioclase, +/- orthopyroxene, clinopyroxene and, in one case, olivine. Much of the post-cumulus clinopyroxene has been replaced by amphibole. Plagioclase in these samples is invariably less altered than in the peridotite and olivine pyroxenite samples. Magnetite with minor ilmenite exsolution is the dominant opaque phase in the ultramafic samples. It occurs as minor disseminated grains in the peridotites and olivine pyroxenites, and as both an euhedral and intercumulus phase in the gabbroic rocks. Minor amounts of chalcopyrite are noted in most samples. Rare inclusions of round, white, high reflectivity grains in olivine are noted, possibly pentlandite. Ultramafic rock outcrops in many cases correspond to strong anomalies in the regional aeromagnetic pattern.

## **Structure**

Foliations within the West Coast Complex, defined by planar fabric of hornblende or biotite, strike northwest and dip 60-75 degrees to the southwest. Near Harris Creek, a large area of Karmutsen basalt is juxtaposed with the West Coast Complex along a shear zone with the same attitude as the pervasive foliation in the diorites. Shear zones defined by cm- to meter thick mylonite horizons within the West Coast Complex have a similar orientation in the westernmost parts of the field area. The common orientation and sense of shear (tops to NE) for all of these shear zones suggest parts of the the West Coast Complex are in a series of east-verging thrust-faulted panels; the easternmost panel has been thrust onto the Karmutsen basalts.

Poles to foliations in the West Coast complex between Gordon River and Harris Creek define a great circle having a pole plunging 50 degrees to the southwest. Minor folds in the West Coast Complex also have axes plunging with the same orientation. These data are interpreted to reflect that the West Coast complex, Island Plutonic and Bonanza group in the field area are all part of a larger fold structure plunging ~ 50 degrees to the southwest, exposing varying structural depth.

## **Synopsis**

Ultramafic rocks occur in several different geologic settings. The hydrous, calc-alkaline nature of the magma that produced the ultramafic cumulates in the West Coast complex around the Port Renfrew area, as attested to by the presence of primary amphibole, phlogopite and magnetite, is inconsistent with an ophiolite association. Furthermore, there is no spatial association of mantle tectonite, pillow lavas or sheeted dikes with the ultramafic bodies or their host rocks.

Several lines of evidence also show that the ultramafic bodies are not part of 'Alaskan-type' intrusions. First and foremost, orthopyroxene is a common phase in many samples, an observation which is inconsistent with Alaskan-type ultramafic occurrences. In addition, the field relations show the peridotite and olivine pyroxenite bodies lack any concentric zoning, and occur rather as blocks and lozenges in the diorite.

Strikingly similar petrography and field relations to the ultramafic rocks of the current study are known from the Giant Mascot deposit of southern BC. Ni-Cu-PGE sulphide ores at Giant Mascot are hosted by ultramafic rocks, including peridotite, pyroxenite, and feldspathic pyroxenite. As in the current study, the Giant Mascot rocks contain cumulus spinel and olivine, poikilolitically enclosed by orthopyroxene and

amphibole. Chemical data is pending for the current study, for further comparison to the Giant Mascot rocks.

Peridotite and pyroxenite are noted to occur in association with gabbro-norite towards the middle and base of crust in exhumed island arc terranes. The Bonanza arc and its setting on Vancouver Island are very similar to the Talkeetna arc in south-central Alaska, and it has been proposed that the two are of similar age and can be correlated along strike.

### **Future Work and Recommendations**

Geochronologic investigations are underway to constrain the exact age of rocks that host the ultramafic bodies. Ultramafic samples collected have been sent for graphite furnace assay of Ni, Cu, Pt, Pd and Au at Global Discovery Labs (Vancouver). These data shed light on the prospectivity of the ultramafic bodies for related Ni-Cu or PGE sulfide bodies in the West Coast complex throughout the Port Renfrew area.

The majority of the ultramafic bodies are no more than a few tens of meters wide. Although discontinuous at the surface, the ultramafic outcrops tend to be distributed in patches throughout the West Coast Complex. Areas of significant concentration are on Fairy Mountain and along Granite Creek mainline. Areas of the West Coast Complex which host ultramafic rocks appear to correspond with magnetic highs in regional and detailed aeromagnetic surveys. The aeromagnetic highs, however, correspond elsewhere in the field area with laterally discontinuous magnetite skarn, and/or the diabase units, which are strongly magnetic in outcrop. If the regional magnetic signal is controlled by the presence of ultramafic rock, there may be a significant amount of these rocks hidden at depth within the West Coast Complex. Geophysical investigations (detailed gravity survey?) or drilling may reveal the continuity between these or other surface ultramafic bodies at depth beneath the area. No significant concentrations of economic minerals were noted in the ultramafic rocks in outcrop, hand sample, or thin section, apart from minor Cu- and Ni-sulphides (chalcopyrite, pentlandite, pyrrhotite).

### **References**

- Muller, J. E., (1977) 1:250 000 Geology of Vancouver Island, British Columbia; Geological Survey of Canada, Open file 463.
- Sumara, M. (2006) Review of Aeromagnetic data over the Pearson Property. Report submitted to Emeralds Fields Resources.

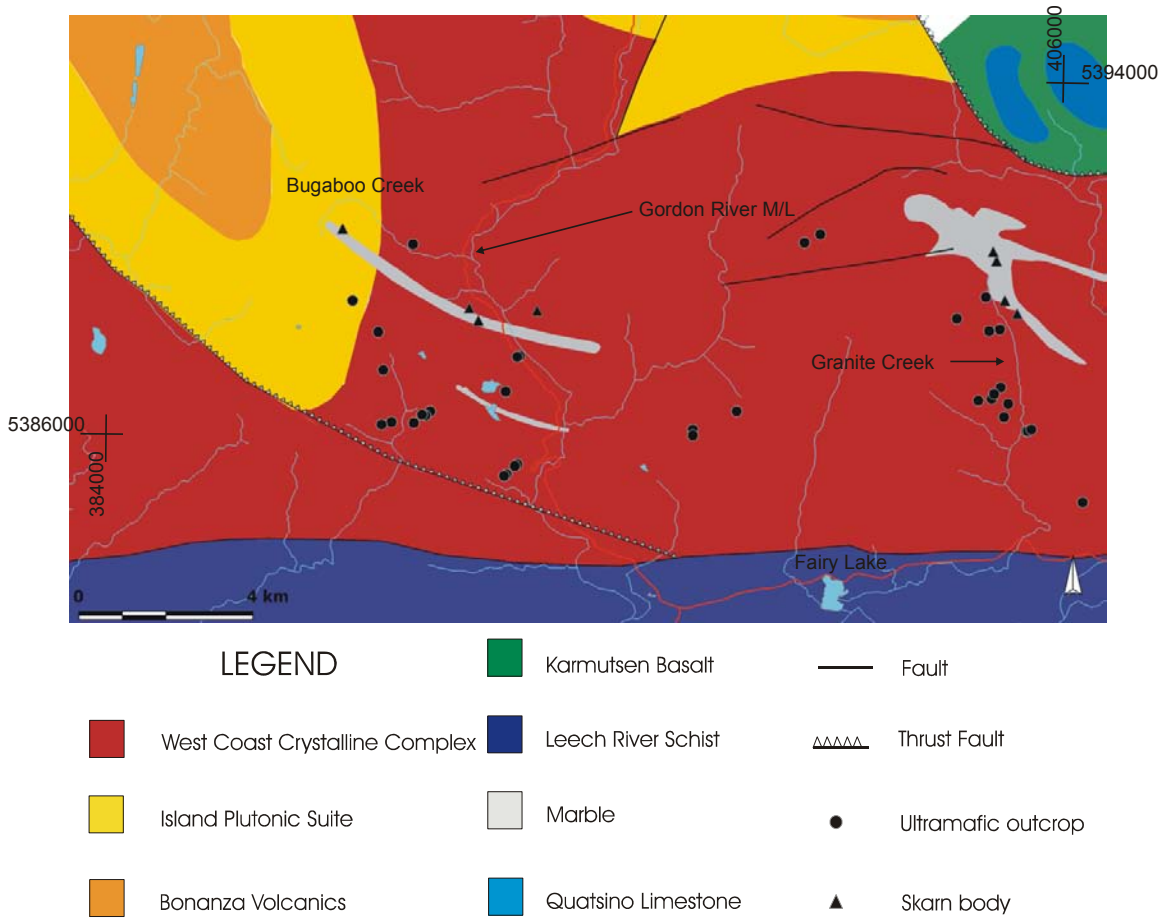


**Figure 1** - 1:50 000 scale geologic map (compiled from 1:20 000 mapping) of field area encompassing the 'Pearson project'. UTM coordinates given for reference. Location of ultramafic and skarn bodies are highlighted by symbols. The latter rock types are not laterally continuous in the map area due to either their size and/or exposure and so are treated as separate units on the map.

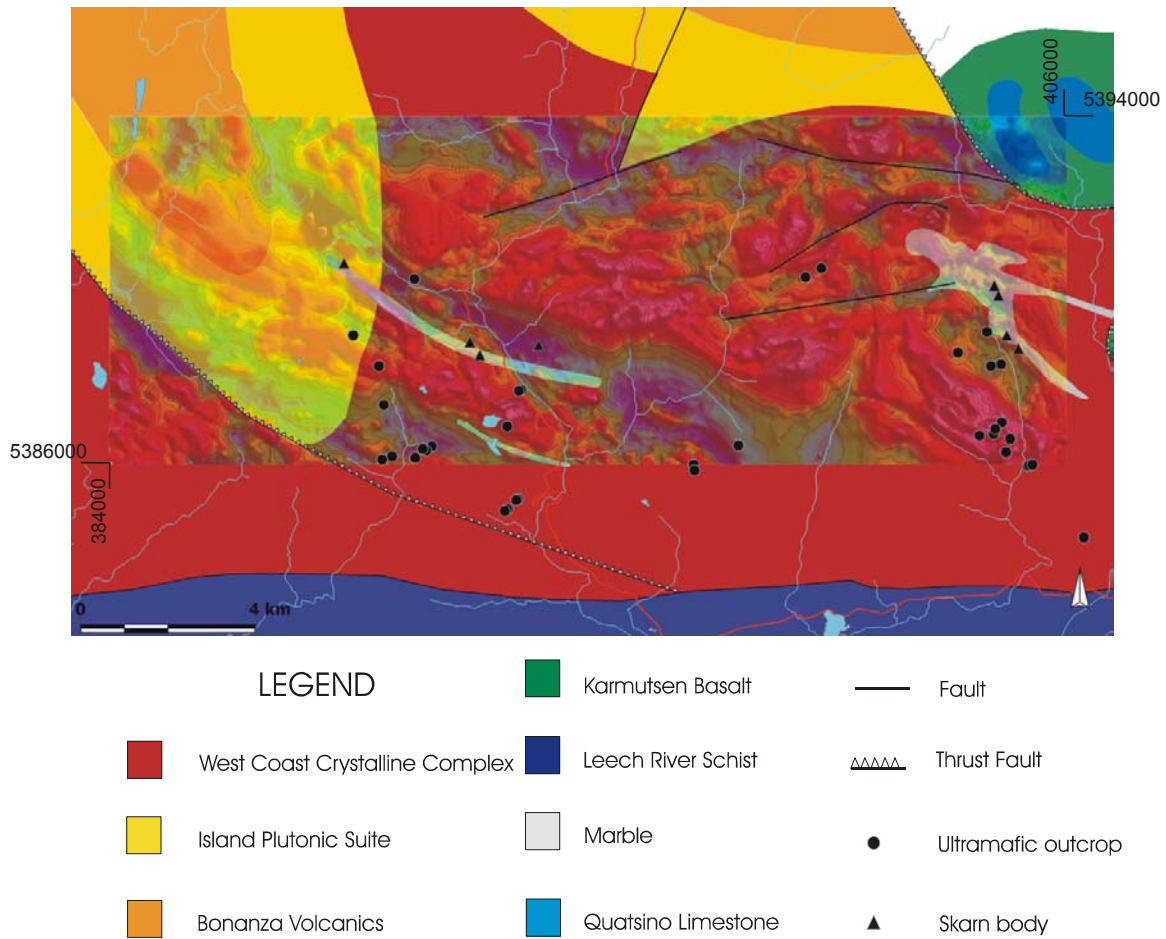


**Figure 2-** 1:50 000 scale geologic map (compiled from 1:20 000 mapping) of field area encompassing the ‘Pearson project’ as per Figure 1, but with high resolution aeromagnetic survey (Sumara, 2006) superimposed on surface geology. Note the correlation of many of the ultramafic and/or skarn bodies with magnetic highs, and the correlation of faults with magnetic lows or offsets.

Appendix D. Preliminary Reports (2) of Pearson Property Geology – Dr.  
Richard Ernst

## PRELIMINARY REPORT OF VISIT TO PEARSON PROPERTY, JULY 2006

Richard Ernst

Ernst Geosciences

7 August 2006

### INTRODUCTION

These are notes based on a visit to the Pearson project in the Port Renfrew area on July 13-16, 2006. The visit mainly focused on the Bugaboo mountain logging-road exposure of the magnetite unit. We also collected a sample from a pegmatitic gabbro near Grierson 1000, for geochronology. In this preliminary report I will comment on the magnetite unit, on the geochronology samples, and on the new aeromagnetic map. Each of these points is expanded upon below. But I should note that this report is preliminary, pending availability of additional datasets as described in each section below.

### BUGABOO MOUNTAIN LOGGING ROAD TRENCHED-EXPOSURE OF MAGNETITE UNIT

A superb exposure of the magnetite unit is available along a logging road on Bugaboo mountain. In the month of June, Gary further improved this outcrop by arranging for trenching along the outcrop and especially along its margins in order to better expose the contacts with the host marble on both side. The contact on the north side (up hill) is vertical with a N80E trend, whereas the contact with marble on the south side is less well exposed and its orientation cannot be determined. Furthermore, the magnetite unit at this locality must be also underlain by marble, given that the David drill hole (located midway along the outcrop) encountered marble at less than 10 m depth. So the structure of the marble unit must be somewhat complex.

The magnetite unit is 71 m wide and broadly consists of a central magnetite-rich unit and bordering skarn/gossans which are in contact with the host marble, although there are some patches of magnetite in contact with marble on the south side of the outcrop. In addition, there are also crosscutting dykes of porphyritic diabase, and probable quartz porphyry. Twelve samples were collected systematically from all units across the outcrop, and these were

submitted by Gary to Vancouver Petrographics for thin section work. In addition, some of the samples have also been submitted for assay, for Au, and other metals. A more complete assessment of the interpretation of the outcrop will be done after the thin section descriptions and assay data are available.

## AEROMAGNETIC INTERPRETATION

With respect to the interpretation of the aeromagnetic data, a more complete interpretation will be possible after the aeromagnetic map is overlain by two other data-types.

- a) Topography: comparison of the aeromagnetic data with topography should allow us to identify any spurious aeromagnetic anomalies. (This point was also made by Dante Canil in his email of 11 July when he asked “Is there any topo influence on the mag signal?”) It is difficult to control the flight elevation over areas of rapidly changing topography. The parameters for the flight elevation according to Monika Sumara’s report are a mean ground clearance of 60 m with a mean variation of 15 m—so the variation can be significant especially in areas where the topography is changing rapidly. Digitally draping of the aeromagnetic data over the topography should help reveal any false aeromagnetic anomalies that might be related to systematic elevation variations.
- b) Gary’s thin section locations: It is important to distinguish which aeromagnetic anomalies are due to the magnetite unit and which are due to the ultramafic units (of the presumed mafic-ultramafic layered intrusion). Given the number (about 60?) of mafic-ultramafic thin sections obtained by Gary, plotting of these on the aeromagnetic map should constrain which aeromagnetic highs are related to the magnetite unit and which are due to ultramafic (serpentinized) bodies.

In the road-side outcrop, along Bugaboo mountain the magnetite unit is 71 m wide and has vertical contact on at least the north side. However, the David drill hole, which is located about midway in the magnetic unit along the roadcut encounters marble starting at a depth of less than 10 m. This is puzzling given the continuous exposure of magnetite on the roadcut behind the drill hole, and would seem to suggest the magnetite unit in this outcrop is very thin. This would contrast with the modeling estimate of 150 m thickness that Monika Sumara obtained by modeling the anomaly characteristic of the region between Daniel,

Conqueror and David drill holes. This puzzle may be explained with reference to the aeromagnetic map. Figure 5 in Monika's report shows that the David drill hole occurs on the edge of the aeromagnetic high, more specifically, on the edge of a slight gap between the aeromagnetic highs associated with the David- Sirdar showings and a separate aeromagnetic high associated with the Conqueror Daniel showings. From this we can conclude that the Bugaboo road outcrop (and the David drill hole) are located on the end (north end) of a segment of the magnetic unit, and this may explain why the David hole encounters marble at such a shallow depth.

#### AGE DATING RATIONALE

A geochronological sample was collected of gabbro pegmatite from a creek located near the Grierson 1000 road. The exact location of the collected sample is 48 degrees, 37.30 minutes N, 124 degrees, 28.42 minutes W. Many mafic-ultramafic outcrops occur along the Grierson 1000 road, and it is reasonable to infer that the gabbro pegmatite is a member of this same mafic-ultramafic assemblage. Therefore a successful U-Pb date on the gabbro pegmatite would also provide an age for the mafic-ultramafic intrusion(s).

The geochronological sample has been submitted to Richard Friedman of the University of British Columbia for U-Pb zircon and baddeleyite dating. The dating is being done on a rush status with a 2 month turn-around. So we will soon have an answer to this fundamental question of whether the mafic-ultramafic layered intrusion in the Port Renfrew area is part of the feeder system for the 230 Ma Wrangellia large igneous province—or not. If yes, the prospects for ore grade Cu-Ni-PGE deposits are improved.

6 October 2006

From:  
Dr. Richard Ernst  
Ernst Geosciences

## GENERAL COMMENTS REGARDING THE PEARSON PROJECT BASED ON THE AEROMAGNETIC MAP AND SUPERIMPOSED THIN SECTION SAMPLES

**IMPORTANCE OF U. VIC MAPPING:** First of all I should again say that the map that the U. Vic crew is producing is the best source of information for accessing the , particularly since I think they are making good use of the aeromagnetic data and also incorporating Gary Pearson's thin section results.

### SITING OF ADDITIONAL DRILLHOLE(S)

I have looked through Monika Sumara's report in some detail, and my comments below on suggested sites for drilling are discussed with respect to her identified anomalies P1 to P19.

P1 is already well characterized with drill holes, which outline the significant distribution of Fe-rich rocks; no further drilling is needed here at this time.

P2 is the key place for drilling. Given that Anomaly P2 (the magnetic high) is roughly on strike with P1, it seems likely that this structure also is caused by a continuation of the Fe body. If road access allows, I would highly recommend drilling into the P2 anomaly to confirm that this aeromagnetic anomaly is due to Fe-rich rocks (and that it is not caused by the serpentinized ultramafics). The continuity of the P2 anomaly suggests that it is a single feature, and the along-strike consistency of the profile suggests that it has a relatively uniform width and depth extent. Also if the source of the P2 anomaly is confirmed to be Fe-rich rocks, this result will considerably increase the Fe reserves in this part of the Pearson project area

Anomalies P7, P8 and P9, are part of a larger magnetic high, and I think the source of this anomaly is more likely (serpentinized) ultramafics rather than Fe. My reasoning is as follows: Although there are no thin section samples in this portion of the magnetic high (in the vicinity of P7, P8 or P9), there is thin section control further to the east. Specifically, in the vicinity of P7-P9 the structure has mostly a ESE strike and about 8 km to the ESE, there are a lot of thin sections showing ultramafic composition. Also about 3 km E-ENE of the P7-9 anomalies there are a couple of thin sections (B3-4) indicating ultramafic compositions. So based on these along-strike correlations, I think it is highly likely that the P7-9 anomalies are due to serpentinized ultramafics and not Fe rich rocks. Therefore, P7-9 would not be a good target for drilling—from the perspective of enhancing Fe deposits. (As a caveat to this conclusion, I should say that I have not

seen the final U-Vic mapping for the P7-9 area) which could give tighter constraints on the geology associated with the P7-P9 anomalies—and maybe lead to a different interpretation).

Anomaly P12 is certainly strongly linked to Fe-rich units. However, the anomaly located about 2 km to the west may be linked with ultramafics (based on B3- an B4 descriptions). So I cannot exclude that the P12 (and nearby P13) anomalies are partially due to ultramafics.

In summary: the obvious choice for further drilling to extend the known Fe reserves is the P2 anomaly.. If it can be shown that P2 is similarly well-endowed in Fe to that of anomaly P1, then the strike length of Fe rich rocks would be more than doubled, which would considerably enhance the economic significance of the Fe deposits of the Pearson Project.

#### PROSPECTING FOR Ni-Cu-PGEs:

I will not comment on this until I have had a chance to think about this some more. As summarized by Gary Pearson in a recent email to me, the anomalous Ni-Cu-PGE values are found in the “porphyritic diabase” which are mapped by the U.Vic team as microdiorites. Certainly the nature of this unit needs to be evaluated.

Ideally an age In any case, I think it is significant that the ultramafic samples do not show anomalous Ni-Cu-PGE values. From the maps that I was sent, the samples with some significant PGEs (and also very high Ni) are 033, 073 and 075 and also Z4. But 033, 074 and 075 are off the aeromagnetic map to the south.

The low values in the ultramafics are perhaps consistent with their lower Ni-Cu-PGE potential given that the age date, 177 Ma, on the pegmatite gabbro phase shows that they are not part of the Wrangellia Large Igneous Province.(